# Fluorometric Detection Of Multiple Bacteria In Water Using Cell Imprinted Polymer Thin Films Integrated Into A Microfluidic Channel

**Islam Mahmoud**

A THESIS SUBMITTED TO THE FACULTY OF GRADUATE STUDIES IN PARTIAL FULFILLMENT OF THE REQUIREMENTS FOR THE DEGREE OF MASTER OF APPLIED SCIENCE

GRADUATE PROGRAM IN MECHANICAL ENGINEERING

YORK UNIVERSITY

TORONTO, ONTARIO

June 2025

© Islam Mahmoud, 2025

# Abstract

Waterborne pathogens pose considerable environmental public health risks, yet conventional bacterial detection methods (i.e., culture plating and molecular assays) are time-consuming, labor-intensive, and typically must be performed in centralized laboratories that render them inappropriate for rapid field monitoring. Rapid biosensors offer a promising solution, yet existing designs rely on fragile biorecognition materials such as antibodies that require cold-chain storage and special handling, undermining field application. To address this issue, synthetic recognition via imprinted polymers, specifically whole-cell imprinted polymers (CIPs), offers a cost-effective and chemically stable solution to bacteria detection that does not require biological reagents. The work in this thesis presents the development of a fluorescence-based microfluidic sensor utilizing CIPs to enable duplex bacteria detection in aqueous samples. Thin films of polymerized CIP, specific to target bacterial species, were in-situ fabricated on the surfaces of microfluidic channels using entire bacterial cells as templates to form selective cavity areas that trap the target cells. By integrating several CIP regions within one chip, each targeting various bacterial species, the device is capable of parallel detection of multiple species. The detection is done through injecting FITC after capturing bacteria, with the FITC concentration optimized to enhance the fluorescence signal intensity. With *Salmonella* as a model target in singleplex format, the sensor exhibited detection and quantification limits of $1.47 \times 10^3$ and $5.28 \times 10^3$ CFU/mL, respectively, with a linear dynamic range across bacterial concentrations from $10^3$ to $10^7$ CFU/mL (log scale). The CIP-based film was also somewhat selective, with preferential capture of *Salmonella* over non-target bacteria at high concentrations. The sensor was additionally evaluated in duplex mode for concurrent detection of *Salmonella* and *E. coli*, using two discrete CIP regions within the microfluidic channel that each bound to selective bacteria. Duplex detection was accomplished at concentrations higher than $10^5$ CFU/mL for both targets in multiplex mode. Despite the sacrifice of sensitivity, the proposed CIP sensor offers profound advantages in terms of simplicity and reagent efficiency; it

requires only small sample volumes and avoids complex sample preparation, thereby highlighting its potential for environmental water quality monitoring. Overall, the results showcase the feasibility of using CIPs as a proficient medium for rapid and discriminatory bacterial identification in environmental water samples using microfluidic fluorescence biosensors. Future efforts must involve continuing to improve detection sensitivity through polymer composition optimization or signal amplification methodologies, and sensor validation with real environmental water samples to move forward with practical field implementation of this technology.

# Dedication

*To my beloved father, Moheb, mother, sister, and brothers, whose constant love and encouragement have been my foundation. To my fiancé, my sweetheart and greatest comfort, whose strength and love have carried me through every challenge.*

## Acknowledgement

The journey of bringing this research to fruition and crafting this thesis has been both demanding and immensely fulfilling. Along the way, I have been fortunate to receive guidance, encouragement, and support from many individuals.

First and foremost, I owe my deepest gratitude to Professor Pouya Rezai. His patient guidance, insightful feedback, and unwavering support have shaped not only the direction of my research but also my development as a scholar. It has been an honor to learn from and collaborate with him, I am grateful for the opportunity to work under his direction.

I am also very grateful to Dr. Ali Doostmohammdi for his hands-on mentorship and direct support. His expertise, patience, and practical advice were invaluable in guiding my research and helping me grow as a researcher. Beyond our work together, I have truly enjoyed getting to know him personally, and his kindness and encouragement have meant a great deal to me.

I am deeply thankful to my fiancée, Heba, whose love, encouragement, and unwavering belief in me have been my greatest source of strength. To my parents, thank you for guiding me with your wisdom, sacrifices, and constant support—you have led me to this milestone and shaped who I am today. And to my brothers and sister, your support and humor have made even the hardest days brighter.

Finaly, I would also like to thank Dr. Noha for all she taught me when I first began my master's—her patience and insights set me on the right path. I'm grateful to Dr. Khaled for his guidance and generous support throughout my studies. And to my friend Mohamed Daoud, thank you for being there at every step, both before I arrived and throughout this journey—you have made all the difference.

# Table of Contents

# List of Figures

# List of Tables

# List of Abbreviations

**AAM:** Acrylamide

**AIE**: Aggregation-induced emission

**AMPs**: Antimicrobial peptides

**ATP**: Adenosine triphosphate

**CBMs**: Carbohydrate-binding modules

**CBP**: Carbohydrate-binding proteins

**CFUs**: Colony-forming units

**CIP**: Cell-imprinted polymer

**CuNCs**: Copper nanoclusters

**DHEBA**: Dihydroxyethylene-bisacrylamide

**DMSO**: Dimethyl sulfoxide

**ECL**: Electrochemiluminescence

**EGDMA**: Ethylene glycol dimethacrylate

**ELFA**: Enzyme-linked fluorescence assay

**ELISA**: Enzyme-linked immunosorbent assay

**FRET**: Fluorescence resonance energy transfer

**HIV**: Human immunodeficiency virus

**ICG**: Immunochromatographic test strip

**IMS**: Immunomagnetic separation

**IPs**: Imprinted polymers

**$K_2S_2O_8$**: Potassium persulfate

**LOD**: Limit of detection

**LOQ**: Limit of quantification

**LPS**: Lipopolysaccharides

**MAA**: Methacrylic acid

**MIP**: Molecularly imprinted polymer

**MMA**: Methyl methacrylate

**MNC**: 2-(4-mesyl-2-nitrobenzoyl)-1,3-cyclohexanedione

**MIT**: Molecular imprinting technique

**N-GQDs**: Nitrogen-doped graphene quantum dots

**NIP**: Non-imprinted polymers

**pAb**: Polyclonal antibodies

**PBS**: Phosphate-buffered saline

**PDA**: Polydopamine

**PEC**: Photoelectrochemical

**PET**: Polyethylene terephthalate

**PFP-OC**: poly(fluorene-co-phenylene) organic semiconductor

**PSA**: Pressure-sensitive adhesive

**POTS**: 1H,1H,2H,2H-perfluorooctyltriethoxysilane

**PCR**: Polymerase chain reaction

**QD**: Quantum dots

**RPA**: Recombinase polymerase amplification

**SAMs**: Self-assembled monolayers

**SD**: Standard deviation

**SELEX**: Systematic evolution of ligands by exponential enrichment

**SEM**: Scanning electron microscopy

**SPR**: Surface plasmon resonance

**SSOs**: Single-stranded oligonucleotides

**VIP**: Virus-imprinted polymers

**VP**: N-vinylpyrrolidone

**WHO**: World Health Organization

# Chapter 1

## 1 Introduction

### 1.1 Research Motivation and Gaps

The ability of bacteria to live in a broad range of environments poses a huge challenge, especially when they contaminate water sources. Pathogenic bacteria such as *E. coli O157:H7*, *Campylobacter jejuni (C. jejuni)*, *Listeria monocytogenes (L. monocytogenes)*, *Shigella spp.*, and *Salmonella* are notable to cause serious health issues [1]. These bacteria are responsible for diseases such as cholera, diarrhea, dysentery, typhoid, and hepatitis A, which are quite common in areas with contaminated water. The consequences are significant; chronic diarrhea accounts for almost 485,000 deaths every year, and a lot of these are young children, according to the World Health Organization (WHO)[2]. The importance of effective methods for the early detection of these pathogens cannot be emphasized enough. Rapid detection is crucial for minimizing the spread of diseases and reducing the significant public health risks associated with bacterial contamination in water. Below, a very brief overview of the conventional and microfluidic bacteria detection methods, and the research gaps in these areas, is provided. These topics are reviewed in more detail in Chapter 2 of the thesis.

Conventional methods for bacterial detection mostly involve biological and biochemical means. Biological detection methods start with culture-dependent methods, where the harmful bacterial strain is isolated using solid or liquid media. Techniques such as plate-culturing and subsequent counting of bacteria colony-forming units (CFUs) are widely used due to their reliability, however, these methods are time-intensive and require specialized equipment, limiting their applicability in scenarios demanding rapid detection [3], [4]. To address these limitations, culture-independent technologies such as polymerase chain reaction (PCR) and gene sequencing have been developed [5], [6], [7], [8]. These advanced methods offer improved speed and precision by identifying target nucleic acid sequences or

proteins. Despite their advantages, these techniques come with challenges, including the need for specialized equipment, complex data analysis, and potential sources of error, such as the formation of chimeric sequences during PCR, which can compromise the accuracy of results. Although immunological methods such as Enzyme-Linked Immunosorbent Assay (ELISA) rely on antigen-antibody interactions and provide robustness, PCR-based techniques generally offer superior accuracy in bacterial detection because of their higher sensitivity and specificity [9]. These methodologies, however, despite their efficiency, are also characterized by several drawbacks – they are time-consuming and labor-intensive, which means that the methods are inefficient in a practical situation where quick point-of-need tests are required [9], [10], [11], [12].

Microfluidic technology has emerged as a key component for biosensor development regarding bacterial detection based on the interdisciplinary knowledge base derived from biology, chemistry, and engineering [13]. These sensors are outstanding at translating biological data into quantitative signals, hence finding quick and accurate detection [14], [15]. The integration of microfluidics allows for the control of fluids within micro-channels with high accuracy, and provides benefits such as reduced costs, enhanced sensitivity, and accelerated processing times [16]. This approach also allows for simultaneous analysis and sample preparation on a single chip, improving efficiency and automation [16], [17].

Optical detection methods, such as colorimetric and fluorescence biosensors, have become promising alternatives to traditional techniques for detecting bacteria. Colorimetric biosensors detect bacteria through visible color changes, making them efficient and requiring less complex equipment [18]. These characteristics make them appropriate for field applications with limited resources. However, their drawbacks, such as low sensitivity, poor selectivity, and long detection times, have driven the development of fluorescence biosensors [19]. Fluorescence biosensors detect changes in fluorescence

intensity when interacting with target bacteria, offering significantly higher sensitivity. For example, fluorescence-based biosensors have been successfully used to detect *Salmonella* and *E. coli* in food samples with a limit of detection (LODs) as low as 9 CFU/mL [18], [20], [21], [22], [23]. Despite their advantages, fluorescence biosensors face challenges when applied to real-world samples. Interference from insoluble particles and the limited stability of biorecognition elements under non-physiological conditions remain significant obstacles [13], [24]. Antibodies are frequently employed among these biorecognition elements because of their high specificity. However, outside of the controlled environment of a laboratory, antibodies are susceptible to denaturation and loss of action when subjected to high temperatures, pH changes, or other harsh environmental circumstances [25], [26]. This instability limits its usefulness for field-based and real-world circumstances because it frequently requires extremely cautious handling and storage, typically under temperature control, with specialized equipment.[24], [27].

As a result, researchers are actively investigating synthetic recognition elements that are more stable and cost-effective as alternatives [28]. Among these, molecularly imprinted polymers (MIPs) and cell-imprinted polymers (CIPs) stand out due to their durability and ability to perform well in challenging environments [29], [30].

Imprinted polymers (IPs) have become widely used in bacterial detection due to their capability to function as fully synthetic, highly specific recognition elements [31]. These polymers are fabricated by polymerizing functional monomers around a template molecule or bacterial cell [32]. After polymerization, removal of the template leaves behind cavities that replicate both the morphological and chemical properties of the original template [31], [33], [34], [35], [36]. This approach creates selective binding sites that can recognize and capture the target bacteria with high specificity [34].

The versatility and robustness of IPs have led to their integration into various biosensing devices. For example, IP-based sensors have been developed for the detection of *E. coli* from water samples by forming specific capturing cavities for bacterial cells within the polymer matrix [37]. These sensors are not only economical but also possess excellent thermal and chemical stability, hence ideal to be used in harsh environments where other conventional biological detection methods may fail. Another device integrates IPs into a microfluidic platform for the rapid on-site detection of *Salmonella*, hence possessing mighty applicative potential in food safety [38]. This versatility makes it possible to adapt IPs for a very wide range of bacterial targets, making them valuable when compared with traditional biological recognition elements. Unlike antibodies, which can be very costly and unstable under non-physiological conditions, IPs could resist harsh environmental conditions without a loss in their effectiveness [38].

While IPs demonstrate good specificity and stability in bacterial detection, significant obstacles remain. These include challenges in completely removing the template, labor-intensive preparation processes, low controllability of polymer layer properties (such as thickness and uniformity), and high costs associated with surface treatment chemicals [39]. Integrating IPs into microfluidic platforms could address these limitations by enabling precise control over polymer synthesis conditions and reducing material usage.

Recent works have demonstrated the combination of microfluidic techniques with CIPs for bacterial detection. Doostmohammadi et al. [40] developed a microfluidic chip incorporating magnetic microstructures designed to immobilize and utilize fluorescent CIP microparticles to detect *E. coli* bacteria cells. This device achieved a LOD as low as $4 \times 10^2$ CFU/mL while successfully differentiating *E. coli* from *Sarcina*. Similarly, Akhtarian et al. [41] fabricated CIP-coated microwires that demonstrated a bacterial capture efficiency of 76% for *E. coli*, highlighting the potential of integrating

the IPs and microfluidic devices for efficient electrical bacterial detection. Yin et al. [42] developed a smartphone-based fluorescent sensor designed to detect *E. coli*, *S. aureus*, and *P. aeruginosa* bacteria. This sensor claims to reach LOD as low as $10^2$ CFU/mL in 40 minutes by utilizing magnetic molecular imprinting and aptamer-based fluorescent probes combined with 3D-printed microfluidic channels. However, the sensor's reliance on aptamers raises concerns about real-world applications. Despite their synthetic nature, aptamers are subject to degradation by nucleases, have limited modification choices, and are sensitive to environmental changes, all of which can reduce the sensor's efficiency [43], [44].

Despite these advancements, most optical IP bacteria sensors integrated with microfluidics to date rely on microparticles as the recognition element. While effective, handling and integrating microparticles into devices can be technically challenging [42], [45], particularly when aiming for consistency and scalability in real-world applications [46]. In this thesis, we address this gap by developing the thin-film CIP coating specifically designed for optical bacterial detection. This approach eliminates the complexity involved with microparticle handling while maintaining high specificity and sensitivity.

## 1.2 Research Opportunity and Thesis Objectives

Despite recent advances in CIP microfluidic biosensors for waterborne bacteria, several specific gaps remain unaddressed. First, no study to date has demonstrated multiplexed bacterial detection using a CIP-only platform – current CIP-based sensors are generally limited to a single target species per device [41]. Second, the integration of fluorescein (FITC)-labeled CIP thin films into microfluidic devices for direct fluorescence-based quantification of captured bacteria has not been reported; prior work has either employed CIP microparticles with fluorescent readouts in a microchannel [46] or used CIP thin films on bulk substrates with non-optical detection methods [47]. Third, most CIP sensor implementations rely on off-chip fabrication of the imprinted polymer (e.g., creating CIP coatings on separate particles or wires), which must then be incorporated into the microfluidic system [41] – a

practice that complicates device assembly and scalability for practical deployment. Finally, there is limited optimization of the template removal process for thin-film CIPs: ensuring that imprinted bacteria templates are fully removed to form clean recognition cavities is still challenging, and few studies have systematically addressed this step [41].

In light of these gaps, the present research is driven by the following questions: How can a CIP-based microfluidic sensor be designed to simultaneously detect multiple bacteria species on a single platform? Can integrating FITC-labeled CIP thin films into microfluidic channels enable sensitive, quantitative fluorescence detection of bound bacterial cells? What on-chip fabrication approaches can eliminate the need for off-chip CIP preparation to improve scalability? And how can the template-removal protocol for thin-film CIPs be optimized to ensure fully formed, specific binding sites? By answering these questions, this thesis aims to advance the development of a fluorescence-based CIP microfluidic sensor that addresses the above limitations.

This thesis addresses these gaps by proposing the development of a microfluidic device integrating thin-film CIPs designed for optical bacterial detection. This innovative approach simplifies the sensor design, enhancing its robustness and scalability while enabling the simultaneous detection of multiple bacterial strains, key for effective environmental monitoring. By focusing on a versatile, easily integrable sensor design that eliminates the need for complex biorecognition elements like aptamers, this work aims to produce an automated device capable of consistent performance in diverse conditions, thus broadening its practical applications beyond laboratory environments.

The goal of this thesis was to develop a fluorescence-based, duplex bacterial detection system using CIP-based microfluidic sensors. To achieve this, the research focused on optimizing the fabrication of CIP thin films for targeted bacterial capture, identifying the optimal concentration of fluorescent dyes

for enhanced detection sensitivity, and integrating these elements into a functional sensor capable of multiplex detection. The following objectives were pursued:

1. **Objective 1: Fabrication of CIP Thin Films** - Develop and optimize fluorescently responsive CIP thin films that can effectively capture target bacteria such as *Salmonella* and integrate these films into a microfluidic device.

2. **Objective 2: Sensor Integration and Singleplex Detection** - Integrate the developed CIP thin films into a microfluidic sensor and characterize its performance in detecting single bacterial species in water samples using fluorescence.

3. **Objective 3: Duplex Detection Enhancement** - Enhance the microfluidic sensor by integrating additional CIP thin films capable of detecting two types of bacterial strains simultaneously to examine the sensor's duplex detection capabilities.

## 1.3 Thesis Organization

The first chapter of the thesis provides a general introduction on the background of bacterial contamination of water, a brief discussion of available sensor technologies focusing on IP-based optical sensors, and identifies critical gaps in current CIP-microfluidic research. The gaps include sensors limited to detecting only one bacterial target, a lack of thin-film CIPs integrated directly into microfluidic channels for fluorescence-based detection, reliance on off-chip CIP fabrication, and insufficient optimization of template removal processes. This thesis addresses these issues by developing an on-chip, fabricated, duplex CIP microfluidic sensor utilizing FITC for enhanced fluorescence detection.

The second chapter begins with an overview of the conventional methods used for bacteria detection. It is followed by the detection of bacteria using natural bio-recognition elements like aptamers and antibodies, highlighting their limitations. The discussion then covers the synthetic bio-recognition elements, specifically imprinted polymers, and their application in bacterial detection, along with an overview of fabrication techniques. This is followed by a focus on fluorometric detection, its advantages, and the role of imprinted polymers in fluorometric bacterial detection. The chapter then further leads to microfluidic sensors combined with IPs for the detection of bacteria, identifying the unexplored gaps in the literature and positioning this thesis to address them.

The third chapter involves the fabrication and integration of thin-film CIPs into a microfluidic device, along with the optimization of the detection mechanism. It involves a detailed description of the device fabrication process, experimental methodologies, and procedural workflows in detail.

Chapter four discusses the results and findings concerning the first two research objectives. It contains an in-depth analysis of the CIP thin-film fabrication process, its optimization methodologies, and experiments conducted to identify the optimal fluorescence dye concentration. These experiments aimed to achieve a detectable fluorescence signal that decreases proportionally with lower bacterial concentrations, enabling clear differentiation across varying bacterial levels. Subsequently, the results of the experimental tests regarding the detection of single bacteria and the determination of sensor performance parameters are discussed.

The fifth chapter provides the results and discussion of expanding the microfluidic sensor to multiple CIP thin film detection zones and the experiments conducted for the detection of two bacterial strains simultaneously.

The sixth and last chapter summarizes the presented thesis findings, discusses the limitations of the work, and provides recommendations for future work.

## 1.4 Author's Contribution

This research integrates CIP thin films directly into microfluidic channels, eliminating off-chip polymer coating steps and improving device scalability, while demonstrating simultaneous FITC-based detection of both *Salmonella* and *E. coli* on a single chip. In addition, the bacterial template-removal process was systematically optimized to ensure well-defined cavities in the thin-film CIPs, thereby enhancing binding specificity.

This thesis is founded on research work in which I had a key role in concept development, design of experimentation, and data analysis. The contents of chapters 1 to 5 are directly influenced by the following publications and presentations, all of which were drafted by me and refined through the guidance of my supervisor, Prof. Pouya Rezai. Prof. Rezai contributed to the conceptual design and improvements in sensor designs, providing valuable feedback throughout my research, while Dr. Ali Doostmohammadi contributed to experimental methodology and manuscript editing.

### 1.4.1 Contributed Journal Papers:

- Mahmoud I., Doostmohammadi A., Rezai P., "Fluorometric Detection of Salmonella in Water Using a Cell Imprinted Polymer Thin Film-based Microfluidic Sensor," submitted to Lab on a Chip.

### 1.4.2 Contributed Conference Papers:

- Mahmoud I., Doostmohammadi A., Kraft G., Rezai P., "Fluorescent Detection of Bacteria Using Cell Imprinted Polymer (CIP) Thin Films Integrated into Microfluidics," MicroFIP 2023, Illinois, USA, June 18–21, 2023.
- Mahmoud I., Doostmohammadi A., Kraft G., Rezai P., "Fluorometric Detection of Salmonella in Water Using Cell Imprinted Polymer Thin Films Integrated into a Microfluidic Channel," MTAS 2023, Katowice, Poland, October 15–19, 2023.

# Chapter 2

## 2 Literature Review and Research Gaps

This chapter begins with an analysis of conventional methods for detecting bacteria in water samples, followed by a review of biosensors utilizing biorecognition elements such as antibodies and aptamers for bacterial detection. In the sections that follow, the state of the art of these biosensors and the problems they are facing are discussed. Then we examine the function of imprinted polymers designed to overcome the disadvantages of previous approaches. The literature review then transitions to fluorometric detection techniques, recognized for their precision and efficacy in bacterial identification. Then, the literature review focuses on IP-based microfluidic sensors as a solution to overcome previous limitations and enhance bacteria detection in different environments. The chapter concludes by identifying significant research gaps, establishing the rationales for the objectives addressed in this thesis.

### 2.1 Conventional Methods for Bacteria Detection

Traditional methods for detecting bacteria in water include culture-based methods as well as immunological and biochemical assays. All these techniques (As shown in Fig. 2-1) have different advantages and disadvantages, which make each one useful in various applications but also indicate that there is a need to improve the technology of detection.

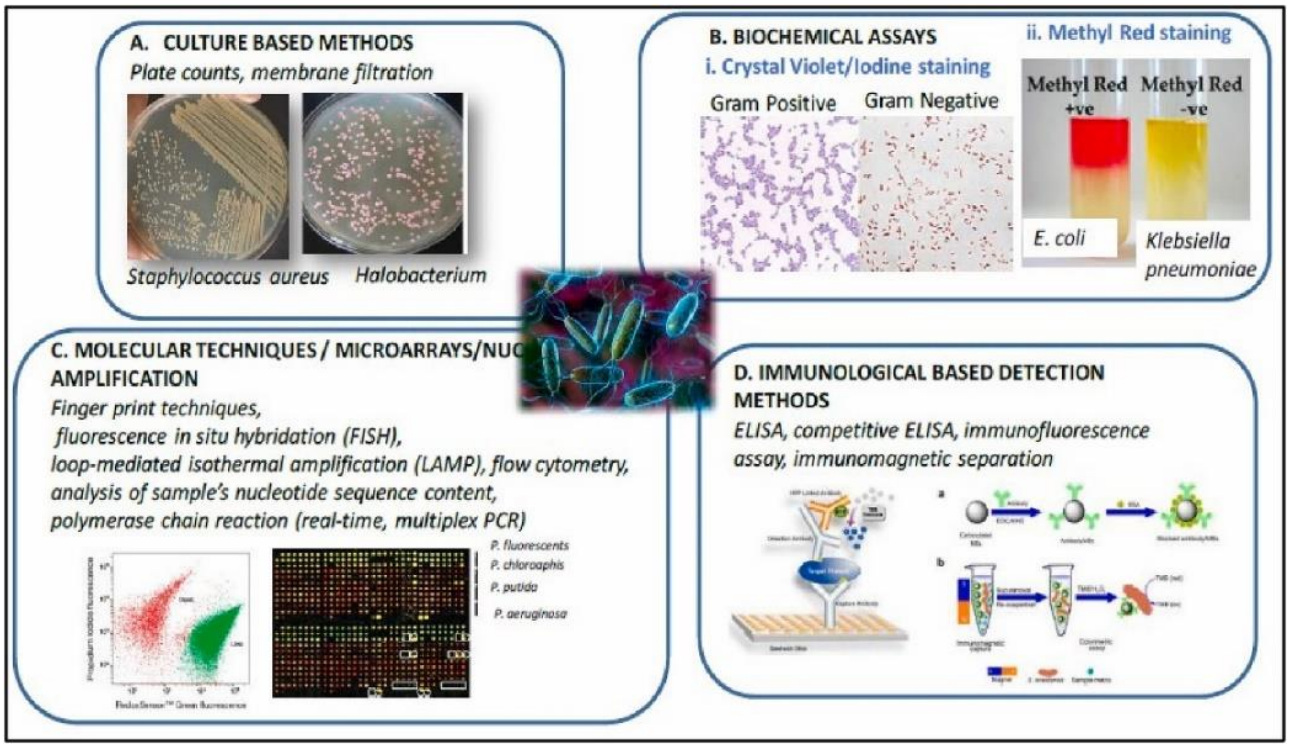


*Fig. 2-1. Conventional Methods for bacteria detection: (A) Culture-based methods like plate counting; (B) Distinguishing between bacterial strains using biochemical assays like staining; (C) Molecular; and (D) Immunological-based techniques. Reproduced with permission from Ref. (Amiri et al., 2018) [48] ,©2018 American Chemical Society*

### 2.1.1 Culture-Based Methods

Culture-based methods are techniques used to isolate and grow bacteria from environmental samples, including water. The methods begin with the application of a defined dilution of a water sample onto a designated growth medium, which enables bacteria cultivation. There are various approaches to utilizing individual culture media and incubation settings, ranging from simple to more complex formulations[49], [50]. Depending on the analysis, different media—either ready-to-use liquid broths (LB) or agar solidified with selective agents that promote coliform proliferation—are chosen. It is crucial to monitor parameters such as culture homogeneity, pH, gelling properties, and incubation temperature to ensure reliable results [51].

Although contemporary microbiological and molecular technologies have increased the sensitivity of bacterial detection, culture methods continue to be essential for the analysis of drinking water and wastewater. These methods allow not only for the detection of microorganisms and the assessment of

waste contamination but also for quantitative analyses of bacterial populations [52], [53], [54], [55]. Among the many advantages of culture-based approaches is their ability to provide detailed information about bacterial isolates, which is important in some types of bacterial studies. In cases where newer techniques or nanotechnological instruments fall short, culture-based methods serve as a critical reference. However, these methods are time-consuming, and some modern technologies may not facilitate the growth of specific bacteria [56].

Other culture-based techniques include the membrane filtration counting method, multiple enzyme colony counting method, most probable number method, culture-counting method, flour-particle tracking method, and Petroff-Hausser counting method [57], [58], [59]. Among these, the membrane filtration technique is considered suitable for its selectivity to specific bacteria and for estimating the number of culturable bacteria. This method protects cell viability while reducing bacterial stress responses caused by harsh filtering conditions. The following are the primary steps in this technique: 1) Sample collection, homogenization, and initial dilution; 2) Electrostatic absorption method of filtering bacteria; 3) Sample filtering and membrane culture; 4) Inoculation and incubation; and 5) Colony counting and determination of detection parameters [57]. A certain volume of the water sample is filtered through a membrane of suitable retention size. The captured cells are cultivated on a suitable nutrient medium and incubated until colonies become visible. After incubation, membranes are transferred onto nutrient plates for further incubation and enumeration of colonies. This filtration system permits analysis of known volumes of water by effectively concentrating bacteria from 100 mL to 1 L of water sample onto the surface of nutrient medium for the growth of individual colonies. The colonies reflect the original concentration of viable bacteria in the samples and are expressed as colony-forming units (CFU) per volume filtered [56],[57]. While both double-agar plating and membrane filtration are widely used culture techniques, membrane filtration is almost used in routine water

analysis. However, mastering these procedural techniques can require significant time and practice for laboratory technicians [57], [59], [60].

### 2.1.2 Biochemical Methods

Biochemical detection methods in microbiology include several methods that utilize the metabolic characteristics and other components of bacterial cells to classify and measure bacterial characteristics. These techniques are categorized into observational and functional biochemical assays. The observational methods start with Gram staining, an elementary method used to categorize bacteria into Gram-positive and Gram-negative based on cell wall composition. Different dye types that interact with the bacterial cell wall structure are utilized in the staining process to facilitate the identification of different bacterial species [61], [62], [63]. After this, the functional biochemical assays, or bioassays, take advantage of the fact that different bacteria have different enzymatic activities. Many of these methods consist of exposing bacteria to different substrates, monitoring the resulting reaction, and subsequently identifying and characterizing the bacteria based on their enzymatic and metabolic characteristics. Examples include the Catalase Test, which shows the presence of the catalase enzyme with bubble growth, and the Oxidase Test, which shows which bacteria can produce cytochrome c oxidase via a color change.[61], [62], [63]. Using antibodies to bind and detect specific bacterial antigens gives these tests the immunological specificity needed to identify particular organisms. Immunologically based assays, such as ELISA and lateral flow assays, target specific bacterial antigens and provide a detailed baseline of bacterial concentrations in water samples [55], [64]. These methods are advantageous for quickly identifying bacterial species and detecting both live and dead cells, with the latter indicating potential pathogenicity. They also provide deeper insights into bacterial metabolic functions and outperform traditional DNA-based analyses [65].

The sensitivity and applicability of the above types of biochemical assays may be restricted, especially in environmental water analysis, where sensitive detection of specific bacterial targets may require preconcentration procedures. This requirement underlines the issues and considerations of deploying biochemical detection approaches in complex matrices. In the following subsections, enzyme-substrate reactions and immunological detection mechanisms will be explored in depth.

#### 2.1.1.1 Enzyme-Substrate Reactions

Enzyme-substrate reactions are one specific category of biochemical methods used in the detection and identification of bacteria. This method relies on the selective and direct detection abilities provided by the different enzymatic functions of several bacterial species. The process initiates with the selection of substrates that are recognized by enzymes specific to the target bacteria. These substrates usually are synthetic and are elaborated to generate a detectable signal-colorimetric, fluorescence, or an electrochemical signal-upon interaction with the bacterial enzyme [65], [66]. The selected substrate interacts with a bacterial enzyme to result in a chemical transformation specific to the enzyme's action. This produces a signal measurable by different instruments depending on the signal type: spectrophotometers in the case of color, fluorometers in cases of fluorescence, and electrochemical sensors for electrical signals. The intensity of this signal is often directly proportional to the amount of enzyme present, hence allowing a quantitative analysis of bacterial concentrations. [65], [67]. These enzyme-substrate interactions target enzymes unique to particular bacterial species, hence showing selective and rapid results. Since only live bacteria can produce active enzymes, this approach separates live and non-viable cells [66], [68]. However, this technique also has a number of drawbacks. There is potential for false positives due to the presence of similar enzymes in non-target organisms, variability in enzyme expression among bacterial strains, and environmental factors that may affect enzyme activity [66], [68]. Recent advances in this area have been aimed at improving the specificity, sensitivity, and automation of such detection methods. Alpha-mannosidase, for example, is used in

industrial water testing to specifically target coliforms, but studies continue into other enzymes and substrates to extend the range of bacteria that can be detected with greater accuracy. It has been suggested that the addition of a dye, which changes color at pH 6.8, would enhance visual analysis, while developments in automation of plate classification and measurement improve the usability and efficiency of the techniques [66], [69], [70], [71].

#### 2.1.1.2 Immunological Detection Methods

The principle of immunological detection techniques is based on a specific antibody-antigen interaction. An antibody is a protein that is produced by the immune system and is specific for binding to a specific foreign substance, called an antigen. Antigens are generally proteins or other molecules present at the surface of a pathogen, including bacteria and viruses. Among the most popular immunological techniques used in food analysis, one can mention ELISA, Enzyme-Linked Fluorescence Assay (ELFA), or Immunomagnetic Separation (IMS) [72]. ELISA uses enzyme-linked antibodies to detect specific antigens. Once bound to the antigen, the enzyme produces a color change that may be detected and quantified. ELFA is similar to an ELISA, except that it employs fluorescent compounds rather than color-changing enzymes for quantifying antigens by measuring fluorescence intensity. IMS employs magnetic beads with specific antibodies to trap and concentrate target pathogens from a sample, where the captured pathogens are then capable of being detected by other methods [9], [10], [11], [72]. In food diagnostics, ELISA is one of the usual immuno-assay methods, while IMS is helpful for the isolation of harmful cells and their concentration, respectively. For simple food diagnostics, an immuno-chromatographic test strip (ICG) has been developed by coupling ELISA and IMS. It is for this reason that ELISA has been combined with immuno-magnetic beads labelled with fluorophores to increase sensitivity in the visual detection of bacteria. Other immunochromatographic techniques, such as lateral flow immunoassays, have enabled the target particle to visually appear when it migrates towards the immobilized antibodies [73]. Among other

technologies, ELISA provides a number of advantages in the form of high specificity, high sensitivity, good reproducibility, and simplicity, thus being particularly suited for large-scale epidemiological investigations. It is low-cost and can be used to replace microscopy and high-performance liquid chromatography techniques in the detection of specific microorganisms. ELISA has also been conducted along with western blotting in detecting viral proteins and in comparative immunological test kits used in detecting shellfish poisons [9], [10], [11]. While classic culture techniques are still useful because of their higher power of detection, the merging of alternative methodologies of detection, like immunological assays and electronic sensors, tends to yield consistent results. Immunoassay combined with other techniques has a good prospect for future applications too [9], [10], [11]. While these techniques have proven their validity concerning detection, their practice entails cumbersome tasks and has always been burdened by longer times of detection.

Conventional methods for detecting bacteria, such as culture-based methods or ELISA, have proven to be effective for bacterial detection. However, there is a growing need for technologies that enable rapid, on-site bacterial detection. This demand has driven the development of biosensors that provide fast, sensitive, and portable solutions for identifying bacterial pathogens. To provide highly specific and sensitive detection, these sensors utilize various biorecognition elements, including antibodies, aptamers, and antimicrobial peptides [74], [75]. We provide further information on these methods in the following section.

## 2.2 Biosensors for Bacteria Detection

The growing need for sensitive detection tools that enhance water quality monitoring and protect consumer safety drives much of the fast development in biosensor technology across many applications. Target bacterial identification in these biosensors depends on biorecognition elements [76], [77], [78]. As seen in Fig. 2-2, these components employ several detection systems: antigen-

antibody interactions, receptor-ligand binding, acid-base reactions, bacterial quorum sensing, and cell lysis techniques. The selection of precise biorecognition elements tailored to specific bacterial species is fundamental to effective water pollution management, particularly in environmental microbiology [79], [80], [81]. When integrated with transducers that increase signal amplification and improve selectivity, these features assist in the development of highly selective biosensors [82], [83].

Sensors are composed of two different units: a sensing unit, which in biosensors is the capturing agent (aptamers, imprinted polymers, etc.), and a transducer, which converts the physical signal into a readable signal. Transduction mechanisms include optical [84], fluorescence [85] electrical and electrochemical [86] methods. Fluorescence biosensors are claimed to be rapid, portable, and cost-effective in addition to being sensitive and specific [87]. The following sections will discuss biosensors capturing agents.

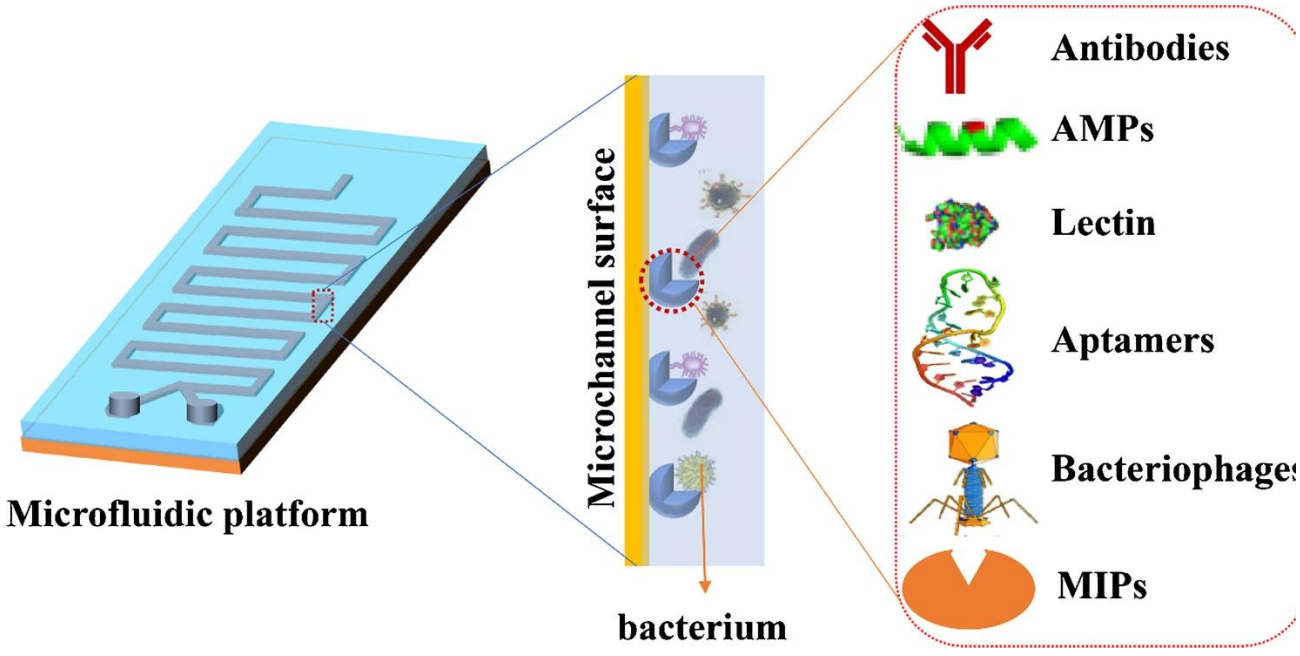


*Fig. 2-2. Types of bio-recognition components that are incorporated into microfluidic devices. Antibodies; AMP: Antimicrobial peptides; Lectin; Aptamers; Bacteriophage; MIP: Molecularly Imprinted Polymers. Reproduced with permission from Ref. (Fang Mi et al., 2022) [13] ,©2022 Analytical and Bioanalytical Chemistry.*

### 2.2.1Antibodies

Antibodies are glycoproteins that are made by white blood cells. They are very important for the immune system to be able to detect and neutralize threats like viruses and bacteria. They bind especially to certain molecular structures on the pathogen known as antigens [88]. Antibodies are effective in identifying pathogens in water since this binding is specific and shows great affinity for target antigens. The development of biosensor platforms depends on the basic process of antibody-antigen interaction. Antibodies on the transducer surface in biosensors help to convey biological selectivity from the molecular level to the bulk phase, therefore allowing the selective and sensitive detection of target analytes in complicated samples [88], [89]. This capability allows for the precise quantification of pathogens, which is essential for monitoring the microbiological quality of water. Additionally, the specific procedures that are used to produce antibodies improve their suitability as bio-recognition elements in biosensors. Antibodies and their modified counterparts offer the resilience needed for sensitive analytical systems, in addition to being selective [88], [90].

Antibodies are often used in bacterial detection, but they have both pros and cons. One main advantage is the high specificity of antibodies, as they only bind to the antigen that is being targeted [91]. Another aspect is that antibodies can be integrated into varied biosensing devices, such as optical and electrochemical sensors [92]. Techniques such as phage display allow us to produce the antibodies quickly and cost-effectively, while traditional methods such as ELISA offer reliable and well-verified detection processes [91], [93].

Despite this, antibody detection methods have several limitations. Some immunoassays have too low sensitivity to detect low levels of pathogens, and environmental factors (such as growth medium variability) can affect the expression of the antigen and produce false results [91]. Cross-reacting with

non-targeted antigens can complicate the interpretation even further, so the need arises to continuously improve and research new recognition elements [94].

Park et al. [95] developed a 3D microfluidic magnetic preconcentrator that could selectively isolate and enrich *E. coli O157:H7* in large sample volumes. The plastic-based device did not require any assembly, and antibody-conjugated Magnetic Nanoparticles (MNPs) were utilized for accomplishing the 700-fold preconcentration of *E. coli* in 100 mL samples within 1 hour. When integrated with an Adenosine Triphosphate (ATP) luminometer, the system was able to detect bacterial concentrations as low as 10 CFU/mL in blood and thus proved its potential to enhance detection sensitivity for large-volume pathogen screening.

### 2.2.2 Antimicrobial Peptides (AMPs)

AMPs have strong antibacterial activity primarily against Gram-negative pathogens and are less toxic to commensal bacteria, making them both odorless and non-cytotoxic [96], [97]. Lipopolysaccharides (LPS) are a unique and universal feature of the outer cell membrane of Gram-negative bacteria. AMPs bind different LPS, such as abraded, pungent, or short hydrophilic side chains, especially the negatively charged core polysaccharides of LPS present in Gram-negative bacteria. The interaction between AMPs and LPS often involves β-sheets, which are secondary structural elements in proteins and peptides. β-sheets are formed by extended polypeptide chains connected by hydrogen bonds to create a pleated sheet-like structure. These β-sheet structures are essential for the antimicrobial activity of AMPs in the context of bacterial membranes, as they facilitate their interaction. The LPS ends attach into the core polysaccharide region of these β-sheets to enable the AMPs to disrupt the bacterial membrane integrity [98], [99]. Therefore, AMPs exhibit electrostatic specificity and hydrophilic sidechain interactions with water-soluble components of the Gram-negative microbial cell membrane [91], [92]. AMPs are particularly effective against Gram-negative bacteria, rapidly identifying and

reacting to them. This quick response is crucial in complex water systems where many types of bacteria are present. AMPs neutralize bacteria primarily through three key actions. First, they create pores in bacterial cell membranes, compromising the bacteria's integrity. Second, they inhibit the synthesis of the cell wall or peptidoglycan, which is vital for bacterial survival. Lastly, they act directly on the bacterial membranes or interfere with essential enzymes within or outside the bacteria. These actions can lead to the leakage of essential ions and molecules from the bacteria, the separation of their DNA, and ultimately, damage to their cell membranes, which can cause the bacteria to die. This process is influenced by the type of bacteria, the nature of their cell walls, and the surrounding ionic conditions. The ability of AMPs to bind electrostatically to the bacteria's cell components is key to their effectiveness. These interactions are crucial for effectively targeting and neutralizing Gram-negative bacteria in water [96], [100].

AMPs are used in bacterial detection, showing both benefits and drawbacks. Among their strengths is the fact that AMPs can be designed for particular target bacteria, thus increasing the specificity of the detection [101]. Moreover, these peptides are broad-spectrum active against a wide range of pathogens, including antibiotic-resistant strains [102]. In addition, the high stability and susceptibility of AMPs to chemical modifications make them ideal for incorporation into optical biosensors that are both clinically and environmentally applicable [101].

However, AMPs have some drawbacks. Their manufacturing is costly, which restricts their practical use [103]. Many AMPs are unstable in real life because they have short half-lives. Furthermore, potential toxicity remains a problem that requires careful research before clinical use [102]. These constraints draw attention to the need for ongoing study on AMPs to maximize safer and efficient bacterial detection and treatment possibilities.

Thuy et al. [104] developed a microfluidic system that integrates a Recombinase Polymerase Amplification (RPA) sensor with the AMP Magainin I for detecting pathogenic bacteria in complex samples. This system allows for real-time, label-free DNA amplification and detection. It achieves detection limits as low as 5 CFU/mL for *Salmonella* and 10 CFU/mL for *Brucella*, all within 60 minutes. Notably, this platform offers a sensitivity that is 10 to 20 times greater than that of traditional nonselective PCR methods, marking a significant improvement in the ability to identify low levels of bacteria quickly and accurately.

### 2.2.3 Aptamers

Aptamers, which are single-stranded oligonucleotides (SSOs) with a length of 20–100 bases, can form a range of secondary and tertiary structures in their molecules. Aptamers have a sequence-specific affinity for various targets, from small ions to bacteria and cancer cells, and are used in a variety of fields such as drug delivery, disease diagnosis, environmental monitoring, and biosensor applications [100], [105]. The benefits of using aptamers as binding reagents include their long-term stability under different storage and environmental conditions. SSO sequences can also be chemically synthesized through simple benchtop methods, and their chemistry can be adjusted with a range of additives such as fluorophores and immobilization agents to aid orientation on surfaces [90], [106]. Since many different aptamers have been introduced to bind to various cellular structures of bacteria and different immune cells, aptamers are used in the water industry to detect many different bacterial pathogens. Because of their tunable sensitivity, immobilization, and high selectivity to bacterial cells in water samples, as a sensitive material, their adoption in biosensor platforms is increasing [13], [107]. To develop an aptamer, an in vitro screening and production method called Systematic Evolution of Ligands by Exponential enrichment (SELEX) is used. This method employs iterative rounds of binding agents and washing and desorption steps to determine the greatest binding affinity and specificity of an aptamer population towards the target. Using substrate-bound targets, a wide range of different non-

specific or even similar targets can be used to select aptamers that can capture a specific high-surface structure on the target surface, such as unique proteins on different cell surfaces [108].

Aptamers present several advantages for bacteria detection. They can be designed to achieve high affinity and specificity, which improves the accuracy of detecting target bacterium strains [109]. Their natural adaptability allows them to be integrated into several detection systems, including electrochemical and optical biosensors [110].

On the other hand, aptamers have certain limitations. Matrices in complex samples could affect their sensitivity [111]. The process of selecting the appropriate aptamer targets is time-consuming. Furthermore, under particular circumstances, some fluorescence detection techniques relying on aptamer conjugates could perform poorly [111]. All considered, these limitations draw attention to the requirement for aptamers for further development to increase their applicability in actual bacterial detection.

Jiang et al. [112] proposed a fluorescence-based microfluidic platform for the detection of *E. coli* O157. PDMS microchannels were modified with DNA aptamers immobilized on poly(amidoamine) dendrimers. This platform employed RCA to amplify the detection signal 50-fold and reached a low detection limit of $10^2$ CFU/mL. For that, multiple binding sites were introduced with dendrimer modification, enhancing the aptamer capture efficiency. Later, Jiang's group developed a dual-RCA method using both capture RCA (cRCA), enhancing bacterial capture, and signal RCA (sRCA) for signal amplification. This approach resulted in a 250-fold increase in the detection signal, with a detection limit of 80 cells/mL in food matrices, hence proving very promising for the rapid and sensitive detection of foodborne bacteria [112]. Integration of aptamers into a test system was further pursued by Wang et al. [113], where a microfluidic chip was used for the simultaneous testing of several bacteria. The chip's nitrocellulose membrane was coated with SELEX-screened biotinylated

aptamers, which underwent chromogenic reactions with tetramethylbenzidine-streptavidin for visualization. This system achieved multiplex detection of three bacterial targets within 35 minutes, thus aptamer-based test systems have great potential in doing fast, specific, portable pathogen detection in practical use [113].

### 2.2.4 Carbohydrate-Binding Proteins (CBP)

CBPs detect specific bacteria by utilizing a complex molecular recognition process. These proteins have specialized binding sites that are similar in shape and chemical properties to specific carbohydrate structures present on bacterial cell surfaces. A CBP produces non-covalent interactions, including hydrogen bonds, van der Waals forces, and hydrophobic interactions, when it encounters its target carbohydrate [114]. The structure and composition of the target carbohydrate in addition to the arrangement of amino acids in the binding site of CBP, define the binding specificity. Some CBPs undergo conformational changes upon binding, a property that can be exploited for signal generation in biosensing applications [115].

Commonly used two main kinds of CBPs in bacterial detection are lectins and carbohydrate-binding modules (CBMs). Lectins bind reversibly to mono- or oligosaccharides and often require metal ions, such as $Ca^{2+}$ to properly fold carbohydrate [116]. They can precipitate glyconjugates or aggregate cells. However, CBMs can operate on their own but normally form part of bigger enzymes. By placing the parent enzyme into proximity with its substrate, they increase its catalytic efficiency and can be built for enhanced specificity or affinity [117].

CBPs provide the bio-recognition element in bacterial detection biosensors. The procedure starts with CBP immobilization on a sensor surface— gold nanoparticles, graphene sheets, or microfluidic channels [118], [119], [120]. The surface carbohydrates of the target bacterium bind to the immobilized CBPs if a sample containing bacteria is presented to the sensor. After that, this binding event is

transduced into an observable signal with either optical (such as fluorescence or colorimetric), electrochemical, or piezoelectric nature. Sometimes further actions are taken to boost the signal, hence enhancing sensitivity. At last, the signal is quantified and detected through a correlation with bacterial concentration[119].

CBPs provide several benefits and some drawbacks. The great specificity of CBPs is one major benefit since it allows exact identification of bacteria depending on distinctive carbohydrate signals on their surfaces, therefore reducing false positives. They are also flexible, helping to identify a broad spectrum of bacterial species, and provide quick, label-free detection, therefore streamlining the testing procedure and lowering the expenses. Furthermore, CBPs fit portable, on-site testing in many environments since they may be included in small devices [121], [122]. However, CBPs also have limitations. Their binding affinity is generally weaker than that of antibody-antigen interactions, which can decrease sensitivity. The limited availability of well-defined carbohydrate scaffolds presents a challenge in the development of CBPs that are specific to bacterial targets. Additionally, the complexity of samples may result in false positives due to cross-reactivity, which is occasionally caused by the diversity of carbohydrate structures [123], [124], [125].

Cooper et al. [126] developed a microfluidic device that was integrated with MBL, coated on magnetic beads, for the detection of pathogens. Such a device could detect *Candida albicans* fungus in human blood within 3 hours at a concentration of 1 cell/mL and could capture *Staphylococcus aureus* from plasma and blood, with a limit of detection of $10^2$ CFU/mL. In this case, the use of MBL underscored its efficacy in binding to terminal mannose and fucose residues on a wide range of pathogens.

### 2.2.5 Imprinted Polymers (IPs)

IPs serve as synthetic recognition components tailored to match specific biomarker targets. The fabrication of IPs involves creating a negative imprint of a target molecule or cell (template) within the

polymer matrix. Polymerization of monomers around the template molecule or cell, followed by its removal, yields a cavity that mirrors both the form and chemical properties of the target molecule.

Fig. 2-3 shows the fabrication procedure of IPs. IPs can be fabricated using various strategies [33], with two main techniques being bulk imprinting and surface imprinting [31], [34]. In bulk imprinting, the template molecules are spread out across the whole polymer matrix. This makes recognition sites distributed across the whole bulk material. Although this approach may suffer from slower mass transfer and less accessibility, it often generates more binding sites [127]. Surface imprinting creates recognition sites mostly on the surface of the material. It has benefits like making binding sites easier to reach, speeding up the binding process, and making it easier to remove the template. Several techniques, such as soft lithography, self-assembled monolayers (SAMs), core-shell particle preparation, and mini-emulsion polymerization, can be used to achieve this goal. Soft lithography uses elastomeric stamps or molds to make patterned surfaces that are very accurate down to the molecular level. This method works well for printing larger biomolecules or whole cells [35], [36]. SAMs provide a versatile platform for creating highly ordered molecular arrangements as templates [128]. The preparation of core-shell particles includes the imprinting of target molecules onto the surface of core particles, which leads to a high surface area and excellent dispersibility [129], [130]. Mini-emulsion polymerization makes it possible to print nanoparticles with precise size and surface qualities, which works especially well for materials that can dissolve in water [131], [132].

IPs are gaining popularity in the field of biosensor development as a result of their significant advantages. IPs are made from inexpensive materials via basic synthesis techniques, which makes them affordable and provides a cost-effective substitute for conventional biological recognition elements. They are designed to recognize a diverse array of target molecules, including small organics, large biomolecules, and even entire cells. IPs also exhibit thermal and chemical stability by retaining their

activity in organic solvents, at high temperatures, and at various pH values. Other advantages of IPs are that they have a long shelf life, unlike biological reagents like antibodies and enzymes.[38].

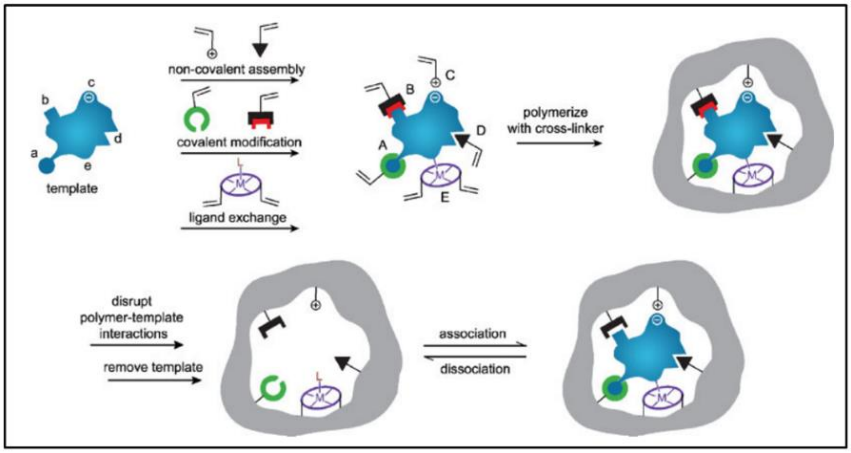


*Fig. 2-3. Molecularly Imprinted Polymers (MIPs) synthesis: Imprinting template into polymer matrix to create a negative imprint for a target molecule. Reproduced with permission from Ref. (Alexander et al., 2006) [133],© Wiley*

An electrochemiluminescence (ECL)-based biosensor (Fig. 2-4a) using nitrogen-doped graphene quantum dots (N-GQDs) and a polydopamine (PDA) imprinted polymer was produced in one study for the detection of *E. coli* in a water sample [134]. Through the combination of N-GQDs with polyclonal antibodies (pAb), this biosensor achieved selective detection, resulting in an enhanced ECL signal in the presence of potassium persulfate ($K_2S_2O_8$). This biosensor's LOD was determined to be 8 CFU/mL [134]. In another study, a micro-contact imprinting technique was employed to fabricate a bacterial sensor. Synthetic receptors for *E. coli* were generated by partially polymerizing monomers and then imprinted onto solid substrates utilizing PDMS bacterial stamps. The resulting functionalized polyurethane films were utilized as the sensor platform, demonstrating the capability to detect bacteria within the range of $10^2$-$10^6$ CFU/mL [135]. A bacteria-based sensor employing molecular imprinting was developed to detect *E. coli* by utilizing surface plasmon resonance (SPR) on a modified gold surface (Fig. 2-4b). Complete cells were imprinted on mass-sensitive and optical devices via micro-contact imprinting. The sensor employed an amino acid-based recognition element and demonstrated

rapid response times and recognition comparable to natural antibodies. Despite this, the detection limits for QCM and SPR were rather high, at $3.72\times10^6$ CFU/mL and $1.54\times10^6$ CFU/mL, respectively [136]. For the detection of *E. coli*, an additional extremely sensitive and selective microcontact imprinted capacitive biosensor was developed (Fig. 2-4d). This biosensor used UV polymerization to create microcontact-*E. coli* imprinted gold electrodes by incorporating unique crosslinkers, monomers, and an amino acid-based recognition element. The sensor achieved real-time detection with a detection limit of 70 CFU/mL and demonstrated outstanding selectivity across a wide range of bacterial concentrations. In addition, the biosensor showed remarkable performance in detecting *E. coli* in river water, with a high recovery rate ranging from 81% to 97% [37].

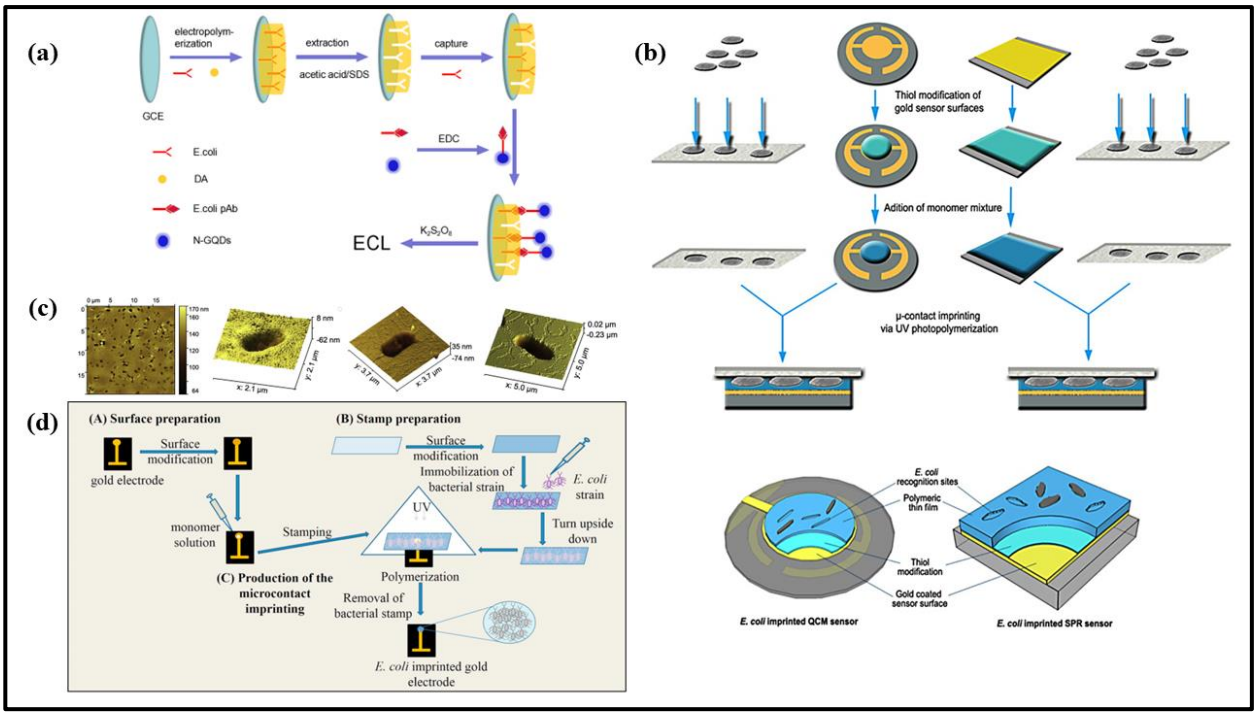


*Fig. 2-4.: E. coli detection using MIP; (a) Development process of MIP based biosensor utilizing electrochemiluminescence (ECL) for E. coli (reproduced with permission from Ref. (Chen et al., 2017), ©2017 American Chemical Society) [134]; (b) Microcontact imprinted SPR surface for the sensor (reproduced with permission from Ref. (Yilmaz et al., 2015), ©2014 Elsevier) [135]; (c) AFM image of the surface area of receptor chip of SIP showing cavities formed (reproduced with permission from Ref. (Cornelis et al., 2019 ), ©2019 Elsevier) [136]; (d) microcontact imprinting of E. coli on polymer surface (reproduced with permission from Ref. (Idil et al., 2017), © 2016 Elsevier).[37] [137]*

The same concepts of molecular imprinting are utilized in whole cell imprinting, such as bacteria, as pursued in this thesis. These imprints are called CIPs. This approach has demonstrated great potential in the detection of bacteria and viruses. Golabi et al [138] developed a CIP bacterial sensor with boronic acid groups. This CIP allows for both the specific capture of target bacteria and their easy release for reuse of the sensor. The sensor successfully detected *Staphylococcus epidermidis* bacteria within a concentration range of $10^3$ to $10^7$ CFU/mL. It also demonstrated good selectivity, differentiating the target bacteria from similar non-target bacteria [138]. Also, Shan et al [139] created a high-speed method for detecting *E. coli* bacteria using a 96-well microplate coated with CIP. This microplate could capture target *E. coli* cells specifically within 30 minutes, differentiating them from other bacteria in a mixture. Sarkhosh et al [140] explored cell-imprinting as a method for *C. parvum* detection in water. Although they exhibited lower affinity than highly specific antibodies, cell-imprinted PDMS surfaces, fabricated via modified stamping, demonstrated comparable binding capacity to standard antibodies, suggesting promise for developing faster and more cost-effective waterborne pathogen detection devices.

In summary, Various biorecognition elements such as antibodies, AMPs, aptamers, and CBPs were investigated to detect bacteria. They have many advantages, including high accuracy and versatility, but are also limited by factors such as sensitivity constraints, high cost of production, and matrix interferences that can compromise detection accuracy. CIPs, however, form artificial binding sites in harsh conditions with higher accuracy and affinity. It has been demonstrated in various studies that CIP-based sensors are capable of capturing whole bacterial cells. The following section discusses imprinted polymer-based sensors' design, development, and application to rapidly detect waterborne pathogens in the field. Among the transduction mechanisms used with biosensors for detection, fluorescence offers particular advantages in sensitivity and rapid detection [87]. Therefore, the next section will review biosensors using imprinted polymers and fluorescence detection.

### 2.2.6 Fluorometric Detection Using Imprinted Polymers

Fluorescence is a photophysical process where molecules absorb photons and cause the excitation of electrons from the ground state to a higher energy singlet state. When the electrons go back to the ground state, the molecule releases a photon with lower energy (corresponding to a longer wavelength). The efficiency of the emission process is measured by the quantum yield, representing the ratio of photons emitted to photons absorbed [141], [142].

For fluorescence-based sensing, important characteristics of fluorophores, including high quantum yield and photostability, are responsible for ensuring stable and reproducible signals over repeated detection cycles. For the detection of bacteria, FITC is especially suitable. FITC couples the stable aromatic backbone of fluorescein, which has a reputation for bright and stable fluorescence, with an isothiocyanate group [143], [144]. The latter is a reactive group that allows FITC to form a covalent bond with biological targets, for example, bacterial surface proteins, and hence constitutes a photobleaching-resistant labeling approach [145].

Fluorescence detection has thus become a sensitive, rapid, and popular analytical method across many fields due to its high sensitivity, broad dynamic range, and non-destructive nature. The advantages of using a fluorescence detection mechanism over the traditional detection methods are often significant. These are mainly advantages from the fact that the fluorescence signal can have enhanced sensitivity and exhibit a wide dynamic range for both small and large analyte concentrations [146], [147]. Additionally, the fluorescence signal can be internally corrected to remove inner-filter effects and any mechanical variations inherent to the measurement system. It can be accomplished on the basis of quantum yield, lifetime, polarization, and frequency of fluorescence. The non-destructive capability of many fluorescence-based analytical and monitoring tools is advantageous and allows for real-time

measurements of dynamic systems, especially of phenomena in biology and microbiology under physiological conditions, including cellular and subcellular studies [145], [146].

Several research groups have developed fluorescence-based MIP sensors for bacteria detection. Guo et al. [150] proposed a bacteria detection method targeting *S. aureus* based on bacteria-imprinting of PDMS combined with a fluorescence resonance energy transfer (FRET) platform. In fabricating the film, specific imprint cavities were formed on PDMS by a stamp-imprinting method using *S. aureus* as a template and modified with 1H,1H,2H,2H-perfluorooctyltriethoxysilane (POTS). This modification enhanced bacterial capture, wherein the imprinted sites were specific to the target bacterium in terms of size and surface features. This detection is based on a FRET mechanism where fluorescent donors are citrate-functional copper nanoclusters (CuNCs) and the acceptors are dopamine-stabilized gold nanoparticles. The negatively charged surface of the modified PDMS film displaced the CuNCs when *S. aureus* bonded to it, causing a fluorescence recovery proportionate to the bacterial concentration. This resulted in a 135-minute detection time with a dynamic range of 10 to $10^7$ CFU/mL and a detection limit of 11.12 CFU/mL. Furthermore, the test demonstrated reliability, with spiked sample recoveries ranging from 97.7% to 101.9% and relative standard deviations smaller than 10% [150].

Similarly, Zhao et al. [151] developed a fluorescence-based MIP for detecting *Listeria monocytogenes* using Pickering emulsion polymerization. The production technique involved creating MIP microspheres with embedded water-soluble CdTe quantum dots as fluorescent identifiers. For the selective recognition, the researchers combined *L. Monoctogenes* with acryloyl-functionalized chitosan coupled to the QDs, serving as the aqueous phase in an oil-in-water emulsion stabilized by solid particles. This arrangement created specific cavity formation on the polymer surface, shaped according to the shape and surface properties of the bacterial template. After the bacteria had been removed, these

cavities acted as highly specific binding sites, selectively capturing *L. monocytogenes* in food samples. The detection mechanism is based on fluorescence quenching upon bacterial binding. Attachment of the *L. monocytogenes* to the imprinted sites changes the fluorescence intensity of the QDs, which may enable qualitative visualization of bacterial presence in real time. This sensor detected *L. monocytogenes* effectively in milk and pork samples with a limit of detection as low as $10^3$ CFU/mL. Moreover, the adsorption capacity of MIP was higher than that of NIP, which confirmed that MIP had enhanced selectivity and binding affinity to the target bacteria [151].

Bezdekova et al. [152] developed magnetic MIPs for the selective detection and isolation of *S. aureus*, using dopamine as a functional monomer. The fabrication involved an imprinted layer on the surface of magnetic particles that easily allowed separation by means of an external magnetic field. Dopamine gets through oxidative polymerization in an alkaline environment, forming a stable poly-dopamine coating on magnetic particles. It was fabricated to detect and selectively bind *S. aureus*. The MIPs were tested on samples of milk and rice. *S. aureus* was detected at as low as $10^3$ CFU/mL concentrations, also complying with the European Union standards for food microbial safety. It showed a high degree of selectivity; MIPs bound to *S. aureus* specifically when Enterococcus faecalis was present as a non-target. The fluorescence signal, which indicated bacterial binding, reached equilibrium after 10 min and showed high sensitivity [152] .

Doostmohammadi et al. [40] reported core-shell microparticles that encapsulated MIP shells for the selective detection and capture of *E. coli OP50*. The fabrication procedure involved the two-step process of polymerization on polystyrene microparticles, enabling precision control of the thickness of the MIP shell between 0.25-3.5 μm. During synthesis, the bacterial template was encapsulated within the shell of MIP, which was removed afterwards to develop cavities tuned to the shape and size of the bacteria. The tailor-made cavities for the selective recognition of bacteria produced selective binding

sites that enhance detection accuracy. It was observed that the MIP microparticles showed higher capture efficiency for *E. coli*. The bacterial uptake ratio reached a maximum of about 74% when $10^3$ MIP-MPs were utilized per milliliter. In contrast, the nonimprinted particles had a much lower binding efficiency, highlighting the high specificity of the MIP-MPs. This study highlighted the possibility of low-cost and very effective biosensors through the MIP fabrication approach developed for various applications, from environmental monitoring to food safety [40].

Zhang et al. [153] developed a photocatalytic organic semiconductor-bacteria imprinted polymer (OBBIPs-PEC) sensor for detecting *S. aureus* at the single-cell level. The detection was based on the inclusion of photocatalytic organic semiconductors, i.e., poly(fluorene-co-phenylene) organic semiconductor (PFP-OC) combined with 2-(4-mesyl-2-nitrobenzoyl)-1,3-cyclohexanedione (MNC), to form heterojunctions. The composites electrostatically interact with the bacterial cell membrane, promoting electron transportation and causing photoelectrochemical (PEC) response upon binding to bacteria. Under irradiation, the excited electrons from the semiconductors are transferred to the captured *S. aureus*, and then followed by reduction of the electron acceptors of NAD+ and FAD+ to NADH and $FADH_2$. The "turn-on" mode sensor achieved an impressive detection limit as low as 10 CFU/mL with selectivity towards other bacteria and stability in complex samples, representing a significant advance over traditional fluorescence detection strategies for food safety and environmental monitoring applications [153].

Lakimova et al. [154] proposed a new approach for the fabrication of surface-imprinted polymers (SIPs) using commercially available 3D printing resin. Polymers were synthesized through spin coating of Clear Resin and subsequent PDMS stamp imprinting with immobilized bacterial templates, which are GFP-expressing *E. coli*. Following imprint formation, cavities with precise complementarity for the size and shape of bacteria allowed selective rebinding, measured by fluorescence microscopy. The

optimized SIPs were highly specific, with non-specific rebinding of bacteria averaging only 7.61% of the signal for specific binding and rebinding target bacteria at concentration levels as low as $5 \times 10^5$ CFU/mL. This new method reduced fabrication time and manual procedures, eliminating the disadvantages of traditional imprinting processes and having the potential for constructing cost-effective and reliable biosensing platforms for environmental monitoring and biotechnology industries [154].

Aside from the detection of bacteria, fluorescent MIP sensors were also used broadly for chemical analytes whose applications are related to bacterial detection. Zhang et al.[155] proposed a hand-held paper-based quantum-dot-MIP sensor to detect herbicide (2,4-D) via fluorescence quenching with a sensitivity of 0.12 µM. Zhang et al. [156] also prepared a microfluidic paper-based FRET sensor for detecting 2,4-dichlorophenoxyacetic acid (2,4-D), in which there is high sensitivity for visual detection at 90 nM. Yang et al. [157] presented microplate-based fluorescent-quenching MIP analysis with CdSe/ZnS quantum dots having a LOD of 2.1 µg/L for the quantification of the pesticide dimethoate. Amjadi et al. [158] utilized a dual-emission, ratio-metric fluorescence-based MIP sensor for the quantification of fungicide diniconazole and demonstrated reusability as well as stability with an LOD of 6.4 µg/L.

Table 2-1 below summarizes the key characteristics of the papers reviewed above.

**Table 2-1. Several fluorescence-based imprinted polymer biosensors to detect various analytes**

| Target analyte | Sensing mechanism | LOD | Ref |
|---|---|---|---|
| ***S. aureus*** | FRET (CuNCs/AuNPs) | 11.12 CFU/mL | [150] |
| ***Listeria monocytogenes*** | Quantum dots (Fluorescence Quenching) | $10^3$ CFU/mL | [151] |
| ***S. aureus*** | Fluorescence quenching | $10^3$ CFU/mL | [152] |
| ***E. coli OP50*** | Fluorescence quenching | NA | [40] |

| | | | |
|---|---|---|---|
| ***S. aureus*** | Photoelectrochemical fluorescence (PEC) | 10 CFU/mL | [153] |
| ***E. coli*** | Fluorescence microscopy (GFP - E. coli) | $5 \times 10^5$ CFU/mL | [154] |
| **2,4-D (Herbicide)** | Quantum Dots (Fluorescence Quenching) | 0.12 µM | [155] |
| **2,4-D (Herbicide)** | FRET (NBD/CdTe QDs) | 90 nM | [156] |
| **Dimethoate (Pesticide)** | Fluorescence quenching | 2.1 µg/L | [157] |
| **Diniconazole (Pesticide)** | (CDs/QDs) | 6.4 µg/L | [158] |

Despite recent advances in fluorescent imprinted polymers-based sensors for bacterial detection, some challenges remain. Current sensors show detection limits no lower than $10^3$ – $10^5$ CFU/mL for pathogens such as *Listeria monocytogenes* and *S. aureus*, limiting their utility for early warning and trace-level detection. Detection times can exceed two hours, which is inadequate for rapid, point-of-care diagnostics or real-time monitoring. Furthermore, most reported systems are limited to single-analyte detection, lacking the multiplexing capability needed for comprehensive pathogen screening in complex samples. Fabrication methods are frequently labor-intensive and require specialized equipment, hindering scalability and routine deployment. Integrating imprinted polymers within microfluidic channels can address these challenges by reducing reagent and sample requirements, speeding up target binding, and enabling multiple-target assays on the same chip. The next section reviews recent efforts to integrate imprinted polymers into microfluidic platforms for bacterial detection.

## 2.3 Imprinted Polymer-Based Microfluidic Sensors for Bacteria Detection

Recently, microfluidics technology has become an efficient method for detection applications due to its features of portability, compact design, automation, multiple sample processing, reduced exposure to toxic materials, and finally, cost-effectiveness [159], [160], [161]. Compared with other technologies, one major advantage of microfluidics is the ability to establish a controlled

microenvironment that allows it to precisely manipulate the fluid flow through microchannels, hence increasing the sensitivity in a detection process [14]. In addition, the entire analysis process, including sample preparation, chemical reactions, separation, and detection, is integrated into microfluidic devices, making them particularly well-suited for use in field testing[160]. The integration of microfluidic technology with imprinted polymer-based sensors provides many advantages for bacterial detection, such as enhanced sensitivity, selectivity, portability, and the potential for rapid integrated analysis.

For instance, Akhtarian et al.[41], developed a microfluidic sensor that used CIP coatings on microwires for the conductometric detection of *E. coli* in water. They fabricated coated stainless steel microwires with a CIP layer imprinted with *E. coli* as a template. This formed the selective cavities that captured the bacteria due to their shape and surface characteristics. These wires were then embedded in a PDMS microchannel and allowed a straightforward setup to measure interwire electrical resistance as a function of bacterial binding. In practical testing, the sensor was specific for *E. coli* over other bacterial strains, such as *Listeria* and *Sarcina*, verifying selectivity. It showed a dynamic range of detection from $10^4$ to $10^7$ CFU/mL. The LOD was $2.1 \times 10^5$ CFU/mL with a LOQ of $7.3 \times 10^5$ CFU/mL. Sensitivity was given as 7.35 µS per CFU/mL in the linear range.

Doostmohammadi et al. [45] developed a microfluidic-based sensor that utilized CIP-coated microparticles for the fluorescent detection of *E. coli* in water. In this instance, the synthesis of CIP microparticles was accomplished by a two-step polymerization process using magnetic polystyrene particles to create surface cavities and selectively capture *E. coli* cells. These CIP particles were then incorporated into a magnetophoretic microfluidic device using ferromagnetic structures to capture the particles in a controlled flow environment and enhance interaction between the bacterial cells and the imprinted sites. Detection was performed by fluorescence intensity measurements, which decreased as

the *E. coli* cells bound to the imprinted cavities, yielding a dose-response relationship. In this paper, the sensor showed a LOD of $4 \times 10^2$ CFU/mL and LOQ of $3 \times 10^3$ CFU/mL in a dynamic range from $10^2$ to $10^7$ CFU/mL. The sensor could also provide specificity for *E. coli* against nontarget bacteria such as *Sarcina*, thus providing the potential for sensitive and specific detection in environmental monitoring.

Also, Yin et al.[42] developed a smartphone-based fluorescence sensor that simultaneously detected multiple pathogenic bacteria, namely *S. aureus, E. coli, and P. aeruginosa*, through the use of magnetic core-shell MIPs combined with aggregation-induced emission (AIE)-based fluorescent probes linked to specific aptamers. The magnetic MIPs enabled the targeted separation of the bacteria under magnetic fields, while the fluorescent probes linked with the aptamers generated specific fluorescent signals that were quantified via smartphone imaging. The system achieved a detection limit of around $10^2$ CFU/mL within 40 minutes, hence proving itself for rapid, portable, and multiplex detection. However, the performance of the sensor relies on the use of aptamers, which, despite the high selectivity they provide, are not free from certain drawbacks, such as susceptibility to degradation under harsh environmental conditions and variability in binding affinity because of their structural instability. In addition, the smartphone-based imaging method may have variability in different ambient light conditions, which could affect accuracy and reproducibility, especially in environments outside laboratory settings.

Apart from bacteria detection, Khan et al. [162] created a multichannel microfluidic sensor for the detection of the H1N1 influenza virus using virus-imprinted polymers (VIP). The sensor uses conducting virus-imprinted polymers synthesized through electropolymerization of 2-amino-1,3,4-thiadiazole monomers onto gold electrodes. After template extraction, cavities were formed with the shape and size of the H1N1 virus. The sensor displayed a linear detection range from 50 to $5 \times 10^6$ $TCID_{50}$/mL, with a low detection limit of 9 $TCID_{50}$/mL and allowing a fast detection time of only 2

minutes. The extensive validation conducted using a range of swine clinical samples validated its selectivity towards non-specific pathogens and revealed its potential for multiple uses through simple regeneration using acetic acid washing. However, the limitations include the potential for poor extraction of integrated viral templates and difficulties in distinguishing between related viral subtypes, thereby demanding more research in improving scalability and differentiation efficacy.

## 2.4 Research Gaps

Despite the significant progress of bacterial sensors, key limitations remain in terms of their robustness, specifically their ability to maintain stable performance under varying environmental conditions such as temperature, ionic strength, and flow rates, as well as their versatility, which refers to their ability to detect multiple bacterial species simultaneously across diverse water matrices. Most of the current microfluidic sensors integrated with CIPs for bacteria detection in the current literature have been fabricated to target *E. coli*. However, practical water quality monitoring typically involves simultaneous detection of multiple bacterial species, which single-target sensors inadequately address. Although several microfluidic platforms have recently demonstrated multiplex bacterial detection[163], [164], [165], [166], [167], these studies typically relied on additional biorecognition elements such as antibodies or aptamers, instead of depending on CIPs only to perform the selective identification of bacteria. For instance, Yin et al. [42] reported multiplex bacterial detection using aptamer-linked fluorescent probes, with magnetic MIPs merely to isolate bacteria rather than directly detect them. This dependence on biological elements increases cost, reduces sensor stability, and complicates device fabrication and operation. Thus, the direct utilization of CIPs alone, without other biological recognition components, to detect several species of bacteria simultaneously has not been thoroughly explored.

Although FITC is a widely used fluorescent label in bioassays, to our knowledge, its integration with thin-film CIPs for on-chip bacterial detection has not been explored. No published studies have demonstrated using FITC-labeled CIPs to enable simple, sensitive, and real-time fluorescence-based readout of bacterial binding events within a microfluidic sensor. This represents a significant opportunity to simplify detection and improve sensitivity by leveraging FITC's well-characterized fluorescence properties.

The CIP-based biosensing approaches that have been used so far, such as those illustrated by Doostmohammadi et al. and Akhtarian et al. [41], [45], rely on external fabrication of CIP coatings on microwires or microparticles, followed by integration into microfluidic devices. These multi-step processes complicate device assembly, reduce reproducibility, and hinder scalability for commercial use. There is a need for a fabrication method that allows direct integration of CIP into microfluidic sensors. To address these gaps, we embedded thin-film CIPs directly into the microfluidic channels, eliminating the need for external polymer coatings, and demonstrated simultaneous detection of *Salmonella* and *E. coli* via FITC fluorescence, providing a practical method for monitoring multiple bacteria in water samples.

# Chapter 3

# 3. Materials and Methods

## 3.1 Materials

All chemicals used for the fabrication of CIPs, including acrylamide (AAM), methacrylic acid (MAA), methylmethacrylate (MMA), N-vinylpyrrolidone (VP), ethylene glycol dimethacrylate (EDGMA), 2,2-Dimethoxy-2-phenylacetophenone (DMPA), dimethyl sulfoxide (DMSO), FITC, acetonitrile, methanol, and acetic acid, were purchased from Sigma-Aldrich, USA.

Materials required for the fabrication of the microfluidic sensor, including polyethylene terephthalate (PET) and pressure-sensitive adhesive (PSA) double-sided tape, were sourced from Adhesives Research, Inc., USA.

The *Salmonella* bacterial strain, utilized as the template and target microorganism for CIP synthesis, was provided by Prof. Lawrence Goodridge from the Department of Food Science at the University of Guelph, Canada. Similarly, heat-killed *E. coli O157:H7* strain was obtained from SeraCare, USA. Additionally, the *Sarcina lutea* (155420) strain, used for specificity evaluation, was acquired from Carolina Biological Supply Company, NC, USA.

## 3.2 Bacteria culturing and sample preparation

*Salmonella enterica* and *Sarcina* lutea strains were cultured in LB liquid medium at 37 °C for 24 hours using a shaker incubator. After incubation, the bacterial suspensions were centrifuged at 4200 rpm for 15 minutes, repeated three times to ensure thorough removal of the supernatant. The resulting bacterial pellets were collected and used in the synthesis of Salmonella-specific CIP islands for integration into the microfluidic sensor. Bacterial concentrations were quantified using standard plate culture and

colony counting methods. The *E. coli* O157:H7 strain, provided in lyophilized form within a dextran matrix at an initial concentration of $10^9$ CFU/mL, was similarly processed. The sample was centrifuged at 4200 rpm for 15 minutes, and the resulting pellet was used for the fabrication of *E. coli*-targeted CIPs. When needed in the abovementioned experiments, serial dilutions were prepared in PBS, followed by centrifugation under the same conditions. Final pellets were resuspended in sterile saline prior to use in binding and detection assays.

## 3.3 FITC fluorescent increase mechanism

Experiments were conducted using FITC as a fluorescent probe [168], [169] to simulate the later-stage on-chip bacterial detection process. FITC was prepared in methanol at three concentrations of 0.5 mg/mL, 0.7 mg/mL, and 0.9 mg/mL. These solutions were mixed with *Salmonella* bacterial suspensions ranging from $10^3$ to $10^8$ CFU/mL inside multi-well plates. Fluorescent images were taken using an upright fluorescent microscope (MZ10F Modular Stereo Microscope, Leica, Germany), then the fluorescence responses of the FITC-bacteria mixtures were measured with ImageJ and compared to a control FITC sample with no bacteria exposure.

## 3.4 NIP and CIP thin films of the microfluidic sensor

The NIP solution was formulated by combining four monomers, a cross-linker, solvent, and a photo-initiator in specific ratios, as detailed in Table 1. Monomer ratios were selected based on work done from literature [170]. These monomers were selected based on previous literature demonstrating their complementary properties for creating effective imprinted polymer cavities. Specifically, AAM provides hydrophilic characteristics and strong hydrogen bonding capacity, facilitating interactions with polar bacterial surface groups. MAA contributes carboxyl functionalities, which enable electrostatic and strong hydrogen bond formation, enhancing polymer-target binding affinity. VP introduces amphiphilic characteristics, which improve polymer compatibility with diverse bacterial

surface chemistries, increasing overall binding efficiency. MMA contributes hydrophobic characteristics and structural rigidity, preserving cavity shape stability under aqueous conditions. Together, these monomers yield a balanced polymer composition, optimizing selectivity, specificity, and stability in bacterial imprinting applications [170]. The mixture was sonicated for 20 minutes to achieve a homogeneous solution. To prepare the CIP prepolymer, a 5 mL suspension of *Salmonella* ($10^8$ CFU/mL) was centrifuged at 4200 rpm for 15 minutes. The supernatant was carefully removed, and 1 mL of the NIP pre-polymer solution was added to the bacterial pellet, followed by thorough mixing for 30 seconds. To study how the number of bacterial cells affects cavity formation efficiency, a second CIP pre-polymer solution was prepared. Using the same method, 3 mL of the source *Salmonella* suspension ($10^8$ CFU/mL) was centrifuged, the supernatant was removed, and 1 mL of the NIP pre-polymer solution was added to the pellet. The mixture was then mixed for 30 seconds.

**Table 3-1. Materials used to prepare the NIP pre-polymer**

| Chemicals | | Quantity |
|---|---|---|
| **Monomers** | AAM | 21 mg |
| | MAA | 180 μL |
| | VP | 4.2 μL |
| | MMA | 5.2 μL |
| **Crosslinker** | EDGMA | 570 μL |
| **Solvent** | DMSO | 1500 μL |
| | Acetonitrile | 300 μL |
| **Initiator** | DMPA | 14.1 mg |

A PSA double-sided tape was laser cut with two 500 μm wide and 20 mm long microchannels and bonded to a PMMA substrate as shown in Fig. 3-1. CIP and NIP pre-polymer solutions were filled into the two channels. These pre-polymers were then cured using a UV lamp with a wavelength of 365 nm for 20 minutes, following a laboratory protocol established before in the lab. Post-polymerization, a

washing procedure was employed to remove the bacterial template and form imprinted cavities within the CIP matrix. The washing step was performed using a methanol-acetic acid solution (7:1, v/v), based on a 9:1 literature protocol but modified in our preliminary tests for more complete template removal [171]. Washing durations of 1, 3, and 5 minutes were then compared to determining the optimal washing time.

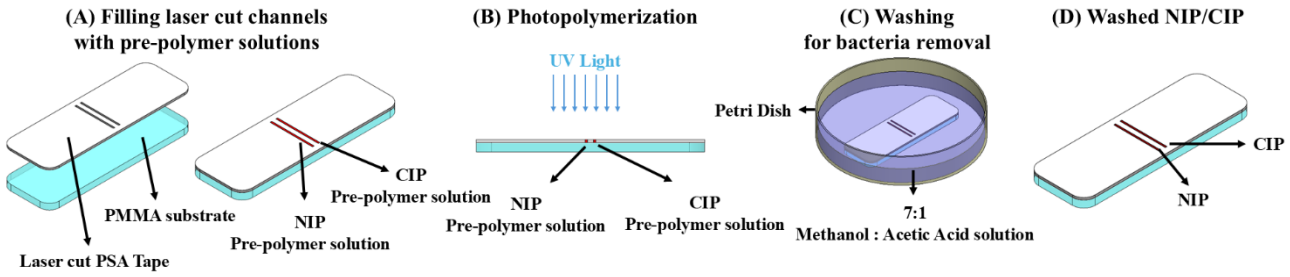


*Fig. 3-1. Schematic illustration of the NIP and CIP thin film patterning process. (A) Bonding PSA tape with laser-cut channels to a PMMA substrate and filling the channels with NIP and CIP pre-polymer solutions. (B) UV curing the NIP and CIP-filled channels. (C) Removing the bacteria template from CIP by 7:1 methanol: acetic acid washing. (D) Final NIP and CIP thin films after washing.*

NIP and CIP thin film morphologies were characterized using scanning electron microscopy (SEM) technique (Hitachi TM4000 SEM, Japan). To reduce charging and increase signal-to-noise ratio during SEM, the samples were coated with 3 nm gold using a Sputter Coater (Leica EM ACE600, Germany).

## 3.5 Fabrication of the singleplex microfluidic bacteria sensor

As illustrated in Fig. 3-2, the microfluidic sensor was fabricated as a four-layer assembly, with each layer measuring 45 × 30 $mm^2$. The base layer consisted of a PMMA substrate. The second layer comprised the PSA double-sided tape with two parallel microchannels, each 500 μm wide, which housed the pre-synthesized NIP and CIP lines (Fig. 3-1). A third layer, also made of PSA double-sided tape, featured two additional parallel microchannels (each 500 μm wide) oriented perpendicular to the NIP and CIP lines. This configuration created four distinct bacteria capture and detection areas at the intersections of the NIP and CIP lines and the microchannels. In this design, one of the microchannels

was intended to introduce a blank solution as a control, while the second channel facilitated the injection of bacterial-spiked solutions. The top layer consisted of a thin PET film, which was cut at four specific locations to serve as inlets and outlets for fluid flow.

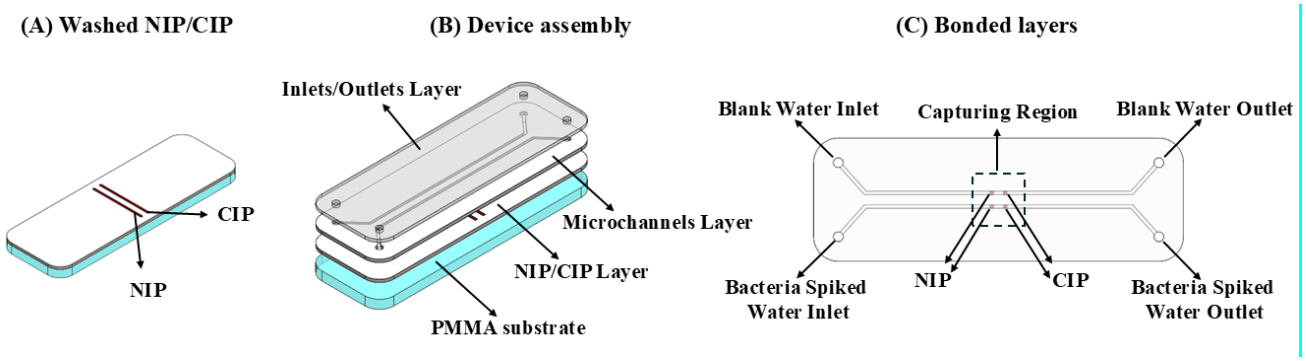


*Fig. 3-2. Illustration of the microfluidic sensor fabrication process: (A) NIP and CIP thin film lines after bacteria template removal, (B) The sensor is composed of four layers: a PMMA substrate as the base layer, a second layer with NIP and CIP thin film lines, a third layer featuring two channels perpendicular to the NIP and CIP lines, and a top layer with inlet and outlet holes, (C) The final microfluidic sensor includes two inlets, two outlets, and a bacteria capturing and detection region with four islands, two for NIP and two for CIP.*

## 3.6 Experimental setup and procedures

The experimental procedure for the microfluidic sensor, as depicted in Fig. 3-3, was developed to assess the re-binding efficiency of CIP for *Salmonella* detection in Chapter 4. As shown in Fig. 3-3A, a dual syringe pump was used to infuse blank water (as a control experiment) and bacteria-spiked water over the NIP and CIP thin films (Fig. 3-3C) inside the microfluidic sensor (Fig. 3-3B). The microfluidic sensor was mounted under a Leica upright microscope and fluorescent images were taken using a MC170 HD color camera (Leica, Germany). The captured fluorescent images (Fig. 3-3D) were analyzed using ImageJ software.

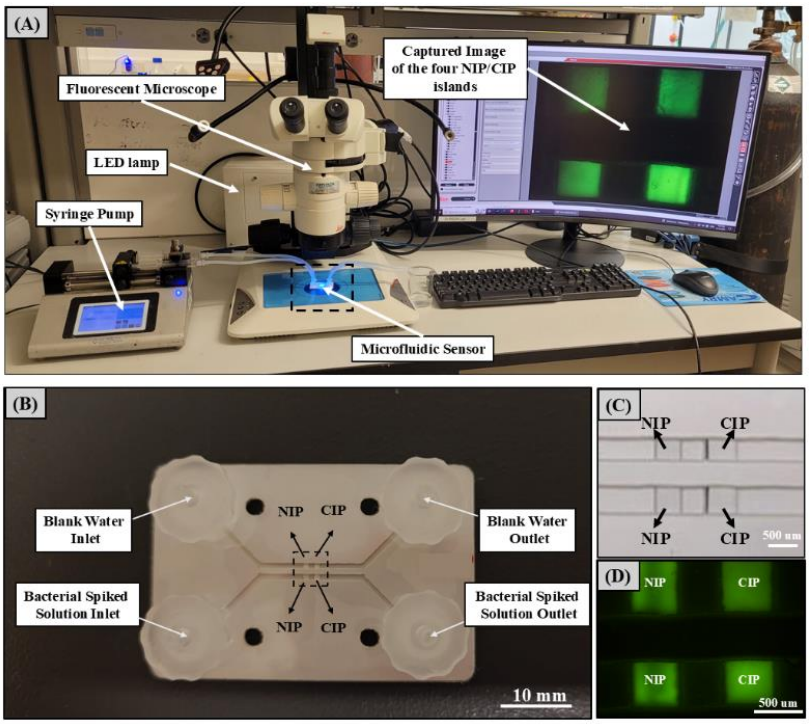


*Fig. 3-3. Experimental setup and microfluidic sensor. (A) Experimental setup with a fluorescent microscope and a dual syringe pump to infuse blank water and bacteria-spiked water through the inlets. (B) Actual image of the fabricated microfluidic sensor. The sensor incorporates two parallel channels with designated inlets and outlets — one for blank water and the other for the bacteria-spiked water samples. These channels intersect with the NIP and CIP thin film regions. (C) The NIP and CIP thin film islands are positioned at the intersection of the two channels. (D) Fluorescent image of the NIP and CIP regions after sample passage, bacteria capturing, and FITC exposure.*

Bacterial water suspensions with concentrations ranging from $10^1$ to $10^8$ CFU/mL were prepared and subjected to centrifugation to pellet the bacterial cells. After centrifugation, the supernatant was carefully removed, and each pellet was resuspended in salinized water at a concentration of 650 ppm of NaCl. The bacterial suspensions were then introduced into one of the two microfluidic channels using a dual syringe pump at a constant flow rate of 0.05 mL/min. The second channel was simultaneously filled with blank water. The bacterial and blank samples were allowed to flow through their respective channels for an incubation period of 60 minutes. Following incubation, a 0.7 mg/mL FITC solution (according to a study described later) was injected into both channels to evaluate the bacterial capture capability of the CIP lines compared to the NIP control. After the injection of FITC solution, both channels were rinsed with DI water and dried using pressurized air. Fluorescence

imaging was then performed using an upright microscope (Fig. 3-3D), and the resulting images were analyzed using fluorescence intensity measurements to assess the capture efficiency of the CIP island.

## 3.7 Specificity and competitive assays

To assess the specificity of the *Salmonella*-imprinted CIP sensor, we introduced *E. coli* O157:H7 as a non-target bacterium through one microfluidic channel while maintaining a blank solution in the parallel channel as a control. The CIP islands in all experiments were made specific to *Salmonella*. After a 60-minute incubation period with continuous flow (0.05 mL/min), fluorescence images were acquired and quantitatively analyzed using ImageJ software to compare the sensor response between the target and non-target bacteria cells.

For the competitive assay, two solutions were prepared, i.e., one containing only non-target bacteria (*E. coli* O157:H7 and *Sarcina*) and another containing both non-target bacteria (*E. coli* O157:H7 and *Sarcina*) along with the target bacterium (*Salmonella*). All bacterial suspensions were prepared at concentrations of $10^7$ CFU/mL. The solution containing only *E. coli* O157:H7 and *Sarcina* was injected into one channel, while the solution containing *E. coli* O157:H7, *Sarcina*, and *Salmonella* was injected into the other channel. The CIP islands in all experiments were made specific to *Salmonella*. Both solutions were allowed to flow through the channels for 60 minutes to evaluate the sensor's ability to selectively capture the target bacterium (*Salmonella*) in the presence of competing microorganisms.

## 3.8 Data analysis and statistics

The fluorescent images acquired from experiments were quantitatively analyzed with ImageJ software. To remove the effect of the carrier fluid, background-subtracted fluorescence intensities were first calculated for the CIP and NIP islands by subtracting the fluorescent intensity of the blank control islands (e.g., top row in Fig. 3-3D) from the fluorescent intensities of the bacteria-exposed islands (bottom row in Fig. 3-3D), as follows:

$$\Delta F_{CIP} = F_{CIP\_bacteria} - F_{CIP\_blank} \quad (3\text{-}1)$$

$$\Delta F_{NIP} = F_{NIP\_bacteria} - F_{NIP\_blank} \quad (3\text{-}2)$$

All experiments were performed three times, and statistical significance between groups was determined using t-test. Standard deviations were determined using the standard error propagation method.

The dose-response curve of the sensor was plotted based on the obtained fluorescent intensity changes (ΔF) as a function of bacteria concentration. The LOD and LOQ of the sensor were determined from the dose-response curve using the 3SD and 10SD method [45] as follows:

$$\Delta F_{LOD} = \Delta F_{blank} + 3SD_{blank} \quad (3\text{-}3)$$

$$\Delta F_{LOQ} = \Delta F_{blank} + 10SD_{blank} \quad (3\text{-}4)$$

LOD and LOQ were determined from the dose-response curve using equations (3-3) and (3-4). First, the average fluorescence intensity ($\Delta F_{blank}$) and standard deviation ($SD_{blank}$) of blank (zero bacteria) samples were calculated. LOD and LOQ were then determined as the bacterial concentrations that correspond to fluorescence intensities equal to $\Delta F_{blank}$ plus three (eq. 3-3) and ten (eq. 3-4) times the $SD_{blank}$, respectively. These calculated intensities were correlated back to bacterial concentrations using a sensor function fit to the dose-response curve.

## 3.9 Duplex microfluidic bacteria sensor

In order to test the capability of our microfluidic method to detect two bacteria species at the same time, i.e., duplex detection, the thin-film bottom polymeric layer of the sensor was redesigned by adding another parallel CIP thin film targeting *E. coli* O157:H7. This configuration established six distinct detection islands, i.e., two serving as NIP controls, two specific for *Salmonella* detection

(S.CIP), and two for *E. coli* O157:H7 (E.CIP), as shown in Fig. 3-4. The fabrication method of NIP and CIP is exactly the same as the ones described in section 3.4.

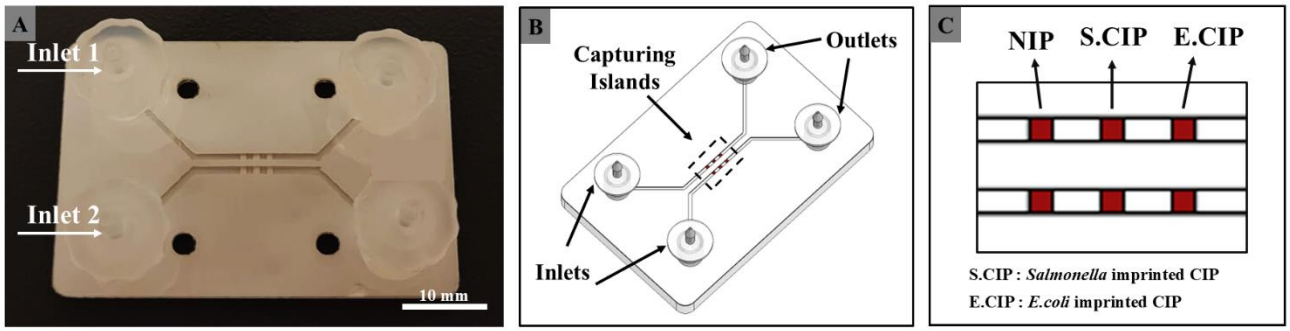


*Fig. 3-4. CIP-integrated microfluidic sensor for duplex bacterial detection. (A) Image and (B) schematic of the microfluidic sensor with six detection islands obtained at overlaying intersections of two sampling microchannels and three NIP/CIP lines as shown in (C).*

The duplex detection capability of the microfluidic sensor was assessed through the simultaneous detection of *E. coli* O157:H7 and *Salmonella* in water samples. Bacterial suspensions in saline buffer (650 ppm NaCl) were prepared at concentrations of $10^4$, $10^5$, and $10^7$ CFU/mL. The experimental procedure was the same as in the singleplex experiment (section 3.6). *Salmonella* and *E. coli* suspensions were injected through Inlet 1 and Inlet 2, respectively, at 0.05 mL/min for 60 minutes, then exposed to 0.7 mg/mL FITC, then washed, and dried. Fluorescence imaging and ImageJ analysis were carried out as described previously to quantify bacterial capture on each CIP island.

Selectivity was evaluated by three competitive binding tests (all at $10^5$ CFU/mL total): *Salmonella* + *Sarcina*, *E. coli* + *Sarcina*, and *Salmonella* + *E. coli*. After 60 minutes of flow and FITC exposure, images were analyzed with ImageJ to quantify fluorescence intensity on each CIP island and confirm target discrimination.

To assess the selectivity of the microfluidic sensor, a series of competitive binding assays were performed using mixtures of target and non-target bacteria. In the first experiment, a mixed bacterial

suspension containing *Salmonella* and *Sarcina* (each at $10^5$ CFU/mL) was introduced simultaneously into both microfluidic channels via Inlets 1 and 2. In the second experiment, a mixture of *E. coli* O157:H7 and *Sarcina* ($10^5$ CFU/mL each) was introduced following the same procedure. The third experiment involved a mixture of *Salmonella* and *E. coli* O157:H7, both at $10^5$ CFU/mL, to evaluate the sensor's ability to discriminate between the two target species. After a 60-minute incubation period to allow for bacterial binding, FITC solution was introduced into each channel to label captured bacteria. Fluorescence imaging was subsequently performed to visualize binding patterns, and the resulting images were analyzed using ImageJ software. Quantitative fluorescence intensity measurements were used to evaluate the specificity of the sensor.

# Chapter 4

# 4 Results and Discussion

## 4.1 Singleplex bacteria detection with the microfluidic sensor

### 4.1.1 Introduction

In this study, we address the first objective, which is stated in Chapter 1, by fabricating *Salmonella*-imprinted CIP thin films and integrating them into a cost-effective microfluidic fluorescent sensing platform. The characterization of the CIP thin films confirms the successful imprinting of *Salmonella*, forming well-defined recognition cavities. To meet the second objective, the developed microfluidic sensor facilitates the sensitive and selective detection of *Salmonella* by leveraging FITC dye for quantification. Specificity tests using *E. coli O157:H7* and *Sarcina lutea* as non-target bacteria further validate the selectivity of the sensor. This work highlights the potential of CIP-based microfluidic biosensors as a robust and scalable solution for rapid bacterial detection in water quality monitoring applications.

### 4.1.2 Determination of FITC concentration to detect *Salmonella*

FITC is commonly used for bacterial labeling due to its covalent binding with surface proteins, expressing fluorescence upon interaction with microbial cells [172]. However, labeling efficiency varies based on bacterial species, cell wall composition, and dye concentration. Although FITC labeling is well-studied, its fluorescence response upon interaction with *Salmonella* and the optimum concentration for quantitative detection are still not fully explored. Therefore, we investigated the optimal FITC concentration for maximizing fluorescence signal. Using the protocol in chapter 3 section 3.3, a multi-well plate was filled with various concentrations of *Salmonella* in the range of 0 to $10^8$ CFU/mL, exposed to FITC at 0 to 0.9 mg/mL, and fluorescently imaged as shown in Fig. 4-1A.

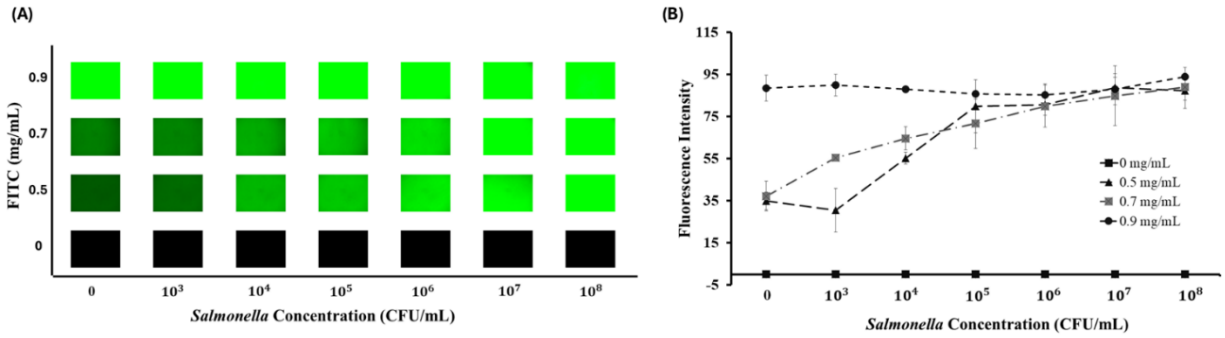


*Fig. 4-1 Effect of Salmonella and FITC concentration on fluorescent expression. (A) Fluorescence images of a multi-well plate showing the effect of different FITC concentrations (0, 0.5, 0.7, and 0.9 mg/mL) on Salmonella suspensions ranging from $10^3$ to $10^8$ CFU/mL, including a blank control water sample. (B) Corresponding fluorescence intensity plots for the same FITC concentrations across the bacterial range.*

As shown in Fig. 4-1A, fluorescence intensity increases with both bacterial and FITC concentration. This fluorescence enhancement is due to the covalent interaction between FITC's isothiocyanate (-N=C=S) group and amine ($-NH_2$) or phosphate ($-PO_4^{3-}$) groups in *Salmonella* lipopolysaccharides (LPS), which forms stable thiourea (-NH-CS-NH-) linkages [173], [174], [175]. Additionally, FITC engages in hydrophobic interactions with bacterial membrane lipids, which reduces the fluorescence quenching and further stabilizes signal detection [173], [176].

Quantitative fluorescence analysis (Fig. 4-1B) further showed the impact of FITC concentration on detection performance. In the absence of FITC (0 mg/mL), no fluorescence signal was detected, which was considered as the baseline. At the highest FITC concentration of 0.9 mg/mL, fluorescence intensity remained consistently high across all bacterial concentrations, including the blank control, indicating that excess unbound FITC contributed to background self-fluorescence [177]. In contrast, at 0.5 mg/mL and 0.7 mg/mL FITC, fluorescence intensity increased proportionally with bacterial concentration. At 0.5 mg/mL, the fluorescence difference between the control and $10^3$ CFU/mL was minimal, but a sharp increase was observed from $10^4$ to $10^5$ CFU/mL, suggesting improved sensitivity beyond a critical bacterial threshold. At 0.7 mg/mL, fluorescence intensity gradually increased across bacterial concentrations, showing that this FITC concentration provides a clear and reliable signal. It maintains

a balance by staying sensitive to low bacterial levels while preventing signal saturation at higher concentrations. This made 0.7 mg/mL FITC an ideal concentration for accurate expression, ensuring consistent and distinguishable fluorescence across the tested range.

### 4.1.3 Characterization of NIP and CIP thin film

The surface morphology of the NIP and CIP thin films fabricated according to Fig. 3-1 procedure was characterized using SEM when they were exposed to the methanol: acetic acid washing solution for up to 5 minutes. CIP samples were prepared at two distinct bacteria-to-pre-polymer ratios of 3:1 and 5:1 as described in the methods chapter. The results are shown in Fig. 4-2.

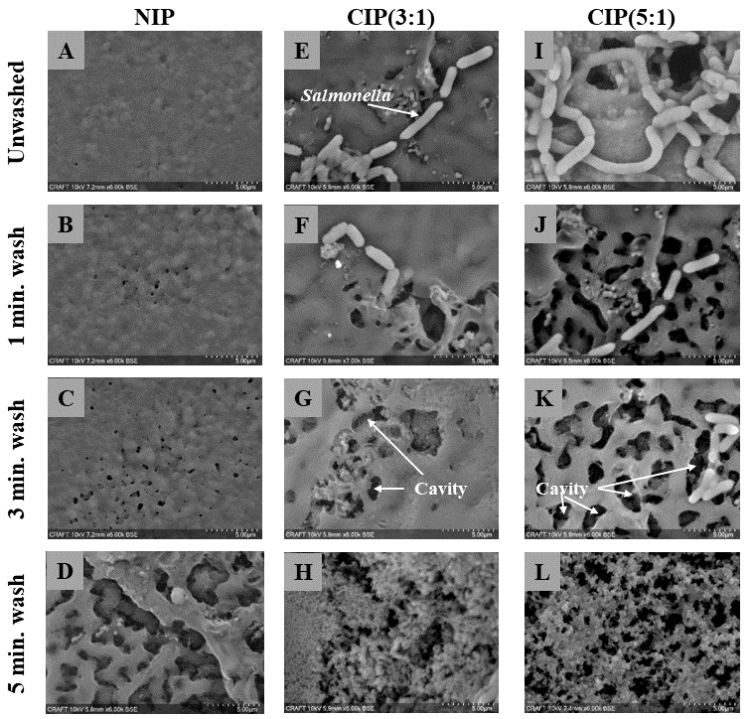


*Fig. 4-2 SEM images of NIP and CIP thin films on PMMA surface and the effect of methanol:acetic acid washing on cavity formation. (A) NIP film after polymerization and before washing; (B–D) Effects of increasing washing duration on NIP surface morphology. (E) CIP film (3:1 bacteria-to-pre-polymer volume ratio) after polymerization and before bacterial template removal; (F-H) Effect of washing duration on bacterial removal and CIP surface morphology (3:1 CIP). (I) CIP film (5:1 bacteria-to-pre-polymer volume ratio) before template removal; (J–L) Effect of washing duration on bacterial removal and cavity formation in 5:1 CIP.*

As illustrated in Fig. 4-2(A-D), the NIP exhibited negligible surface alterations after a 1-minute wash, with only minor degradation observed on the polymer surface. After 3 minutes of washing, the etching

remained minimal; however, following a 5-minute wash, significant surface degradation was evident, marked by the formation of multiple etching-induced holes within the polymer matrix.

For the CIP films prepared at the 3:1 ratio, SEM analysis showed the presence of *Salmonella* bacteria embedded in the polymer matrix prior to washing, as shown in Fig. 4-2E. After 1 minute of washing in Fig. 4-2F, some portions of the bacteria remained within the polymer, with only few cavities visible. Increasing the wash time to 3 minutes in Fig. 4-2G resulted in the complete removal of *Salmonella*, leaving behind more well-defined cavities. However, after a 5-minute wash, the polymer structure exhibited significant etching, leading to the degradation of the CIP surface integrity.

In contrast, the CIP films fabricated at the 5:1 ratio initially displayed a higher density of *Salmonella* bacteria, as depicted in Fig. 4-2I. Following a 1-minute wash in Fig. 4-2J, bacterial removal commenced, and cavities began to form, although some bacteria remained embedded. Extending the wash duration to 3 minutes in Fig. 4-2K facilitated further bacterial removal and the exposure of additional cavities. However, similar to the 3:1 CIP, prolonged washing for 5 minutes resulted in pronounced etching and structural degradation of the polymer as shown in Fig. 4-2L.

The washing optimization experiments showed that a 3-minute wash for CIP films prepared at a 5:1 bacteria-to-pre-polymer ratio provided an optimal balance between cavity formation and preservation of surface morphology. This wash duration effectively removed the *Salmonella* bacteria while minimizing excessive polymer erosion. Shorter wash durations were insufficient for complete bacterial removal, whereas longer durations caused significant damage to the polymer surface. Therefore, the 3-minute wash duration was selected as the optimal condition, ensuring the formation of well-defined cavities without compromising the polymer integrity. Maintaining this balance is essential for the functional performance of CIP films, especially in applications demanding precise cell recognition and binding.

### 4.1.4 Fluorescent detection of *Salmonella* in the microfluidic sensor

In this section, the bacteria capturing performance of CIP thin films and the effectiveness of FITC-based post-capture fluorescence detection were evaluated in the context of the microfluidic sensor shown in Fig. 3-3B. The focus was on assessing the rebinding efficiency of *Salmonella* and optimizing fluorescence labeling for accurate bacteria quantification. We hypothesized that CIP thin films would exhibit selective binding in comparison to NIP thin films, and FITC fluorescence would enable reliable quantification of captured bacteria at CIP islands. After incubating bacteria at a concentration of $10^5$ CFU/mL for 60 minutes in the bottom microchannels of the sensor, FITC at a concentration of 0.7 mg/mL was introduced into the channels to enable fluorescence-based stimulation of CIP and NIP islands. The top channel was exposed to blank water as a control experiment. Fluorescent images were captured using an upright fluorescence microscope. As illustrated in Fig. 4-3A, the fluorescent images of the NIP and CIP islands before bacteria culturing appear entirely black. Following bacterial capture and exposure to the FITC solution (Fig. 4-3B), the fluorescent image reveals the four CIP and NIP islands exhibiting green fluorescence, confirming the presence of captured bacteria. Fig. 4-3C quantifies the fluorescent intensities of these CIP and NIP islands. When exposed to the blank water (upper row in Fig. 4-3B), both islands exhibit similar background fluorescence of approximately 38 a.u. However, when exposed to bacteria (lower row in Fig. 4-3B), the CIP island showed a higher fluorescence of ~70 a.u. than the NIP island (43 a.u.), which confirms that the increased signal is due to specific bacterial binding to CIP as compared to non-specific binding of bacteria onto the NIP island.

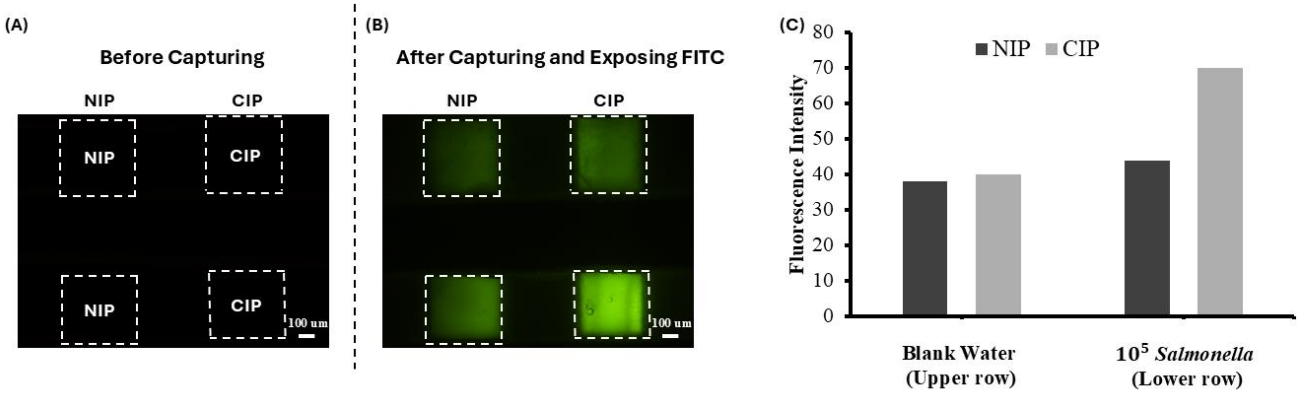


*Fig. 4-3 Salmonella capturing and FITC-based detection in the microfluidic sensor. (A) Fluorescent image of sensor's NIP and CIP islands before bacterial capture showing no green fluorescence. (B) Fluorescent image after exposure to FITC following bacteria capture, with the upper row exposed to blank water and the bottom row exposed to $10^5$ CFU/mL Salmonella. (C) Fluorescence intensity measurements of the NIP and CIP islands of (B).*

The NIP and CIP islands in the upper row of Fig. 4-3B and their intensities in Fig. 4-3C were used for background noise determination, as they were only exposed to blank water samples with no bacteria. The signals from the NIP and CIP islands in the bottom microchannel, which were exposed to the bacterial solution, were then used for the determination of background-subtracted fluorescence intensities.

### 4.1.5 Dose-response characterization of the microfluidic sensor for *Salmonella* quantification

The effect of bacterial concentration on the FITC-induced fluorescent stimulation of the sensor was evaluated by comparing the background-subtracted fluorescence intensities of CIP and NIP islands, as shown in Fig. 4-4. These ΔF intensities were calculated using Equations 3-1 and 3-2, which enable a direct comparison between CIP and NIP fluorescence after bacterial capture.

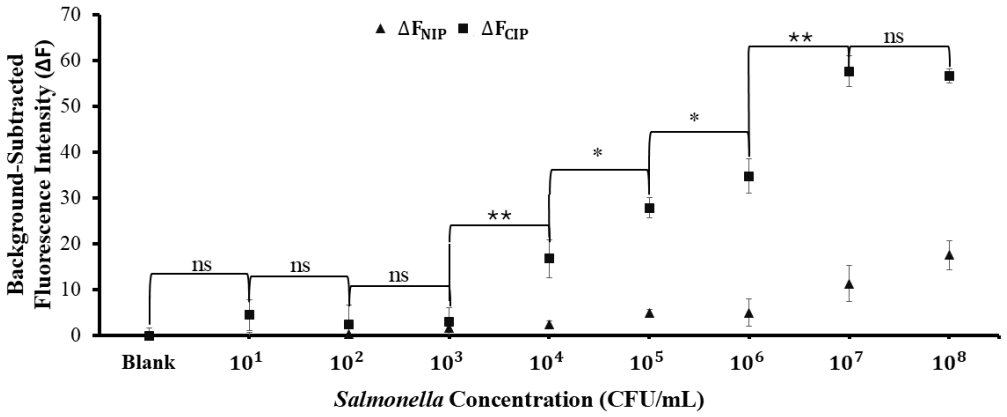


*Fig. 4-4 Background-subtracted fluorescence intensity (ΔF) measurements of NIP and CIP islands after 60 minutes of Salmonella incubation at concentrations ranging from 0 (blank) to $10^8$ CFU/mL, followed by exposure to 0.7 mg/mL FITC. Each data point represents the mean of three independent experiments under the same conditions. Error bars indicate standard deviations (SD), ns: not significant, *: p<0.05, **: p < 0.01.*

NIP islands show low ΔF variations at bacterial concentrations ranging from 0 to $10^4$ CFU/mL, followed by a gradual increase from $10^5$ to $10^8$ CFU/mL. Similarly, CIP islands maintained a baseline fluorescence at lower concentrations of 0 to $10^3$ CFU/mL, indicating minimal bacterial capture. However, a notable and statistically significant increase in fluorescence was observed from $10^3$ to $10^7$ CFU/mL. The highest ΔF was measured at the bacterial concentration of $10^7$ CFU/mL, which did not rise any further at $10^8$ CFU/mL. At $10^7$ CFU/mL, the imprinting factor was calculated to be 4.07 using equation 4-1 [178].

$$\alpha = \frac{\Delta F_{CIP\_bacteria}}{\Delta F_{NIP\_bacteria}} \tag{4-3}$$

These results indicate the enhanced bacterial binding capacity of CIP compared to NIP while also suggesting a quantitative increase in bacterial capturing in the range of $10^3$ to $10^7$ CFU/mL. A linear fit to the CIP data in this range revealed a sensor function of $\Delta F_{CIP} = 5.51\, Ln(C_s) - 35.41$ ($C_s$: *Salmonella* concentration) with a goodness of fit of $R^2$=0.967.

Using the 3SD method in Equation (3-3) and the sensor function above, the LOD of the sensor was determined to be 1.47 × $10^3$ CFU/mL, while the LOQ, based on the 10SD method in Equation (3-4),

was calculated as $5.28 \times 10^3$ CFU/mL. The sensitivity of the sensor was 5.51 a.u. per CFU/mL, defined as the slope of the linear fit, within the $10^3$–$10^7$ CFU/mL range.

In our study, the CIP-functionalized islands demonstrated a significant fluorescence response for bacterial concentrations above $10^3$ CFU/mL, which aligns with detection limits reported in previous studies employing MIP-based bacterial sensing approaches [45], [46], [179], [180], [181]. For example, Akhtarian et al [170]. reported that metal microwires functionalized with multi-functional CIP coatings achieved bacterial capture efficiencies of approximately 76% at $10^4$ CFU/mL. Similarly, a microfluidic sensor incorporating CIP-coated microwires for conductometric detection exhibited a dynamic detection range between $10^4$ and $10^7$ CFU/mL, though its LOD was slightly higher, around $2.1 \times 10^5$ CFU/mL [180]. These findings suggest that CIP-based sensors can provide reliable bacterial detection within an environmentally relevant range, which makes them a strong alternative to conventional biosensing approaches.

Unlike conventional biosensors that rely on antibodies, aptamers, or enzyme-based recognition, our IP-based microfluidic sensor offers several advantages, including enhanced shelf stability, ease of fabrication, and reduced susceptibility to environmental degradation [182], [183], [184]. These characteristics make CIPs particularly suitable for implementation in continuous monitoring systems across critical domains such as environmental water quality monitoring, which requires durable sensing platforms.

Despite these advantages, our study also highlights the limitations of the current sensor design. Specifically, the device showed reduced sensitivity below $10^3$ CFU/mL, which may restrict its applicability in cases where very low bacterial concentrations must be detected, such as early-stage infections or trace-level contamination in water supplies [185], [186]. To overcome this limitation, future research should focus on optimizing the polymerization process [170], incorporating

nanostructured materials (e.g., graphene oxide, gold nanoparticles) to enhance bacterial binding efficiency [187], [188]. Additionally, further modifications to the microfluidic design, such as increasing the surface area of the CIP regions or implementing multi-stage bacterial pre-concentration steps, could significantly improve the sensor's analytical performance [171].

### 4.1.6 Specificity and competitive detection assays using the singleplex sensor

The specificity of the *Salmonella*-imprinted CIP thin films was evaluated using the microfluidic sensor to assess their ability to differentiate between *Salmonella* (target bacterium) and *E. coli* O157:H7 (non-target bacterium). The results, presented in Fig. 4-5A, illustrate the NIP-subtracted fluorescence intensity (ΔF) of CIP films upon exposure to *Salmonella* and *E. coli* O157:H7. The CIP films exhibited significantly higher fluorescence intensity when exposed to *Salmonella* compared to *E. coli* O157:H7, with statistical analysis confirming a significant difference ($p < 0.01$). At $10^7$ CFU/mL, the selectivity factor was calculated to be 2.7 using equation 4-2 [178], where $\alpha_{Salmonella}$ was 4.07 and $\alpha_{E.coli}$ was 1.5

$$\beta = \frac{\alpha_{analyte}}{\alpha_{analogues}} \tag{4-2}$$

These findings indicate that the microfluidic sensor demonstrates a measurable degree of selectivity for *Salmonella* over *E. coli* O157:H7. However, while the observed distinction is statistically significant, it may not be sufficient to claim a high degree of specificity. The residual binding observed with *E. coli* O157:H7 suggests potential cross-reactivity, which could impact detection accuracy. To further refine specificity, additional investigations are needed. Future studies should explore the performance of CIP films in competitive binding assays involving complex bacterial mixtures.

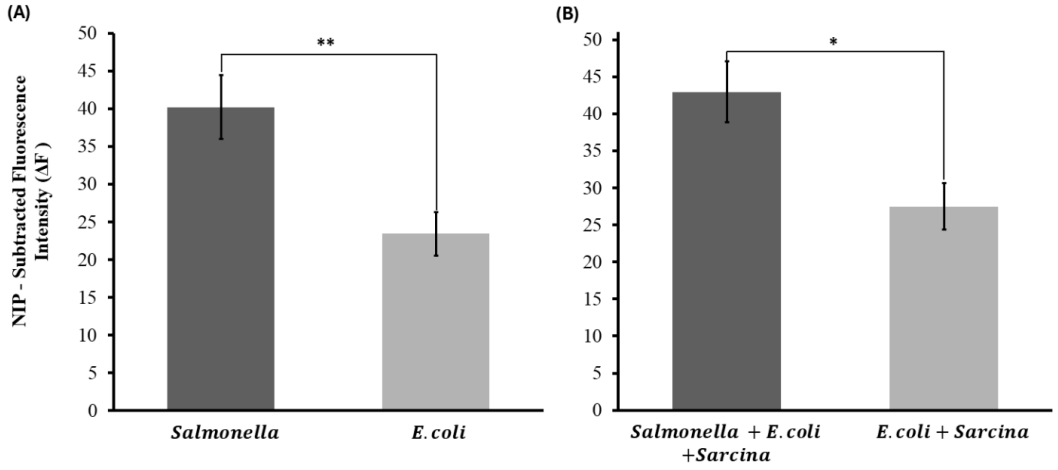


*Fig. 4-5* Specificity and selectivity of *Salmonella-imprinted* CIP thin films. (A) NIP-subtracted fluorescence intensity (ΔF) of *Salmonella*-imprinted CIP thin films when exposed to *Salmonella* (target) versus *E. coli* O157:H7 (non-target) at $10^7$ CFU/mL. (B) NIP-subtracted fluorescence intensity (ΔF) of CIP films exposed to a bacterial mixture containing *Salmonella*, *E. coli* O157:H7, and *Sarcina* ($10^7$ CFU/mL) compared to films exposed to only *E. coli* O157:H7 and *Sarcina*. The values in the graph represent the mean values of three experiments per condition. Error bars indicate standard deviations (SD), and statistical significance is denoted as *: $p < 0.05$, **: $p < 0.01$.

Fig. 4-5B presents the normalized fluorescence intensity of *Salmonella*-imprinted CIP films upon exposure to a bacterial mixture containing *Salmonella*, *E. coli* O157:H7, and *Sarcina* at a concentration of $10^7$ CFU/mL, compared to the same CIP films exposed to a control solution containing only *E. coli* O157:H7 and *Sarcina*. The results demonstrate that the CIP films exhibited significantly higher fluorescence intensity when exposed to the more complex but *Salmonella*-containing solution, with statistical analysis confirming a significant difference ($p < 0.05$). These findings indicate that the *Salmonella*-imprinted CIP films are capable of detecting *Salmonella* even in the presence of multiple bacterial species at a high concentration. This suggests that the imprinting process confers a degree of selectivity to the CIP films, enabling them to boost response to the target bacterium in complex mixtures. However, further investigations involving a broader range of bacterial species and varying concentrations are necessary to fully assess the robustness and selectivity of the sensor under real-world conditions.

The developed microfluidic CIP-thin film sensor demonstrated detection limits and dynamic ranges comparable to state-of-the-art biosensors employing biological recognition elements [189], [190].

However, unlike biological counterparts, the integration of CIP within the sensor confers robustness and cost-efficiency [191]. This advantage stems from the inherent stability of CIP materials, which eliminate the degradation and storage constraints typically associated with biological receptors. A key innovation in this work was the direct incorporation of CIP thin films into the microfluidic sensor during fabrication. This design significantly enhances the sensor's suitability for point-of-need applications by streamlining operation and removing the need for complex assembly steps or external modifications, which are often required in other CIP-based microfluidic platforms [41], [45], [46], [171], [179], [180]. Specificity assessments confirmed the sensor's ability to distinguish *Salmonella* from non-target bacteria, such as *E. coli* O157:H7, at a bacterial concentration of $10^7$ CFU/mL. While the observed selectivity is promising, further optimization is necessary to enhance specificity in complex, heterogeneous microbiological samples.

## 4.2 Duplex bacteria detection with the microfluidic sensor

### 4.2.1 Introduction

To address the need for simultaneous detection of multiple pathogens, we designed a microfluidic chip integrating two CIP thin films (Fig. 3-4) for duplex fluorescence detection of *Salmonella enterica* and *E. coli* O157:H7 in water. This layout reduces sample volume and assay time compared to single-target detection methods and uses only standard FITC labeling without additional signal enhancers. The platform's performance was validated using a series of rebinding and competitive assays across bacterial concentrations of $10^4$, $10^5$, and $10^7$ CFU/mL.

### 4.2.2 Duplex fluorometric detection of *Salmonella* and *E. coli* using CIP thin films

This experiment examined whether *Salmonella* and *E. coli* imprinted CIP islands in a single microfluidic sensor exhibit fluorescence intensities that correlate with bacterial concentration. Bacterial suspensions ($10^4$, $10^5$, and $10^7$ CFU/mL) of *Salmonella* and *E. coli* were introduced into the top and bottom microchannels of the sensor, respectively, incubated for 60 minutes, exposed to 0.7

mg/mL FITC, and then imaged by fluorescence microscopy to quantify the signal response. Fig. 4-6 presents six images arranged in two rows corresponding to the above bacterial concentrations; the top table row shows the fluorescent images of sensor regions before bacterial capture, and the bottom table row shows the matching fluorescence images after FITC exposure.

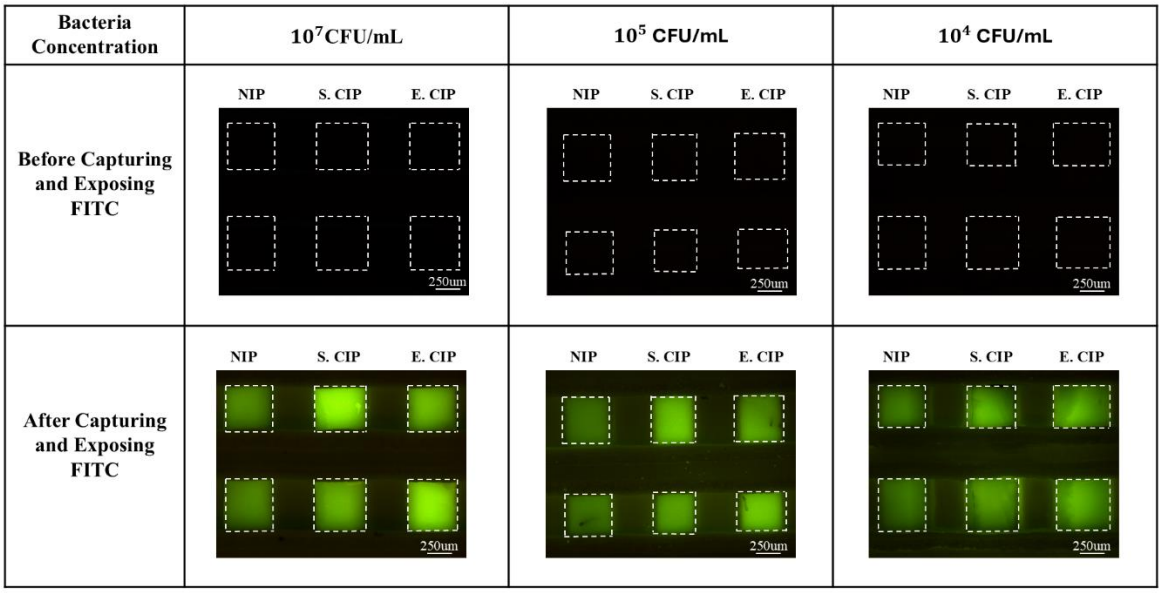


*Fig. 4-6 Fluorescence images of NIP, Salmonella-imprinted CIP (S.CIP), and E. coli-imprinted CIP (E.CIP) islands exposed to bacterial concentrations of $10^7$, $10^5$, and $10^4$ CFU/mL. The top row shows each region before bacterial capture and FITC exposure. The bottom row shows the same regions after bacteria capture and exposure to FITC. Within each image inside the table cells, the top NIP, S.CIP and E.CIP islands were exposed to Salmonella while the bottom islands were exposed to E. coli.*

In each table cell of Figure 4-6, six fluorescent images related to NIP, S.CIP, and E.CIP islands are displayed. These images were captured following exposure to *Salmonella* (top islands) and *E. coli* (bottom islands) at various concentrations arranged from left to right. At $10^7$ CFU/mL, the S.CIP island shows higher fluorescence (94.3 a.u.) compared to the E.CIP (73.9 a.u.). At $10^5$ CFU/mL, S.CIP again shows slightly higher fluorescence (68.5 a.u.) than E.CIP (55.2 a.u.). However, at $10^4$ CFU/mL, no difference was observed (51.2 a.u. vs 50.3 a.u.). A similar trend is observed in the *E. coli* exposures. At $10^7$ CFU/mL, E.CIP shows higher fluorescence (90.4 a.u.) compared to S.CIP (75.3 a.u.), and $10^5$ CFU/mL, it again shows greater fluorescence (64.3 a.u. vs 54.4 a.u.). At $10^4$ CFU/mL, both islands

show the same level of fluorescence (52.1 a.u. vs 50.2 a.u.). This demonstrated that the sensor is potentially capable of differentiating between the two bacterial species at higher concentrations of $10^7$ and $10^5$ CFU/mL.

In order to study the above observations quantitatively, duplex bacteria measurements were performed in three independent trials. The fluorescent intensities of the S.CIP and E.CIP islands (F′) were normalized by the corresponding fluorescent intensity of the NIP island (F) in the same microchannel line. These normalized fluorescence intensities (F′/F) of the microfluidic sensor at various bacterial concentrations are presented in Fig. 4-7A for both strains. For better observation, Fig. 4-7 B and C show the *Salmonella* and *E. coli* specific dose-response curves in separate panels.

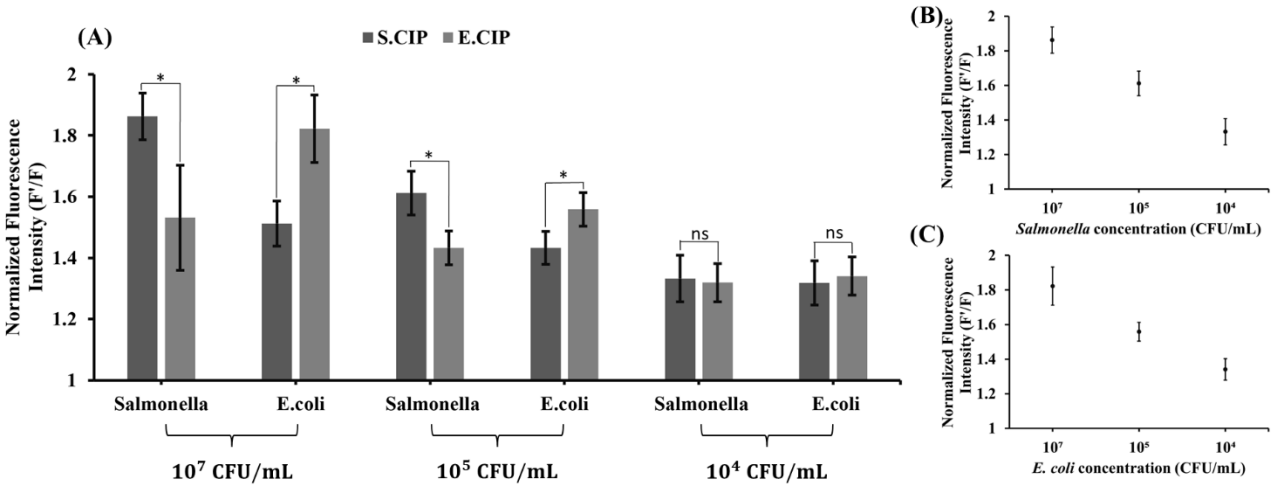


*Fig. 4-7. Dose-response curves of the duplex microfluidic sensor for Salmonella and E. coli detection at $10^7$, $10^5$, and $10^4$ CFU/mL concentrations. (A) Normalized fluorescence intensity of the duplex microfluidic sensor with integrated S.CIP and E.CIP thin films are shown for both Salmonella and E. coli for side-by-side comparison. (B) and (C) separately show these normalized fluorescence intensities for Salmonella and E. coli, respectively. Each data point represents the mean of three independent experiments under the same conditions. Error bars indicate standard deviations (SD), and statistical significance is denoted as *: $p < 0.05$, and ns: not significant.*

At a bacterial concentration of $10^7$ CFU/mL, *Salmonella* in the top microchannel of the sensor, a statistical difference ($p < 0.05$) was observed between the S.CIP and the E.CIP normalized fluorescence intensities. Similarly, at $10^7$ CFU/mL *E. coli* in the bottom microchannel of the sensor, a statistical difference ($p < 0.05$) was observed between the E.CIP and the S.CIP, indicating the potential for each

CIP island to selectively bind its designated target at $10^7$ CFU/mL concentration. At $10^5$ CFU/mL, the CIP islands imprinted with target bacteria similarly showed a statistical difference in their corresponding microchannels, with $p < 0.05$ for their respective target bacteria. However, at $10^4$ CFU/mL, no significant difference in the normalized fluorescence intensity was observed between the two bacterial species, suggesting that this microfluidic sensor for multiplex bacterial detection can differentiate between the two tested bacteria at concentrations of $10^5$ and $10^7$ CFU/mL.

The findings of this study indicate that our CIP thin-film microfluidic sensor, with parallel imprints for *Salmonella* and *E. coli* O157:H7, may selectively capture its target bacteria. We observed an increase in normalized fluorescence intensity (F′/F) at $10^7$ CFU/mL for each target ($p < 0.05$), a response in line with selective binding by the imprinted cavities. In contrast, at $10^4$ CFU/mL, the fluorescence response was negligible and not statistically different from controls, indicating a practical detection limit around $10^5$ CFU/mL under the current configuration. While this LOD is higher than those reported for some enhanced CIP sensors – for example, devices using magnetic nanoparticle-enriched CIPs or electrochemical impedance readouts have achieved LODs in the $10^2$–$10^3$ CFU/mL range – those approaches often involve more complex fabrication or instrumentation [45], [46], [179], [180]. Doostmohammadi et al. [45], [46] and others, for instance, improved sensitivity to the $10^3$ CFU/mL level by incorporating magnetically concentrated CIP microparticles and fluorescence detection, or by leveraging electrochemical signal amplification in microfluidic CIPs [179], [180]. In contrast, our focus was on simplicity and multiplexing: we employ a straightforward in situ UV-polymerized film within a microfluidic chip, enabling dual-bacteria detection using standard fluorescence microscopy. This design prioritizes ease of use and field deployability, which are especially valuable for environmental monitoring and food safety screening applications.

### 4.2.3 Competitive assay

The ability of each CIP area to selectively capture its target bacterium under competitive binding conditions was assessed by introducing mixtures containing equal concentrations of two bacterial species into the sensor. Mixed suspensions of *Salmonella* + *Sarcina*, *E. coli* + *Sarcina*, and *Salmonella* + *E. coli* (each at $10^5$ CFU/mL) were infused into the sensor for 60 min, followed by 0.7 mg/mL FITC exposure. Fig. 4-8 shows the fluorescent images taken before and after bacterial capturing.

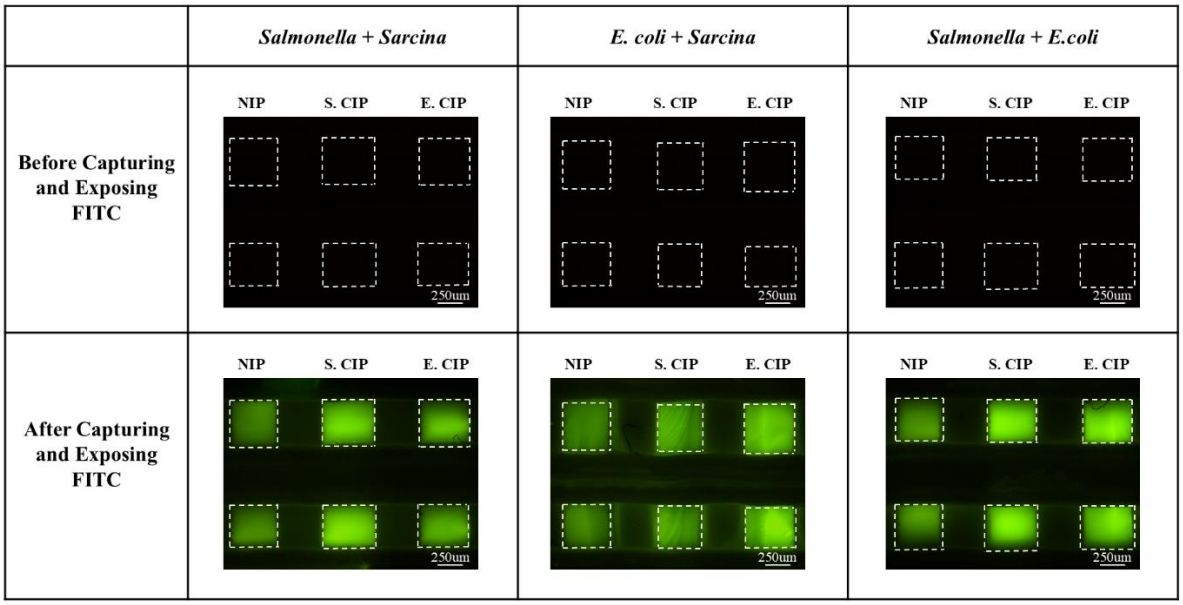


*Fig. 4-8 Fluorescence images of NIP, Salmonella-imprinted CIP (S.CIP), and E. coli-imprinted CIP (E.CIP) islands before and after exposure to mixed bacteria suspensions ($10^5$ CFU/mL each) of Salmonella + Sarcina, E. coli + Sarcina, and Salmonella + E. coli. The top row shows each region before bacterial capture and FITC exposure. The bottom row shows the same regions after capture and FITC exposure.*

In the *Salmonella* + *Sarcina* mixture, S.CIP shows higher fluorescence (~88 a.u.) compared to E.CIP (~ 75 a.u.), while in *E. coli* + *Sarcina* mixture, E.CIP fluorescence signal (~87 a.u.) is slightly higher than S.CIP (~79 a.u.). Lastly, in the *Salmonella* + *E. coli* mixture, no difference was observed between S.CIP and E.CIP (~90 a.u. vs ~89 a.u.). These results indicate that each CIP island is more likely to bind to its target bacteria even in the presence of a competitor (left and middle columns of Fig. 4-8),

leading to potential for duplex detection in the *Salmonella* + *E. coli* mixtures (right column of Fig. 4-8).

The above competitive experiments were performed in triplicate for quantitative assessment of sensor performance using the normalized fluorescent intensity metric as described before. As shown in Fig. 4-9, the S.CIP island showed a higher fluorescence than the E.CIP in the *Salmonella* + *Sarcina* assay with minimal statistical difference ($P < 0.05$). Similarly, in the *E. coli* + *Sarcina* assay, the E.CIP showed a higher signal than the S.CIP ($P < 0.05$). In the *Salmonella* + *E. coli* assay, both CIP islands exhibited comparable high fluorescence intensities, which were not statistically different from each other. These observations likely reflect non-specific adhesion of the larger, spherical *Sarcina* cells to the CIP surface, where they can obstruct or foul the imprinted cavities and produce elevated background fluorescence [192]. *Sarcina* cells often form tetrads or clusters that cannot fit into the rod-shaped imprint cavities but can nonetheless adhere non-specifically to the polymer surface through electrostatic or hydrophobic interactions [193]. As a result, the high *Sarcina*-derived signal narrows the gap between target and non-target responses ($P < 0.05$), reducing statistical confidence in distinguishing bacteria in mixed-bacteria assays.

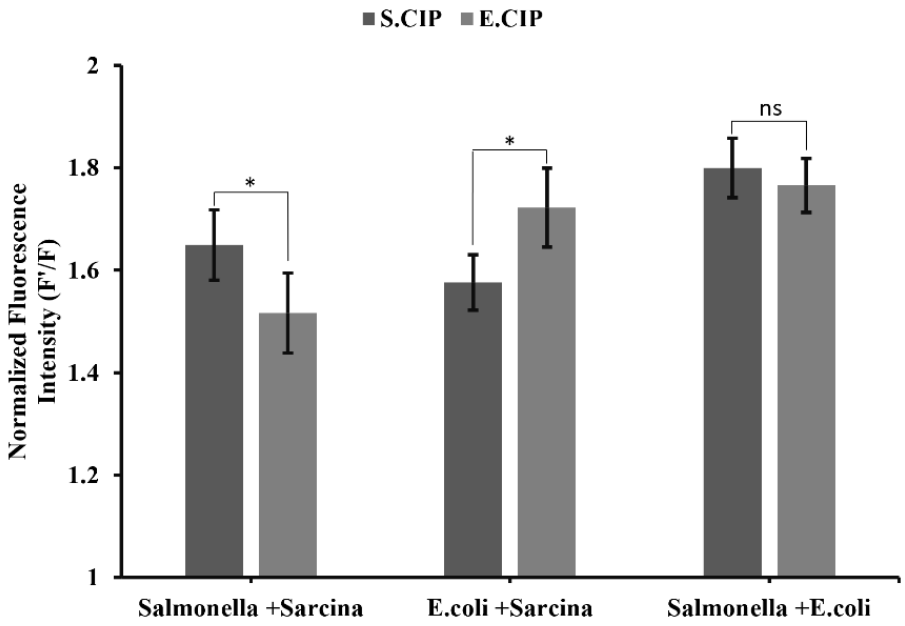


*Fig. 4-9. Selectivity experiments conducted using three bacterial mixtures (each at $10^5$ CFU/mL) in channels containing NIP, Salmonella-imprinted CIP (S.CIP), and E. coli-imprinted CIP (E.CIP). The tested mixtures included Salmonella with Sarcina, E. coli O157:H7 with Sarcina, and Salmonella with E. coli O157:H7. Each data point represents the mean of three independent experiments under the same conditions. Error bars indicate standard deviations (SD), statistical significance is denoted as *: $p < 0.05$ and ns: not significant.*

These results suggest that our dual-CIP microfluidic sensor may provide a practical means of detecting both *Salmonella* and *E. coli* on a single chip without antibodies or DNA probes. Existing fluorescence-based CIP microfluidic devices typically target only one species and report LODs around $8 \times 10^3$ CFU/mL in water samples [45], while impedance-based CIP sensors integrated into microchannels have achieved LODs near $2 \times 10^2$ CFU/mL but require electrodes and electronic readers [179].In comparison, aptamer-linked fluorescent assays can detect multiple bacteria at 10–25 CFU/mL, yet they involve nanoparticle conjugation and complex probe selection [194], and immunosensors with dual antibodies reach ~40 CFU/mL but demand multi-step surface modification and precise optics [195]. Table 4-1below shows a comparison between different bacteria detection biosensors with our sensor.

**Table 4-1. Comparison of Bacterial Detection Biosensors**

| **Target** | **Detection Method** | **Recognition Element** | **LOD** (CFU/mL) | **Range** (CFU/mL) | **Time** | **Specificity** | **Cost** | **Ref** |
|---|---|---|---|---|---|---|---|---|
| ***Salmonella*** | Electrochemical impedance | Antibody | 73 | $1.6 \times 10^2$ – $1.6 \times 10^6$ | 1 h | High | Moderate | [196] |
| ***Salmonella*** | Differential Pulse Voltammetry (DPV) | Antibody | 89 | $10^2$ - $10^6$ | 40 min. | Moderate | Moderate | [197] |
| ***E. coli*** | Amperometry | Antibody | 52 | $10^2$ -$10^6$ | 35 min | Moderate | High | [198] |
| ***E. coli*** | Electrochemical Impedance Spectroscopy (EIS) | MIP | $10^3$ | $10^3$ -$10^8$ | 1 h | Moderate | Moderate | [199] |
| ***B. cereus*** | Cyclic Voltammetry | MIP | Not available | $10^2$-$10^5$ | 5 min | Moderate | Moderate | [200] |
| ***P. aeruginosa*** | Linear Sweeping Voltammetry (LSV) | Antibody | $9 \times 10^2$ | $10^1$-$10^7$ | 15 min | Low | High | [201] |

| | | | | | | | | |
|---|---|---|---|---|---|---|---|---|
| ***E. coli*** | Fluorescence Detection | CIP-Micro particles | $4 \times 10^2$ | $10^2$- $10^7$ | 30 min | Low | Moderate | [45] |
| ***E. coli*** | Conductometric Detection | CIP-Micro Wires | $2.1 \times 10^5$ | $10^4$-$10^7$ | 110 sec. | Moderate | Low | [180] |
| ***Salmonella*** + ***E. coli*** | Fluorescence Detection | CIP-Thin Films | $10^5$ | Not available | 1 h | Very Low | Low | This work (Duplex) |
| ***Salmonella*** | Fluorescence Detection | CIP-Thin Films | $1.47 \times 10^3$ | $10^3$ - $10^7$ | 1 h | Low | Low | This work (Singleplex) |

By contrast, our method uses UV-cured thin films imprinted in micro channels and a single FITC staining step to achieve simultaneous detection, with a sensitivity of $10^5$ CFU/mL in duplex detection and 1.47 x $10^3$ CFU/mL limit of detection for singleplex detection of *Salmonella*. Although the sensitivity is modest, the simplified fabrication and the absence of biological recognition elements or electronics may make this approach well suited for rapid, on-site water quality monitoring and food safety screening.

# Chapter 5

# 5 Thesis Summary and Prospect

## 5.1 Thesis summary

### 5.1.1 Restatement of Objectives

Four primary objectives guided this research toward the development of a microfluidic, fluorescence-based bacterial sensor that utilizes CIP thin films. First, uniform CIP thin-film lines were fabricated directly within microfluidic channels so that they could be used as surfaces for target bacteria to bind to. Second, FITC dye concentration was optimized to enhance the signal-to-noise ratio while preventing background saturation. Third, singleplex performance was evaluated by detecting *Salmonella*, determining its LOD, and assessing both specificity and selectivity against non-target strains. Finally, multiplex detection was shown by capturing and differentiating *Salmonella* and *E. coli* O157:H7 simultaneously within the same sensor. Competitive binding assays were employed selective recognition in mixed samples.

### 5.1.2 Synthesis of CIP Thin-Film Lines

CIP thin films were fabricated in situ within microfluidic channels by a photopolymerization reaction. A pre-polymer mixture was formulated by dissolving four functional monomers (AAM, MAA, VP, MMA) along with the crosslinker EDGMA and photoinitiator DMPA in DMSO. For *Salmonella*-specific CIP, a suspension of *Salmonella* was centrifuged, the supernatant removed, and the pre-polymer solution added to the bacterial pellet with mixing to ensure homogeneous monomer–template interaction. A PSA film, laser cut with 500 μm-wide channels and bonded to a PMMA substrate. After filling the channels with CIP (and NIP for control) pre-polymer solutions, UV curing initiated cross-linking and solidification of the polymer films in microchannels. Following

post-polymerization, bacterial templates were removed by washing the CIP channels with a methanol–acetic acid mixture. Washing durations of 1, 3, and 5 minutes were evaluated to optimize template removal without sacrificing polymer integrity. SEM characterization revealed that a 3-minute wash effectively removed embedded bacteria and generated imprint cavities, without degrading the overall film structure. Shorter washes left behind residual cells, while longer washes caused excessive etching and pore collapse.

This optimized synthesis and template-removal protocol produced uniform CIP thin-film lines with high cavity density that form the selective binding element of the fluorescence-based microfluidic sensor.

### 5.1.3 Optimization of Fluorescence Dye Concentration

A series of FITC concentrations (0, 0.5, 0.7, and 0.9 mg/mL) was examined in preliminary suspension assays to identify the conditions that provide the optimal signal-to-background ratio. The 0.5 mg/mL concentration yielded only modest fluorescence increases at $10^3$–$10^4$ CFU/mL, while 0.9 mg/mL produced excessive baseline signal. The 0.7 mg/mL FITC condition delivered an approximately linear response from $10^3$ to $10^8$ CFU/mL. When applied in the microfluidic sensor, this concentration produced consistent signals in replicate assays, allowing reliable LOD and specificity determinations.

### 5.1.4 Singleplex Detection of *Salmonella*

The singleplex detection performance of the sensor was explored by detection of *Salmonella* over a range of $10^1$–$10^8$ CFU/mL. LOD was approximated as $1.47 \times 10^3$ CFU/mL, and LOQ as $5.28 \times 10^3$ CFU/mL. The dynamic sensitivity of the sensor varied from $10^3$ to $10^7$ CFU/mL, demonstrating quantification within this range. Specificity was assessed by exposing *Salmonella*-imprinted CIP channels and NIP controls to $10^7$ CFU/mL of *Salmonella* versus *E. coli* O157:H7. The CIP films gave higher fluorescence responses when exposed to *Salmonella*

compared with *E. coli* O157:H7 ($p < 0.01$), demonstrating somehow selective recognition of the target bacterium. Competitive binding assays, which utilized mixtures of *E. coli* O157:H7 and *Sarcina*, showed that CIP regions did not generate high fluorescent signals, except in the presence of *Salmonella*, whereas signals remained near baseline for non-target mixtures. Together, these results are validation that microfluidic CIP sensor functions with sensitive levels of *Salmonella* detection with statistical difference against the non-target bacteria, thereby serving the singleplex detection function.

### 5.1.5 Duplex Bacterial Detection

The duplex capability of the microfluidic CIP sensor was evaluated by introducing mixed suspensions of *Salmonella* and *E. coli* O157:H7 at concentrations of $10^4$, $10^5$, and $10^7$ CFU/mL into parallel imprinted islands. Fluorescence microscopy images show that at $10^7$ CFU/mL, the *Salmonella*-imprinted island exhibited slightly higher fluorescence when exposed to *Salmonella* than the *E. coli*-imprinted region, and vice versa for *E. coli* exposures ($p < 0.05$). At $10^5$ CFU/mL, the target-specific CIP regions still produced significantly higher fluorescence than the non-target regions, although the differences were less observed ($p < 0.05$). However, at $10^4$ CFU/mL, there was no significant difference in fluorescence between the two imprints, indicating that under the current conditions, the practical multiplex limit of detection is at $10^5$ CFU/mL. Competitive binding assays further explored selectivity by flowing mixtures of *Salmonella* + *Sarcina*, *E. coli* + *Sarcina*, and *Salmonella* + *E. coli* (each at a total of $10^5$ CFU/mL) through the sensor. In the Salmonella + Sarcina and *E. coli* + *Sarcina* tests, each target-imprinted island produced statistically higher fluorescence ($p < 0.05$) than the non-target region, while in the *Salmonella* + *E. coli* mixture, both imprints yielded comparable high signals (not significant). Overall, these results suggest that the CIP-based microfluidic sensor can distinguish between two bacterial targets at concentrations of $10^5$ CFU/mL and above, but that sensitivity is reduced below this level. While this duplex LOD is higher than that achieved in some

single-analyte CIP devices, the preliminary demonstration of simultaneous recognition on a simple, portable chip provides a foundation for further refinement. Future work might focus on lowering the duplex LOD through adjustments to polymer film thickness, imprint fidelity, or incorporation of signal-amplification strategies to strengthen the sensor's multiplex performance.

## 5.2 Thesis Prospects

### 5.2.1 Limitations and Challenges

Although the microfluidic CIP sensor demonstrated ability for singleplex and multiplex bacterial detection, there are some limitations that must be addressed before it can be applied practically. Firstly, the detection limits $3 \times 10^3$ CFU/mL for singleplex and $10^5$ CFU/mL for multiplex remain higher than are required for many applications in the real world, such as detecting low-level bacterial contamination in drinking water or environmental water bodies where concentrations are often lower [202]. The requirement for relatively high bacterial concentrations could potentially make the sensor ineffective unless upstream sample concentration or signal-amplification methods are used.

Secondly, the stability of CIP films during reuse was not investigated; prolonged exposure to solvents or mechanical stress during sample flow can reduce imprint quality and selectively limit selectivity from one cycle to the next [203], [204]. The reusability and long-term stability of the sensor surfaces are to be assessed.

Third, the design has only been demonstrated with limited bacterial species (*Salmonella* and *E. coli* O157:H7) in buffer solutions. The performance in field matrices such as food extracts, wastewater, or blood could be disrupted by non-specific adsorption, fouling, or interference from particulates and other biomolecules [205], [206]. Finally, external fluorescence microscopy readout limits portability and requires skilled users, thus limiting field application in resource-limited environments.

Resolving these challenges will be required to transition the technology from laboratory demonstration to a user-friendly, high-throughput diagnostic platform.

### 5.2.2 Future Work

#### 5.2.2.1 Enhancing Sensitivity

To reduce the detection limitations of the CIP-based microfluidic sensor, future studies should investigate methods to increase polymer–analyte interactions and amplify signals. Integrating nanomaterials (such as carbon nanotubes, MXene sheets, or gold or silver nanoparticles) into the CIP matrix to boost fluorescence intensity via plasmonic enhancement or by adding more fluorophore binding sites is one possible strategy [207], [208], [209]. Alternatively, the fluorescent signal could be catalytically amplified by enzyme-linked reporters after capture, allowing detection at lower bacterial concentrations [207].

CIP film thickness and porosity can also be optimized to increase sensitivity: thinner films can reduce diffusion limitations and allow faster binding of the analyte, and designed pore sizes can provide greater template–polymer surface contact [210]. Cumulatively, these enhancements can reduce the practical multiplex LOD well below $10^5$ CFU/mL, which will move the sensor closer to real-world applicability.

#### 5.2.2.2 Expanding the Range of Imprinted Targets

Future research would apply the CIP imprinting technique to a broader variety of microorganisms and analytes to evaluate its adaptability and applicability. This could involve developing dedicated CIP regions for other bacterial pathogens (*Listeria monocytogenes*, *Staphylococcus aureus*, or *Campylobacter jejuni*) and customizing the imprinting parameters (monomer composition, polymerization duration) to accommodate cells of varying size, morphology, and surface chemistry. Application to non-bacterial targets, such as e.g., virus or bacteriophage, would establish the platform

further as versatile [211], [212]. Furthermore, manufacture of multiplex arrays with more than two imprints, where each imprint addresses a distinct organism, could provide comprehensive screening panels. Comparison of imprint quality and binding performance from this extended target group will define the boundaries of whole-cell imprinting and guide optimizations in polymer formulation for biosensing.

#### 5.2.2.3 Real-Sample Validation

To assess real-world performance, the sensor should be evaluated using real water samples (tap, river, or wastewater) against standard culture methods to measure recovery and accuracy. Simple pretreatments like filtration can help remove debris without adding complexity. Testing in these matrices will reveal any interference from organic matter or other microbes and guide necessary adjustments for reliable field use.

#### 5.2.2.4 Field-Deployable Sensor

To convert this sensor into a product, the microfluidic sensor should be integrated into a compact housing that mounts a small, battery-powered peristaltic pump linked to onboard sample and waste reservoirs. A portable fluorescence reader comprising a miniature microscope will be fixed above the microfluidic sensor and interfaced with a touchscreen tablet running custom acquisition software. Following assembly, the complete unit will undergo on-site testing with real water samples to validate its analytical performance, ease of use, and robustness under field conditions.

# References


[1] A. Marušić, “Food safety and security: What were favourite topics for research in the last decade?,” *J Glob Health*, vol. 1, no. 1, pp. 72–78, 2011.

[2] Y.-L. Oon, Y.-S. Oon, M. Ayaz, M. Deng, L. Li, and K. Song, “Waterborne pathogens detection technologies: advances, challenges, and future perspectives,” *Front Microbiol*, vol. 14, Nov. 2023, doi: 10.3389/fmicb.2023.1286923.

[3] C. Davis, “Enumeration of probiotic strains: Review of culture-dependent and alternative techniques to quantify viable bacteria,” *J Microbiol Methods*, vol. 103, pp. 9–17, Aug. 2014, doi: 10.1016/j.mimet.2014.04.012.

[4] P. Billard and M. S. DuBow, “Bioluminescence-Based Assays for Detection and Characterization of Bacteria and Chemicals in Clinical Laboratories,” *Clin Biochem*, vol. 31, no. 1, pp. 1–14, Feb. 1998, doi: 10.1016/S0009-9120(97)00136-7.

[5] T. C. GLENN, “Field guide to next-generation DNA sequencers,” *Mol Ecol Resour*, vol. 11, no. 5, pp. 759–769, Sep. 2011, doi: 10.1111/j.1755-0998.2011.03024.x.

[6] M. Nayak *et al.*, “Integrated sorting, concentration and real time PCR based detection system for sensitive detection of microorganisms,” *Sci Rep*, vol. 3, no. 1, p. 3266, Nov. 2013, doi: 10.1038/srep03266.

[7] M. Moriconi, E. Acke, D. Petrelli, and S. Preziuso, “Multiplex PCR-based identification of Streptococcus canis, Streptococcus zooepidemicus and Streptococcus dysgalactiae subspecies from dogs,” *Comp Immunol Microbiol Infect Dis*, vol. 50, pp. 48–53, Feb. 2017, doi: 10.1016/j.cimid.2016.11.011.

[8] A. Fraisse *et al.*, “Digital RT-PCR method for hepatitis A virus and norovirus quantification in soft berries,” *Int J Food Microbiol*, vol. 243, pp. 36–45, Feb. 2017, doi: 10.1016/j.ijfoodmicro.2016.11.022.

[9] D. Singh, A. Sharma, and G. K. Saini, “Biochemical and molecular characterisation of the bacterial endophytes from native sugarcane varieties of Himalayan region,” *3 Biotech*, vol. 3, no. 3, pp. 205–212, Jun. 2013, doi: 10.1007/s13205-012-0084-2.

[10] A.-L. Välimaa, A. Tilsala-Timisjärvi, and E. Virtanen, “Rapid detection and identification methods for Listeria monocytogenes in the food chain – A review,” *Food Control*, vol. 55, pp. 103–114, Sep. 2015, doi: 10.1016/j.foodcont.2015.02.037.

[11] S. Nagaraj, S. Ramlal, J. Kingston, and H. V. Batra, “Development of IgY based sandwich ELISA for the detection of staphylococcal enterotoxin G (SEG), an egc toxin,” *Int J Food Microbiol*, vol. 237, pp. 136–141, Nov. 2016, doi: 10.1016/j.ijfoodmicro.2016.08.009.

[12] S. Hameed, L. Xie, and Y. Ying, “Conventional and emerging detection techniques for pathogenic bacteria in food science: A review,” *Trends Food Sci Technol*, vol. 81, pp. 61–73, Nov. 2018, doi: 10.1016/j.tifs.2018.05.020.

[13] F. Mi *et al.*, “Recent advancements in microfluidic chip biosensor detection of foodborne pathogenic bacteria: a review,” *Anal Bioanal Chem*, vol. 414, no. 9, pp. 2883–2902, Apr. 2022, doi: 10.1007/s00216-021-03872-w.

[14] B. Nasseri, N. Soleimani, N. Rabiee, A. Kalbasi, M. Karimi, and M. R. Hamblin, “Point-of-care microfluidic devices for pathogen detection,” *Biosens Bioelectron*, vol. 117, pp. 112–128, Oct. 2018, doi: 10.1016/j.bios.2018.05.050.

[15] W. Zhou, J. Le, Y. Chen, Y. Cai, Z. Hong, and Y. Chai, “Recent advances in microfluidic devices for bacteria and fungus research,” *TrAC Trends in Analytical Chemistry*, vol. 112, pp. 175–195, Mar. 2019, doi: 10.1016/j.trac.2018.12.024.

[16] D. Gao, Z. Ma, and Y. Jiang, “Recent advances in microfluidic devices for foodborne pathogens detection,” *TrAC Trends in Analytical Chemistry*, vol. 157, p. 116788, Dec. 2022, doi: 10.1016/j.trac.2022.116788.

[17] T. Karasu, E. Özgür, and L. Uzun, “MIP-on-a-chip: Artificial receptors on microfluidic platforms for biomedical applications,” *J Pharm Biomed Anal*, vol. 226, p. 115257, Mar. 2023, doi: 10.1016/j.jpba.2023.115257.

[18] L. Sun *et al.*, “A novel, simple and low-cost paper-based analytical device for colorimetric detection of Cronobacter spp.,” *Anal Chim Acta*, vol. 1036, pp. 80–88, Dec. 2018, doi: 10.1016/j.aca.2018.05.061.

[19] V. G. Panferov and J. Liu, “Optical and Catalytic Properties of Nanozymes for Colorimetric Biosensors: Advantages, Limitations, and Perspectives,” *Adv Opt Mater*, vol. 12, no. 30, Oct. 2024, doi: 10.1002/adom.202401318.

[20] P. Yan, Z. Ding, X. Li, Y. Dong, T. Fu, and Y. Wu, “Colorimetric Sensor Array Based on Wulff-Type Boronate Functionalized AgNPs at Various pH for Bacteria Identification,” *Anal Chem*, vol. 91, no. 19, pp. 12134–12137, Oct. 2019, doi: 10.1021/acs.analchem.9b03172.

[21] J. C. Jokerst, J. A. Adkins, B. Bisha, M. M. Mentele, L. D. Goodridge, and C. S. Henry, “Development of a Paper-Based Analytical Device for Colorimetric Detection of Select Foodborne Pathogens,” *Anal Chem*, vol. 84, no. 6, pp. 2900–2907, Mar. 2012, doi: 10.1021/ac203466y.

[22] M. Srisa-Art, K. E. Boehle, B. J. Geiss, and C. S. Henry, “Highly Sensitive Detection of *Salmonella typhimurium* Using a Colorimetric Paper-Based Analytical Device Coupled with Immunomagnetic Separation,” *Anal Chem*, vol. 90, no. 1, pp. 1035–1043, Jan. 2018, doi: 10.1021/acs.analchem.7b04628.

[23] T. Hormsombut, P. Rijiravanich, W. Surareungchai, and S. Kalasin, “Highly sensitive and selective antibody microarrays based on a Cy5-antibody complexes coupling ES-biochip for *E. coli* and *Salmonella* detection,” *RSC Adv*, vol. 12, no. 38, pp. 24760–24768, 2022, doi: 10.1039/D2RA03391G.

[24] C. Justino, A. Duarte, and T. Rocha-Santos, “Recent Progress in Biosensors for Environmental Monitoring: A Review,” *Sensors*, vol. 17, no. 12, p. 2918, Dec. 2017, doi: 10.3390/s17122918.

[25] Y. Wang, Z. Wang, P. Gupta, J. J. Morrissey, R. R. Naik, and S. Singamaneni, “Enhancing the Stability of COVID-19 Serological Assay through Metal–Organic Framework Encapsulation,” *Adv Healthc Mater*, vol. 10, no. 18, Sep. 2021, doi: 10.1002/adhm.202100410.

[26] S. Sharma, H. Byrne, and R. J. O’Kennedy, “Antibodies and antibody-derived analytical biosensors,” *Essays Biochem*, vol. 60, no. 1, pp. 9–18, Jun. 2016, doi: 10.1042/EBC20150002.

[27] A. Makaraviciute and A. Ramanaviciene, “Site-directed antibody immobilization techniques for immunosensors,” *Biosens Bioelectron*, vol. 50, pp. 460–471, Dec. 2013, doi: 10.1016/j.bios.2013.06.060.

[28] H. Chen *et al.*, “A review on electronic bio-sensing approaches based on non-antibody recognition elements,” *Analyst*, vol. 141, no. 8, pp. 2335–2346, 2016, doi: 10.1039/C5AN02623G.

[29] S. Akgönüllü, E. Özgür, and A. Denizli, “Recent Advances in Quartz Crystal Microbalance Biosensors Based on the Molecular Imprinting Technique for Disease-Related Biomarkers,” *Chemosensors*, vol. 10, no. 3, p. 106, Mar. 2022, doi: 10.3390/chemosensors10030106.

[30] P. Lenain, S. De Saeger, B. Mattiasson, and M. Hedström, “Affinity sensor based on immobilized molecular imprinted synthetic recognition elements,” *Biosens Bioelectron*, vol. 69, pp. 34–39, Jul. 2015, doi: 10.1016/j.bios.2015.02.016.

[31] B. Fresco-Cala, A. D. Batista, and S. Cárdenas, “Molecularly Imprinted Polymer Micro- and Nano-Particles: A Review,” *Molecules*, vol. 25, no. 20, p. 4740, Oct. 2020, doi: 10.3390/molecules25204740.

[32] Polyakov MV, “Adsorption properties and structure of silica gel.,” *Zhurnal Fizieskoj Khimii/Akademiya SSSR*, vol. 2, pp. 799-805., 1931.

[33] W. J. Cheong, S. H. Yang, and F. Ali, “Molecular imprinted polymers for separation science: A review of reviews,” *J Sep Sci*, vol. 36, no. 3, pp. 609–628, Feb. 2013, doi: 10.1002/jssc.201200784.

[34] D. Refaat *et al.*, “Strategies for Molecular Imprinting and the Evolution of MIP Nanoparticles as Plastic Antibodies—Synthesis and Applications,” *Int J Mol Sci*, vol. 20, no. 24, p. 6304, Dec. 2019, doi: 10.3390/ijms20246304.

[35] D. Forchheimer, G. Luo, L. Montelius, and L. Ye, “Molecularly imprinted nanostructures by nanoimprint lithography,” *Analyst*, vol. 135, no. 6, p. 1219, 2010, doi: 10.1039/c0an00132e.

[36] H. Lalo, C. Ayela, E. Dague, C. Vieu, and K. Haupt, “Nanopatterning molecularly imprinted polymers by soft lithography: a hierarchical approach,” *Lab Chip*, vol. 10, no. 10, p. 1316, 2010, doi: 10.1039/b924315a.

[37] N. Idil, M. Hedström, A. Denizli, and B. Mattiasson, “Whole cell based microcontact imprinted capacitive biosensor for the detection of Escherichia coli,” *Biosens Bioelectron*, vol. 87, pp. 807–815, Jan. 2017, doi: 10.1016/j.bios.2016.08.096.

[38] A. K. Yadav, D. Verma, N. Dalal, A. Kumar, and P. R. Solanki, “Molecularly imprinted polymer-based nanodiagnostics for clinically pertinent bacteria and virus detection for future pandemics,” *Biosens Bioelectron X*, vol. 12, p. 100257, Dec. 2022, doi: 10.1016/j.biosx.2022.100257.

[39] K. K. Dar, S. Shao, T. Tan, and Y. Lv, “Molecularly imprinted polymers for the selective recognition of microorganisms,” *Biotechnol Adv*, vol. 45, p. 107640, Dec. 2020, doi: 10.1016/j.biotechadv.2020.107640.

[40] A. Doostmohammadi *et al.*, “Molecularly imprinted polymer (MIP) based core-shell microspheres for bacteria isolation,” *Polymer (Guildf)*, vol. 251, p. 124917, Jun. 2022, doi: 10.1016/j.polymer.2022.124917.

[41] S. Akhtarian, A. Doostmohammadi, D.-E. Archonta, G. Kraft, S. K. Brar, and P. Rezai, “Microfluidic Sensor Based on Cell-Imprinted Polymer-Coated Microwires for Conductometric Detection of Bacteria in Water,” *Biosensors (Basel)*, vol. 13, no. 10, p. 943, Oct. 2023, doi: 10.3390/bios13100943.

[42] P. Yin *et al.*, “A smartphone-based fluorescent sensor for rapid detection of multiple pathogenic bacteria,” *Biosens Bioelectron*, vol. 242, p. 115744, Dec. 2023, doi: 10.1016/j.bios.2023.115744.

[43] K. Varty, C. O’Brien, and A. Ignaszak, “Breast Cancer Aptamers: Current Sensing Targets, Available Aptamers, and Their Evaluation for Clinical Use in Diagnostics,” *Cancers (Basel)*, vol. 13, no. 16, p. 3984, Aug. 2021, doi: 10.3390/cancers13163984.

[44] R. Thevendran *et al.*, “The Diagnostic Potential of RNA Aptamers against the NS1 Protein of Dengue Virus Serotype 2,” *Biology (Basel)*, vol. 12, no. 5, p. 722, May 2023, doi: 10.3390/biology12050722.

[45] A. Doostmohammadi, K. Youssef, S. Akhtarian, G. Kraft, and P. Rezai, “Fluorescent bacteria detection in water using cell imprinted polymer (CIP) coated microparticles in a magnetophoretic microfluidic device,” *Talanta*, vol. 268, p. 125290, Feb. 2024, doi: 10.1016/j.talanta.2023.125290.

[46] A. Doostmohammadi, H. Huang, S. Naushad, and P. Rezai, “Portable cell imprinted polymer-based microfluidic sensor for bacteria detection in real water,” *Microchemical Journal*, vol. 206, p. 111611, Nov. 2024, doi: 10.1016/j.microc.2024.111611.

[47] R. B. Jamal, S. Shipovskov, and E. E. Ferapontova, “Electrochemical Immuno- and Aptamer-Based Assays for Bacteria: Pros and Cons over Traditional Detection Schemes,” *Sensors*, vol. 20, no. 19, p. 5561, Sep. 2020, doi: 10.3390/s20195561.

[48] M. Amiri, A. Bezaatpour, H. Jafari, R. Boukherroub, and S. Szunerits, “Electrochemical Methodologies for the Detection of Pathogens,” *ACS Sens*, vol. 3, no. 6, pp. 1069–1086, Jun. 2018, doi: 10.1021/acssensors.8b00239.

[49] M. Bonnet, J. C. Lagier, D. Raoult, and S. Khelaifia, “Bacterial culture through selective and non-selective conditions: the evolution of culture media in clinical microbiology,” *New Microbes New Infect*, vol. 34, p. 100622, Mar. 2020, doi: 10.1016/j.nmni.2019.100622.

[50] F. Huang, L. Pan, Z. He, M. Zhang, and M. Zhang, “Identification, interactions, nitrogen removal pathways and performances of culturable heterotrophic nitrification-aerobic denitrification bacteria from mariculture water by using cell culture and metagenomics,” *Science of The Total Environment*, vol. 732, p. 139268, Aug. 2020, doi: 10.1016/j.scitotenv.2020.139268.

[51] J. K. Patra, G. Das, S. K. Das, and H. Thatoi, “Isolation, Culture, and Biochemical Characterization of Microbes,” 2020, pp. 83–133. doi: 10.1007/978-981-15-6252-5_4.

[52] C. Schreiber *et al.*, “Clinically relevant antibiotic-resistant bacteria in aquatic environments – An optimized culture-based approach,” *Science of The Total Environment*, vol. 750, p. 142265, Jan. 2021, doi: 10.1016/j.scitotenv.2020.142265.

[53] B. R. McConn *et al.*, “An analysis of culture-based methods used for the detection and isolation of Salmonella spp., Escherichia coli, and Enterococcus spp. from surface water: A systematic review,” *Science of The Total Environment*, vol. 927, p. 172190, Jun. 2024, doi: 10.1016/j.scitotenv.2024.172190.

[54] S. Zhang *et al.*, “Molecular Methods for Pathogenic Bacteria Detection and Recent Advances in Wastewater Analysis,” *Water (Basel)*, vol. 13, no. 24, p. 3551, Dec. 2021, doi: 10.3390/w13243551.

[55] R. C. Nnachi *et al.*, “Biosensors for rapid detection of bacterial pathogens in water, food and environment,” *Environ Int*, vol. 166, p. 107357, Aug. 2022, doi: 10.1016/j.envint.2022.107357.

[56] N. N. Wijayawardene *et al.*, “Current Insight into Culture-Dependent and Culture-Independent Methods in Discovering Ascomycetous Taxa,” *Journal of Fungi*, vol. 7, no. 9, p. 703, Aug. 2021, doi: 10.3390/jof7090703.

[57] A. Canciu, M. Tertis, O. Hosu, A. Cernat, C. Cristea, and F. Graur, “Modern Analytical Techniques for Detection of Bacteria in Surface and Wastewaters,” *Sustainability*, vol. 13, no. 13, p. 7229, Jun. 2021, doi: 10.3390/su13137229.

[58] K. P. Goswami and G. Pugazhenthi, “Credibility of polymeric and ceramic membrane filtration in the removal of bacteria and virus from water: A review,” *J Environ Manage*, vol. 268, p. 110583, Aug. 2020, doi: 10.1016/j.jenvman.2020.110583.

[59] J. Li, Y. Zhu, X. Wu, and M. R. Hoffmann, “Rapid Detection Methods for Bacterial Pathogens in Ambient Waters at the Point of Sample Collection: A Brief Review,” *Clinical Infectious Diseases*, vol. 71, no. Supplement_2, pp. S84–S90, Jul. 2020, doi: 10.1093/cid/ciaa498.

[60] T. Pluym, F. Waegenaar, B. De Gusseme, and N. Boon, “Microbial drinking water monitoring now and in the future,” *Microb Biotechnol*, vol. 17, no. 7, Jul. 2024, doi: 10.1111/1751-7915.14532.

[61] E. Kandeler, “Physiological and biochemical methods for studying soil biota and their functions,” in *Soil Microbiology, Ecology and Biochemistry*, Elsevier, 2024, pp. 193–227. doi: 10.1016/B978-0-12-822941-5.00007-7.

[62] M. Kieliszek, K. Pobiega, K. Piwowarek, and A. M. Kot, “Characteristics of the Proteolytic Enzymes Produced by Lactic Acid Bacteria,” *Molecules*, vol. 26, no. 7, p. 1858, Mar. 2021, doi: 10.3390/molecules26071858.

[63] A. Singh *et al.*, “Biological remediation technologies for dyes and heavy metals in wastewater treatment: New insight,” *Bioresour Technol*, vol. 343, p. 126154, Jan. 2022, doi: 10.1016/j.biortech.2021.126154.

[64] S. Meile, S. Kilcher, M. J. Loessner, and M. Dunne, “Reporter Phage-Based Detection of Bacterial Pathogens: Design Guidelines and Recent Developments,” *Viruses*, vol. 12, no. 9, p. 944, Aug. 2020, doi: 10.3390/v12090944.

[65] P. Song *et al.*, “Limitations and opportunities of technologies for the analysis of cell-free DNA in cancer diagnostics,” *Nat Biomed Eng*, vol. 6, no. 3, pp. 232–245, Jan. 2022, doi: 10.1038/s41551-021-00837-3.

[66] S. B. Ebrahimi, D. Samanta, and C. A. Mirkin, “DNA-Based Nanostructures for Live-Cell Analysis,” *J Am Chem Soc*, vol. 142, no. 26, pp. 11343–11356, Jul. 2020, doi: 10.1021/jacs.0c04978.

[67] S. Miller and C. Chiu, “The Role of Metagenomics and Next-Generation Sequencing in Infectious Disease Diagnosis,” *Clin Chem*, vol. 68, no. 1, pp. 115–124, Dec. 2021, doi: 10.1093/clinchem/hvab173.

[68] F. Marchetti *et al.*, “Error-corrected next generation sequencing – Promises and challenges for genotoxicity and cancer risk assessment,” *Mutation Research/Reviews in Mutation Research*, vol. 792, p. 108466, Jul. 2023, doi: 10.1016/j.mrrev.2023.108466.

[69] Y. Huang *et al.*, “Selection of DNA-encoded chemical libraries against endogenous membrane proteins on live cells,” *Nat Chem*, vol. 13, no. 1, pp. 77–88, Jan. 2021, doi: 10.1038/s41557-020-00605-x.

[70] E. J. Duncavage *et al.*, “Genomic profiling for clinical decision making in myeloid neoplasms and acute leukemia,” *Blood*, vol. 140, no. 21, pp. 2228–2247, Nov. 2022, doi: 10.1182/blood.2022015853.

[71] Q. Gao *et al.*, “Circulating cell-free DNA for cancer early detection,” *The Innovation*, vol. 3, no. 4, p. 100259, Jul. 2022, doi: 10.1016/j.xinn.2022.100259.

[72] S. Thakur, N. K. Mishra, H. S. Tuli, and A. K. Sharma, “Principles of Immunodetection and Immunotechniques: A Preview and Emerging Applications,” in *Immunology*, Jenny Stanford Publishing, 2019, pp. 201–212. doi: 10.1201/b22453-9.

[73] Y. Lu, W. Sheng, B. Liu, and S. Wang, “ELISA-based Sensing in Food Safety and Quality Analysis,” in *Sensing Techniques for Food Safety and Quality Control*, The Royal Society of Chemistry, 2017, pp. 141–163. doi: 10.1039/9781788010528-00141.

[74] X. Feng *et al.*, “Ultra-sensitive and rapid detection of Salmonella enterica and Staphylococcus aureus to single-cell level by aptamer-functionalized carbon nanotube field-effect transistor

biosensors," *Biosens Bioelectron*, vol. 257, p. 116333, Aug. 2024, doi: 10.1016/j.bios.2024.116333.

[75] R. N. Lopes *et al.*, "Development of an Immunocapture-Based Polymeric Optical Fiber Sensor for Bacterial Detection in Water," *Polymers (Basel)*, vol. 16, no. 6, p. 861, Mar. 2024, doi: 10.3390/polym16060861.

[76] X. Su, L. Sutarlie, and X. J. Loh, "Sensors, Biosensors, and Analytical Technologies for Aquaculture Water Quality," *Research*, vol. 2020, Jan. 2020, doi: 10.34133/2020/8272705.

[77] H. Sohrabi *et al.*, "Recent advances on portable sensing and biosensing assays applied for detection of main chemical and biological pollutant agents in water samples: A critical review," *TrAC Trends in Analytical Chemistry*, vol. 143, p. 116344, Oct. 2021, doi: 10.1016/j.trac.2021.116344.

[78] S. Gavrilaș, C. Ștefan Ursachi, S. Perța-Crișan, and F.-D. Munteanu, "Recent Trends in Biosensors for Environmental Quality Monitoring," *Sensors*, vol. 22, no. 4, p. 1513, Feb. 2022, doi: 10.3390/s22041513.

[79] H. Jayan, H. Pu, and D.-W. Sun, "Recent development in rapid detection techniques for microorganism activities in food matrices using bio-recognition: A review," *Trends Food Sci Technol*, vol. 95, pp. 233–246, Jan. 2020, doi: 10.1016/j.tifs.2019.11.007.

[80] R. Ali and D. V. Singh, "Biosensors: A Biotechnological Tool for Monitoring Environmental Pollution," in *Bioremediation and Biotechnology, Vol 3*, Cham: Springer International Publishing, 2020, pp. 331–348. doi: 10.1007/978-3-030-46075-4_15.

[81] Y. Hui, Z. Huang, M. E. E. Alahi, A. Nag, S. Feng, and S. C. Mukhopadhyay, "Recent Advancements in Electrochemical Biosensors for Monitoring the Water Quality," *Biosensors (Basel)*, vol. 12, no. 7, p. 551, Jul. 2022, doi: 10.3390/bios12070551.

[82] K. B. Shivaram, P. Bhatt, M. S. Verma, K. Clase, and H. Simsek, "Bacteriophage-based biosensors for detection of pathogenic microbes in wastewater," *Science of The Total Environment*, vol. 901, p. 165859, Nov. 2023, doi: 10.1016/j.scitotenv.2023.165859.

[83] S. S. Arya, N. K. Morsy, D. K. Islayem, S. A. Alkhatib, C. Pitsalidis, and A.-M. Pappa, "Bacterial Membrane Mimetics: From Biosensing to Disease Prevention and Treatment," *Biosensors (Basel)*, vol. 13, no. 2, p. 189, Jan. 2023, doi: 10.3390/bios13020189.

[84] C. Fricke, H. Harms, and T. Maskow, "Rapid Calorimetric Detection of Bacterial Contamination: Influence of the Cultivation Technique," *Front Microbiol*, vol. 10, Nov. 2019, doi: 10.3389/fmicb.2019.02530.

[85] E. Elcin and H. A. Öktem, "Whole-cell fluorescent bacterial bioreporter for arsenic detection in water," *International Journal of Environmental Science and Technology*, vol. 16, no. 10, pp. 5489–5500, Oct. 2019, doi: 10.1007/s13762-018-2077-0.

[86] E. T. S. G. da Silva, D. E. P. Souto, J. T. C. Barragan, J. de F. Giarola, A. C. M. de Moraes, and L. T. Kubota, "Electrochemical Biosensors in Point-of-Care Devices: Recent Advances

and Future Trends," *ChemElectroChem*, vol. 4, no. 4, pp. 778–794, Apr. 2017, doi: 10.1002/celc.201600758.

[87] J. Zhang *et al.*, "Recent advances of fluorescent sensors for bacteria detection-A review," *Talanta*, vol. 254, p. 124133, Mar. 2023, doi: 10.1016/j.talanta.2022.124133.

[88] G. Pantaleo, B. Correia, C. Fenwick, V. S. Joo, and L. Perez, "Antibodies to combat viral infections: development strategies and progress," *Nat Rev Drug Discov*, vol. 21, no. 9, pp. 676–696, Sep. 2022, doi: 10.1038/s41573-022-00495-3.

[89] G. Karuppaiah, A. Vashist, M. Nair, M. Veerapandian, and P. Manickam, "Emerging trends in point-of-care biosensing strategies for molecular architectures and antibodies of SARS-CoV-2," *Biosens Bioelectron X*, vol. 13, p. 100324, May 2023, doi: 10.1016/j.biosx.2023.100324.

[90] D. Li *et al.*, "Recent advances on aptamer-based biosensors for detection of pathogenic bacteria," *World J Microbiol Biotechnol*, vol. 37, no. 3, p. 45, Mar. 2021, doi: 10.1007/s11274-021-03002-9.

[91] P. P. Banada and A. K. Bhunia, "Antibodies and Immunoassays for Detection of Bacterial Pathogens," in *Principles of Bacterial Detection: Biosensors, Recognition Receptors and Microsystems*, New York, NY: Springer New York, pp. 567–602. doi: 10.1007/978-0-387-75113-9_21.

[92] "Antibody-Based Biosensors," in *Biosensors*, Wiley, 2024, pp. 91–137. doi: 10.1002/9781394268238.ch4.

[93] O. I. Guliy, S. S. Evstigneeva, and L. A. Dykman, "The Use of Phage Antibodies for Microbial Cells Detection (Review)," *Прикладная биохимия и микробиология*, vol. 59, no. 2, pp. 150–166, Mar. 2023, doi: 10.31857/S0555109923020083.

[94] R. K. Verma and A. Jain, "*Retracted* : Antibodies to mycobacterial antigens for diagnosis of tuberculosis," *FEMS Immunol Med Microbiol*, vol. 51, no. 3, pp. 453–461, Dec. 2007, doi: 10.1111/j.1574-695X.2007.00302.x.

[95] C. Park, J. Lee, Y. Kim, J. Kim, J. Lee, and S. Park, "3D-printed microfluidic magnetic preconcentrator for the detection of bacterial pathogen using an ATP luminometer and antibody-conjugated magnetic nanoparticles," *J Microbiol Methods*, vol. 132, pp. 128–133, Jan. 2017, doi: 10.1016/j.mimet.2016.12.001.

[96] T. D. Tavares *et al.*, "Activity of Specialized Biomolecules against Gram-Positive and Gram-Negative Bacteria," *Antibiotics*, vol. 9, no. 6, p. 314, Jun. 2020, doi: 10.3390/antibiotics9060314.

[97] A. Bin Hafeez, X. Jiang, P. J. Bergen, and Y. Zhu, "Antimicrobial Peptides: An Update on Classifications and Databases," *Int J Mol Sci*, vol. 22, no. 21, p. 11691, Oct. 2021, doi: 10.3390/ijms222111691.

[98] N. P. Giordano, M. B. Cian, and Z. D. Dalebroux, "Outer Membrane Lipid Secretion and the Innate Immune Response to Gram-Negative Bacteria," *Infect Immun*, vol. 88, no. 7, Jun. 2020, doi: 10.1128/IAI.00920-19.

[99] S. He and C. M. Deber, “Interaction of designed cationic antimicrobial peptides with the outer membrane of gram-negative bacteria,” *Sci Rep*, vol. 14, no. 1, p. 1894, Jan. 2024, doi: 10.1038/s41598-024-51716-1.

[100] Z. Watkins, A. Karajic, T. Young, R. White, and J. Heikenfeld, “Week-Long Operation of Electrochemical Aptamer Sensors: New Insights into Self-Assembled Monolayer Degradation Mechanisms and Solutions for Stability in Serum at Body Temperature,” *ACS Sens*, vol. 8, no. 3, pp. 1119–1131, Mar. 2023, doi: 10.1021/acssensors.2c02403.

[101] C. Cuntín-Abal, B. Jurado-Sánchez, and A. Escarpa, “Playing with biological selectivity: Antimicrobial peptides and bacteriophages-based optical biosensors for pathogenic bacteria detection,” *TrAC Trends in Analytical Chemistry*, vol. 172, p. 117565, Mar. 2024, doi: 10.1016/j.trac.2024.117565.

[102] B. S. Lopes, A. Hanafiah, R. Nachimuthu, S. Muthupandian, Z. N. Md Nesran, and S. Patil, “The Role of Antimicrobial Peptides as Antimicrobial and Antibiofilm Agents in Tackling the Silent Pandemic of Antimicrobial Resistance,” *Molecules*, vol. 27, no. 9, p. 2995, May 2022, doi: 10.3390/molecules27092995.

[103] S. Ji *et al.*, “Antimicrobial peptides: An alternative to traditional antibiotics,” *Eur J Med Chem*, vol. 265, p. 116072, Feb. 2024, doi: 10.1016/j.ejmech.2023.116072.

[104] T. N. T. Dao, E. Y. Lee, B. Koo, C. E. Jin, T. Y. Lee, and Y. Shin, “A microfluidic enrichment platform with a recombinase polymerase amplification sensor for pathogen diagnosis,” *Anal Biochem*, vol. 544, pp. 87–92, Mar. 2018, doi: 10.1016/j.ab.2017.12.030.

[105] J. Chung *et al.*, “Effects of storage conditions on the performance of an electrochemical aptamer-based sensor,” *Sensors & Diagnostics*, vol. 3, no. 6, pp. 1044–1050, 2024, doi: 10.1039/D4SD00066H.

[106] M. Saad and S. P. Faucher, “Aptamers and Aptamer-Coupled Biosensors to Detect Water-Borne Pathogens,” *Front Microbiol*, vol. 12, Feb. 2021, doi: 10.3389/fmicb.2021.643797.

[107] A. Mansouri, K. Abnous, M. S. Nabavinia, M. Ramezani, and S. M. Taghdisi, “In vitro selection of tacrolimus binding aptamer by systematic evolution of ligands by exponential enrichment method for the development of a fluorescent aptasensor for sensitive detection of tacrolimus,” *J Pharm Biomed Anal*, vol. 177, p. 112853, Jan. 2020, doi: 10.1016/j.jpba.2019.112853.

[108] M. Banakar *et al.*, “Electrochemical Biosensors for Pathogen Detection: An Updated Review,” *Biosensors (Basel)*, vol. 12, no. 11, p. 927, Oct. 2022, doi: 10.3390/bios12110927.

[109] Y. Tang, Y. Li, P. Chen, S. Zhong, and Y. Yang, “Nucleic Acid Aptamer-Based Sensors for Bacteria Detection: A Review,” *BioEssays*, vol. 47, no. 3, Mar. 2025, doi: 10.1002/bies.202400111.

[110] V. Léguillier, B. Heddi, and J. Vidic, “Recent Advances in Aptamer-Based Biosensors for Bacterial Detection,” *Biosensors (Basel)*, vol. 14, no. 5, p. 210, Apr. 2024, doi: 10.3390/bios14050210.

[111] J. G. Bruno, J. C. Sivils, and T. Phillips, “Aptamer–Magnetic Bead Quantum Dot Sandwich Assays for Foodborne Pathogen Detection: Pros, Cons, and Lessons Learned,” *J AOAC Int*, vol. 100, no. 4, pp. 895–899, Jul. 2017, doi: 10.5740/jaoacint.17-0163.

[112] Y. Jiang, S. Zou, and X. Cao, “A simple dendrimer-aptamer based microfluidic platform for E. coli O157:H7 detection and signal intensification by rolling circle amplification,” *Sens Actuators B Chem*, vol. 251, pp. 976–984, Nov. 2017, doi: 10.1016/j.snb.2017.05.146.

[113] C.-H. Wang, J.-J. Wu, and G.-B. Lee, “Screening of highly-specific aptamers and their applications in paper-based microfluidic chips for rapid diagnosis of multiple bacteria,” *Sens Actuators B Chem*, vol. 284, pp. 395–402, Apr. 2019, doi: 10.1016/j.snb.2018.12.112.

[114] V. G. Correia *et al.*, “Mapping Molecular Recognition of β1,3-1,4-Glucans by a Surface Glycan-Binding Protein from the Human Gut Symbiont Bacteroides ovatus,” *Microbiol Spectr*, vol. 9, no. 3, Dec. 2021, doi: 10.1128/Spectrum.01826-21.

[115] C. P. Sager, D. Eriş, M. Smieško, R. Hevey, and B. Ernst, “What contributes to an effective mannose recognition domain?,” *Beilstein Journal of Organic Chemistry*, vol. 13, pp. 2584–2595, Dec. 2017, doi: 10.3762/bjoc.13.255.

[116] S. Guo *et al.*, “Structural Basis of Ligand Selectivity by a Bacterial Adhesin Lectin Involved in Multispecies Biofilm Formation,” *mBio*, vol. 12, no. 2, Apr. 2021, doi: 10.1128/mBio.00130-21.

[117] F. Bonnardel *et al.*, “Proteome-wide prediction of bacterial carbohydrate-binding proteins as a tool for understanding commensal and pathogen colonisation of the vaginal microbiome,” *NPJ Biofilms Microbiomes*, vol. 7, no. 1, p. 49, Jun. 2021, doi: 10.1038/s41522-021-00220-9.

[118] O. B. Daramola *et al.*, “Bio-Receptors Functionalized Nanoparticles: A Resourceful Sensing and Colorimetric Detection Tool for Pathogenic Bacteria and Microbial Biomolecules,” *Frontiers in Nanotechnology*, vol. 4, Apr. 2022, doi: 10.3389/fnano.2022.885803.

[119] A. Pennacchio *et al.*, “A bacterial biosensor based on gold nanoparticles functionalized by a hydrophobin-chimera and combined with machine learning for user-friendly detection,” *Sens Actuators B Chem*, vol. 410, p. 135645, Jul. 2024, doi: 10.1016/j.snb.2024.135645.

[120] F. Cheng Y, “Biosensors for Bacterial Detection,” *Int J Biosens Bioelectron*, vol. 2, no. 6, Jul. 2017, doi: 10.15406/ijbsbe.2017.02.00048.

[121] H. Liu, “Pathogenic Bacterial Sensors Based on Carbohydrates as Sensing Elements,” in *Principles of Bacterial Detection: Biosensors, Recognition Receptors and Microsystems*, New York, NY: Springer New York, pp. 659–687. doi: 10.1007/978-0-387-75113-9_24.

[122] L. Otten, E. Fullam, and M. I. Gibson, “Discrimination between bacterial species by ratiometric analysis of their carbohydrate binding profile,” *Mol Biosyst*, vol. 12, no. 2, pp. 341–344, 2016, doi: 10.1039/C5MB00720H.

[123] B. P. M. Lake and A. F. Rullo, “Offsetting Low-Affinity Carbohydrate Binding with Covalency to Engage Sugar-Specific Proteins for Tumor-Immune Proximity Induction,” *ACS Cent Sci*, vol. 9, no. 11, pp. 2064–2075, Nov. 2023, doi: 10.1021/acscentsci.3c01052.

[124] B. B. Haab, “Using lectins in biomarker research: Addressing the limitations of sensitivity and availability,” *Proteomics Clin Appl*, vol. 6, no. 7–8, pp. 346–350, Aug. 2012, doi: 10.1002/prca.201200014.

[125] X. Zeng, C. A. S. Andrade, M. D. L. Oliveira, and X.-L. Sun, “Carbohydrate–protein interactions and their biosensing applications,” *Anal Bioanal Chem*, vol. 402, no. 10, pp. 3161–3176, Apr. 2012, doi: 10.1007/s00216-011-5594-y.

[126] R. M. Cooper *et al.*, “A microdevice for rapid optical detection of magnetically captured rare blood pathogens,” *Lab Chip*, vol. 14, no. 1, pp. 182–188, 2014, doi: 10.1039/C3LC50935D.

[127] A. Katz and M. E. Davis, “Molecular imprinting of bulk, microporous silica,” *Nature*, vol. 403, no. 6767, pp. 286–289, Jan. 2000, doi: 10.1038/35002032.

[128] E. Kim *et al.*, “Selective detection of estradiol using a molecularly imprinted self-assembled monolayer on gold surface,” *Toxicol Environ Health Sci*, vol. 1, no. 2, pp. 117–121, Aug. 2009, doi: 10.1007/BF03216472.

[129] R. Gao, X. Su, X. He, L. Chen, and Y. Zhang, “Preparation and characterisation of core–shell CNTs@MIPs nanocomposites and selective removal of estrone from water samples,” *Talanta*, vol. 83, no. 3, pp. 757–764, Jan. 2011, doi: 10.1016/j.talanta.2010.10.034.

[130] X. Kong, R. Gao, X. He, L. Chen, and Y. Zhang, “Synthesis and characterization of the core–shell magnetic molecularly imprinted polymers (Fe3O4@MIPs) adsorbents for effective extraction and determination of sulfonamides in the poultry feed,” *J Chromatogr A*, vol. 1245, pp. 8–16, Jul. 2012, doi: 10.1016/j.chroma.2012.04.061.

[131] M. Pourfarzib, M. Shekarchi, H. Rastegar, B. Akbari-Adergani, A. Mehramizi, and R. Dinarvand, “Molecularly imprinted nanoparticles prepared by miniemulsion polymerization as a sorbent for selective extraction and purification of efavirenz from human serum and urine,” *Journal of Chromatography B*, vol. 974, pp. 1–8, Jan. 2015, doi: 10.1016/j.jchromb.2014.10.012.

[132] Z. Wang, T. Qiu, L. Guo, J. Ye, L. He, and X. Li, “The synthesis of molecular recognition polymer particles via miniemulsion polymerization,” *React Funct Polym*, vol. 126, pp. 1–8, May 2018, doi: 10.1016/j.reactfunctpolym.2018.02.013.

[133] C. Alexander *et al.*, “Molecular imprinting science and technology: a survey of the literature for the years up to and including 2003,” *Journal of Molecular Recognition*, vol. 19, no. 2, pp. 106–180, Mar. 2006, doi: 10.1002/jmr.760.

[134] S. Chen, X. Chen, L. Zhang, J. Gao, and Q. Ma, “Electrochemiluminescence Detection of *Escherichia coli* O157:H7 Based on a Novel Polydopamine Surface Imprinted Polymer Biosensor,” *ACS Appl Mater Interfaces*, vol. 9, no. 6, pp. 5430–5436, Feb. 2017, doi: 10.1021/acsami.6b12455.

[135] E. Yilmaz, D. Majidi, E. Ozgur, and A. Denizli, “Whole cell imprinting based Escherichia coli sensors: A study for SPR and QCM,” *Sens Actuators B Chem*, vol. 209, pp. 714–721, Mar. 2015, doi: 10.1016/j.snb.2014.12.032.

[136] P. Cornelis *et al.*, "Sensitive and specific detection of E. coli using biomimetic receptors in combination with a modified heat-transfer method," *Biosens Bioelectron*, vol. 136, pp. 97–105, Jul. 2019, doi: 10.1016/j.bios.2019.04.026.

[137] A. K. Yadav, D. Verma, N. Dalal, A. Kumar, and P. R. Solanki, "Molecularly imprinted polymer-based nanodiagnostics for clinically pertinent bacteria and virus detection for future pandemics," *Biosens Bioelectron X*, vol. 12, p. 100257, Dec. 2022, doi: 10.1016/j.biosx.2022.100257.

[138] M. Golabi, F. Kuralay, E. W. H. Jager, V. Beni, and A. P. F. Turner, "Electrochemical bacterial detection using poly(3-aminophenylboronic acid)-based imprinted polymer," *Biosens Bioelectron*, vol. 93, pp. 87–93, Jul. 2017, doi: 10.1016/j.bios.2016.09.088.

[139] X. Shan, T. Yamauchi, Y. Yamamoto, H. Shiigi, and T. Nagaoka, "A rapid and specific bacterial detection method based on cell-imprinted microplates," *Analyst*, vol. 143, no. 7, pp. 1568–1574, 2018, doi: 10.1039/C7AN02057K.

[140] T. Sarkhosh, E. Mayerberger, K. Jellison, and S. Jedlicka, "Development of cell-imprinted polymer surfaces for Cryptosporidium capture and detection," *Water Res*, vol. 205, p. 117675, Oct. 2021, doi: 10.1016/j.watres.2021.117675.

[141] P. T. So and C. Y. Dong, "Fluorescence Spectrophotometry," in *Encyclopedia of Life Sciences*, Wiley, 2001. doi: 10.1038/npg.els.0002978.

[142] R. Redmond, "Introduction To Fluorescence And Photophysics," in *Handbook of Biomedical Fluorescence*, CRC Press, 2003. doi: 10.1201/9780203912096.pt1.

[143] Y. Huang, W. Chen, J. Chung, J. Yin, and J. Yoon, "Recent progress in fluorescent probes for bacteria," *Chem Soc Rev*, vol. 50, no. 13, pp. 7725–7744, 2021, doi: 10.1039/D0CS01340D.

[144] Y. Kong, Q. Jiang, F. Zhang, and Y. Yang, "Small Molecular Fluorescent Probes: Application Progress of Specific Bacteria Detection and Antibacterial Phototherapy," *Chem Asian J*, vol. 18, no. 11, Jun. 2023, doi: 10.1002/asia.202300178.

[145] S. A. Yoon, S. Y. Park, Y. Cha, L. Gopala, and M. H. Lee, "Strategies of Detecting Bacteria Using Fluorescence-Based Dyes," *Front Chem*, vol. 9, Aug. 2021, doi: 10.3389/fchem.2021.743923.

[146] Y. Shen, L. Xu, and Y. Li, "Biosensors for rapid detection of *Salmonella* in food: A review," *Compr Rev Food Sci Food Saf*, vol. 20, no. 1, pp. 149–197, Jan. 2021, doi: 10.1111/1541-4337.12662.

[147] C. H. Woo, S. Jang, G. Shin, G. Y. Jung, and J. W. Lee, "Sensitive fluorescence detection of SARS-CoV-2 RNA in clinical samples via one-pot isothermal ligation and transcription," *Nat Biomed Eng*, vol. 4, no. 12, pp. 1168–1179, Sep. 2020, doi: 10.1038/s41551-020-00617-5.

[148] H. Gunter, C. Bradley, D. M. Hannah, S. Manaseki-Holland, R. Stevens, and K. Khamis, "Advances in quantifying microbial contamination in potable water: Potential of fluorescence-based sensor technology," *WIREs Water*, vol. 10, no. 1, Jan. 2023, doi: 10.1002/wat2.1622.

[149] J. A. Huffman *et al.*, “Real-time sensing of bioaerosols: Review and current perspectives,” *Aerosol Science and Technology*, vol. 54, no. 5, pp. 465–495, May 2020, doi: 10.1080/02786826.2019.1664724.

[150] Y. Guo, J. Li, X. Song, K. Xu, J. Wang, and C. Zhao, “Label-Free Detection of *Staphylococcus aureus* Based on Bacteria-Imprinted Polymer and Turn-on Fluorescence Probes,” *ACS Appl Bio Mater*, vol. 4, no. 1, pp. 420–427, Jan. 2021, doi: 10.1021/acsabm.0c00897.

[151] X. Zhao, Y. Cui, J. Wang, and J. Wang, “Preparation of Fluorescent Molecularly Imprinted Polymers via Pickering Emulsion Interfaces and the Application for Visual Sensing Analysis of Listeria Monocytogenes,” *Polymers (Basel)*, vol. 11, no. 6, p. 984, Jun. 2019, doi: 10.3390/polym11060984.

[152] J. Bezdekova *et al.*, “Magnetic molecularly imprinted polymers used for selective isolation and detection of Staphylococcus aureus,” *Food Chem*, vol. 321, p. 126673, Aug. 2020, doi: 10.1016/j.foodchem.2020.126673.

[153] W. Zhang, X. Zang, W. Guo, Y. Fang, and B. Cui, “Photocatalytic Organic Semiconductor-Bacteria Imprinted Polymers for Highly Selective Determination of *Staphylococcus aureus* at the Single-Cell Level,” *Anal Chem*, vol. 97, no. 4, pp. 2273–2282, Feb. 2025, doi: 10.1021/acs.analchem.4c05450.

[154] T. M. Iakimova, B. Heidt, and A. Q. Shen, “Surface-imprinted polymers based on 3D printing resin for selective bacteria detection,” *Cell Rep Phys Sci*, vol. 5, no. 8, p. 101853, Aug. 2024, doi: 10.1016/j.xcrp.2024.101853.

[155] Z. Zhang, X. Ma, M. Jia, B. Li, J. Rong, and X. Yang, “Deposition of CdTe quantum dots on microfluidic paper chips for rapid fluorescence detection of pesticide 2,4-D,” *Analyst*, vol. 144, no. 4, pp. 1282–1291, 2019, doi: 10.1039/C8AN02051E.

[156] Z. Zhang *et al.*, “Fluorescence detection of 2,4-dichlorophenoxyacetic acid by ratiometric fluorescence imaging on paper-based microfluidic chips,” *Analyst*, vol. 145, no. 3, pp. 963–974, 2020, doi: 10.1039/C9AN01798D.

[157] Y. Yang *et al.*, “Fluorometric microplate-based dimethoate assay using CdSe/ZnS quantum dots coated with a molecularly imprinted polymer,” *Microchimica Acta*, vol. 186, no. 8, p. 589, Aug. 2019, doi: 10.1007/s00604-019-3649-5.

[158] M. Amjadi and R. Jalili, “Molecularly imprinted mesoporous silica embedded with carbon dots and semiconductor quantum dots as a ratiometric fluorescent sensor for diniconazole,” *Biosens Bioelectron*, vol. 96, pp. 121–126, Oct. 2017, doi: 10.1016/j.bios.2017.04.045.

[159] Y. Gao *et al.*, “Fluorescence-enhanced microfluidic sensor for highly sensitive in-situ detection of copper ions in lubricating oil,” *Mater Des*, vol. 191, p. 108693, Jun. 2020, doi: 10.1016/j.matdes.2020.108693.

[160] X. Zhao, M. Li, and Y. Liu, “Microfluidic-Based Approaches for Foodborne Pathogen Detection,” *Microorganisms*, vol. 7, no. 10, p. 381, Sep. 2019, doi: 10.3390/microorganisms7100381.

[161] L. Zhou *et al.*, “Microfluidic-RT-LAMP chip for the point-of-care detection of emerging and re-emerging enteric coronaviruses in swine,” *Anal Chim Acta*, vol. 1125, pp. 57–65, Aug. 2020, doi: 10.1016/j.aca.2020.05.034.

[162] R. R. Khan, H. Ibrahim, G. Rawal, J. Zhang, M. Lu, and L. Dong, “Multichannel microfluidic virus sensor for rapid detection of respiratory viruses using virus-imprinted polymer for digital livestock farming,” *Sens Actuators B Chem*, vol. 389, p. 133920, Aug. 2023, doi: 10.1016/j.snb.2023.133920.

[163] Y. Shang, G. Xing, H. Lin, Y. Sun, S. Chen, and J.-M. Lin, “Development of nucleic acid extraction and real-time recombinase polymerase amplification (RPA) assay integrated microfluidic biosensor for multiplex detection of foodborne bacteria,” *Food Control*, vol. 155, p. 110047, Jan. 2024, doi: 10.1016/j.foodcont.2023.110047.

[164] G. Xing *et al.*, “A microfluidic biosensor for multiplex immunoassay of foodborne pathogens agitated by programmed audio signals,” *Chinese Chemical Letters*, vol. 35, no. 10, p. 109491, Oct. 2024, doi: 10.1016/j.cclet.2024.109491.

[165] S. B. Somvanshi *et al.*, “Microfluidic paper-based aptasensor devices for multiplexed detection of pathogenic bacteria,” *Biosens Bioelectron*, vol. 207, p. 114214, Jul. 2022, doi: 10.1016/j.bios.2022.114214.

[166] X. Hu, C. Lin, G. Li, T. Jiang, and J. Shen, “A microfluidic chip-based multiplex PCR-reverse dot blot hybridization technique for rapid detection of enteropathogenic bacteria,” *J Microbiol Methods*, vol. 211, p. 106785, Aug. 2023, doi: 10.1016/j.mimet.2023.106785.

[167] G. Xing, N. Li, H. Lin, Y. Shang, Q. Pu, and J.-M. Lin, “Microfluidic biosensor for one-step detection of multiplex foodborne bacteria ssDNA simultaneously by smartphone,” *Talanta*, vol. 253, p. 123980, Feb. 2023, doi: 10.1016/j.talanta.2022.123980.

[168] Jr. , N. F. Fell *et al.*, “Concentration, size, and excitation power effects on fluorescence from microdroplets and microparticles containing tryptophan and bacteria</title>,” J. Leonelli and M. L. Althouse, Eds., Jan. 1999, pp. 52–63. doi: 10.1117/12.336843.

[169] L. F. Wolff *et al.*, “Bacterial Concentration Fluorescence Immunoassay (BCFIA) for the Detection of Periodontopathogens in Plaque,” *J Periodontol*, vol. 63, no. 12S, pp. 1093–1101, Dec. 1992, doi: 10.1902/jop.1992.63.12s.1093.

[170] S. Akhtarian, A. Doostmohammadi, K. Youssef, G. Kraft, S. Kaur Brar, and P. Rezai, “Metal Microwires Functionalized with Cell-Imprinted Polymer for Capturing Bacteria in Water,” *ACS Appl Polym Mater*, vol. 5, no. 5, pp. 3235–3246, May 2023, doi: 10.1021/acsapm.2c01886.

[171] A. Doostmohammadi *et al.*, “Molecularly imprinted polymer (MIP) based core-shell microspheres for bacteria isolation,” *Polymer (Guildf)*, vol. 251, p. 124917, Jun. 2022, doi: 10.1016/j.polymer.2022.124917.

[172] L. K. Chaganti, N. Venkatakrishnan, and K. Bose, “An efficient method for FITC labelling of proteins using tandem affinity purification,” *Biosci Rep*, vol. 38, no. 6, Dec. 2018, doi: 10.1042/BSR20181764.

[173] M. Eskenazy, G. Konstantinov, R. Ivanova, and D. Strahilov, “Detection by Immunofluorescence of Common Antigenic Determinants in Unrelated Gram-Negative Bacteria and Their Lipopolysaccharides,” *Journal of Infectious Diseases*, vol. 135, no. 6, pp. 965–969, Jun. 1977, doi: 10.1093/infdis/135.6.965.

[174] E. Grunberg and R. Cleeland, “Fluorescence and Viability of *Proteus mirabilis* Stained Directly with Fluorescein Isothiocyanate,” *J Bacteriol*, vol. 92, no. 1, pp. 23–27, Jul. 1966, doi: 10.1128/jb.92.1.23-27.1966.

[175] Y. Tian, M. Yu, Z. Li, J. Han, L. Yang, and S. Han, “Optical Tracking of Phagocytosis with an Activatable Profluorophore Metabolically Incorporated into Bacterial Peptidoglycan,” *Anal Chem*, vol. 87, no. 16, pp. 8381–8386, Aug. 2015, doi: 10.1021/acs.analchem.5b01633.

[176] A. M. Powl, J. Carney, P. Marius, J. M. East, and A. G. Lee, “Lipid interactions with bacterial channels: fluorescence studies,” *Biochem Soc Trans*, vol. 33, no. 5, p. 905, Oct. 2005, doi: 10.1042/BST20050905.

[177] L. Y. Ma, H. Y. Wang, H. Xie, and L. X. Xu, “A long lifetime chemical sensor: study on fluorescence property of fluorescein isothiocyanate and preparation of pH chemical sensor,” *Spectrochim Acta A Mol Biomol Spectrosc*, vol. 60, no. 8–9, pp. 1865–1872, Jul. 2004, doi: 10.1016/j.saa.2003.10.004.

[178] G. Zhang *et al.*, “Defect-rich Co,N-doped Ti3C2Tx/C/poly (3,4-ethylenedioxy thiophene) molecularly imprinted sensor for ultrasensitive electrochemical detection of gatifloxacin,” *Talanta*, vol. 295, p. 128364, Dec. 2025, doi: 10.1016/j.talanta.2025.128364.

[179] S. Akhtarian, S. Kaur Brar, and P. Rezai, “Electrochemical Impedance Spectroscopy-Based Microfluidic Biosensor Using Cell-Imprinted Polymers for Bacteria Detection,” *Biosensors (Basel)*, vol. 14, no. 9, p. 445, Sep. 2024, doi: 10.3390/bios14090445.

[180] S. Akhtarian, A. Doostmohammadi, D.-E. Archonta, G. Kraft, S. K. Brar, and P. Rezai, “Microfluidic Sensor Based on Cell-Imprinted Polymer-Coated Microwires for Conductometric Detection of Bacteria in Water,” *Biosensors (Basel)*, vol. 13, no. 10, p. 943, Oct. 2023, doi: 10.3390/bios13100943.

[181] X. Zheng *et al.*, “Towards Clean and Safe Water: A Review on the Emerging Role of Imprinted Polymer-Based Electrochemical Sensors,” *Sensors*, vol. 21, no. 13, p. 4300, Jun. 2021, doi: 10.3390/s21134300.

[182] G. P. González, P. F. Hernando, and J. S. Durand Alegría, “A MIP-based flow-through fluoroimmunosensor as an alternative to immunosensors for the determination of digoxin in serum samples,” *Anal Bioanal Chem*, vol. 394, no. 4, pp. 963–970, Jun. 2009, doi: 10.1007/s00216-008-2584-9.

[183] M. C. Moreno-Bondi *et al.*, “Molecularly imprinted polymers as biomimetic receptors for fluorescence-based optical sensors,” Jul. 2007, p. 66190C. doi: 10.1117/12.738347.

[184] H. D. ERTUĞRUL UYGUN and M. N. DEMİR, “The Role of Molecularly Imprinted Polymers In Sensor Technology: Electrochemical, Optical and Piezoelectric Sensor Applications,” *Journal of the Turkish Chemical Society Section A: Chemistry*, vol. 10, no. 4, pp. 1081–1098, Nov. 2023, doi: 10.18596/jotcsa.1285655.

[185] N. K. Rajan, X. Duan, and M. A. Reed, “Performance limitations for nanowire/nanoribbon biosensors,” *WIREs Nanomedicine and Nanobiotechnology*, vol. 5, no. 6, pp. 629–645, Nov. 2013, doi: 10.1002/wnan.1235.

[186] N. Couniot, D. Flandre, L. A. Francis, and A. Afzalian, “Signal-to-noise ratio optimization for detecting bacteria with interdigitated microelectrodes,” *Sens Actuators B Chem*, vol. 189, pp. 43–51, Dec. 2013, doi: 10.1016/j.snb.2012.12.008.

[187] R. Chaudhary, N. B. Singh, G. Nagpal, F. K. Saah, and A. K. Singh, “Nanomaterials in bacterial detection: current trends and future outlook,” *Zastita Materijala*, vol. 66, no. 1, pp. 56–65, Mar. 2025, doi: 10.62638/ZasMat1256.

[188] T. M. Le and N. T. Tran, “Investigating the Antibacterial Activities of Graphene Oxide Loaded Spiky Gold Nanocomposites via Chitosan linker,” *Journal of Technical Education Science*, no. 80, pp. 55–61, Dec. 2023, doi: 10.54644/jte.80.2023.1484.

[189] F. Mi *et al.*, “Recent advancements in microfluidic chip biosensor detection of foodborne pathogenic bacteria: a review,” *Anal Bioanal Chem*, vol. 414, no. 9, pp. 2883–2902, Apr. 2022, doi: 10.1007/s00216-021-03872-w.

[190] A. Ahmed, J. V. Rushworth, N. A. Hirst, and P. A. Millner, “Biosensors for Whole-Cell Bacterial Detection,” *Clin Microbiol Rev*, vol. 27, no. 3, pp. 631–646, Jul. 2014, doi: 10.1128/CMR.00120-13.

[191] P. Qi, Y. Wan, and D. Zhang, “Impedimetric biosensor based on cell-mediated bioimprinted films for bacterial detection,” *Biosens Bioelectron*, vol. 39, no. 1, pp. 282–288, Jan. 2013, doi: 10.1016/j.bios.2012.07.078.

[192] A. Karrat and A. Amine, “Innovative approaches to suppress non-specific adsorption in molecularly imprinted polymers for sensing applications,” *Biosens Bioelectron*, vol. 250, p. 116053, Apr. 2024, doi: 10.1016/j.bios.2024.116053.

[193] D. Tartaglia *et al.*, “Sarcina Ventriculi infection: a rare but fearsome event. A Systematic Review of the Literature,” *International Journal of Infectious Diseases*, vol. 115, pp. 48–61, Feb. 2022, doi: 10.1016/j.ijid.2021.11.027.

[194] S. Wu, N. Duan, Z. Shi, C. Fang, and Z. Wang, “Simultaneous Aptasensor for Multiplex Pathogenic Bacteria Detection Based on Multicolor Upconversion Nanoparticles Labels,” *Anal Chem*, vol. 86, no. 6, pp. 3100–3107, Mar. 2014, doi: 10.1021/ac404205c.

[195] M. Angelopoulou, P. Petrou, K. Misiakos, I. Raptis, and S. Kakabakos, “Simultaneous Detection of Salmonella typhimurium and Escherichia coli O157:H7 in Drinking Water and

Milk with Mach–Zehnder Interferometers Monolithically Integrated on Silicon Chips," *Biosensors (Basel)*, vol. 12, no. 7, p. 507, Jul. 2022, doi: 10.3390/bios12070507.

[196] Y. Liu *et al.*, "A microfluidic biosensor for rapid detection of Salmonella typhimurium based on magnetic separation, enzymatic catalysis and electrochemical impedance analysis," *Chinese Chemical Letters*, vol. 33, no. 6, pp. 3156–3160, Jun. 2022, doi: 10.1016/j.cclet.2021.10.064.

[197] J. Fei, W. Dou, and G. Zhao, "Amperometric immunoassay for the detection of Salmonella pullorum using a screen - printed carbon electrode modified with gold nanoparticle-coated reduced graphene oxide and immunomagnetic beads," *Microchimica Acta*, vol. 183, no. 2, pp. 757–764, Feb. 2016, doi: 10.1007/s00604-015-1721-3.

[198] M. Xu, R. Wang, and Y. Li, "An electrochemical biosensor for rapid detection of E. coli O157:H7 with highly efficient bi-functional glucose oxidase-polydopamine nanocomposites and Prussian blue modified screen-printed interdigitated electrodes," *Analyst*, vol. 141, no. 18, pp. 5441–5449, 2016, doi: 10.1039/C6AN00873A.

[199] J. Wu, R. Wang, Y. Lu, M. Jia, J. Yan, and X. Bian, "Facile Preparation of a Bacteria Imprinted Artificial Receptor for Highly Selective Bacterial Recognition and Label-Free Impedimetric Detection," *Anal Chem*, vol. 91, no. 1, pp. 1027–1033, Jan. 2019, doi: 10.1021/acs.analchem.8b04314.

[200] A. Ait Lahcen, F. Arduini, F. Lista, and A. Amine, "Label-free electrochemical sensor based on spore-imprinted polymer for Bacillus cereus spore detection," *Sens Actuators B Chem*, vol. 276, pp. 114–120, Dec. 2018, doi: 10.1016/j.snb.2018.08.031.

[201] N. Krithiga, K. B. Viswanath, V. S. Vasantha, and A. Jayachitra, "Specific and selective electrochemical immunoassay for Pseudomonas aeruginosa based on pectin–gold nano composite," *Biosens Bioelectron*, vol. 79, pp. 121–129, May 2016, doi: 10.1016/j.bios.2015.12.006.

[202] Y. Zhang, C. Xu, T. Guo, and L. Hong, "An automated bacterial concentration and recovery system for pre-enrichment required in rapid Escherichia coli detection," *Sci Rep*, vol. 8, no. 1, p. 17808, Dec. 2018, doi: 10.1038/s41598-018-35970-8.

[203] J. Kupai, M. Razali, S. Buyuktiryaki, R. Kecili, and G. Szekely, "Long-term stability and reusability of molecularly imprinted polymers," *Polym Chem*, vol. 8, no. 4, pp. 666–673, 2017, doi: 10.1039/C6PY01853J.

[204] D. M. Arm and A. F. Tencer, "Effects of cyclical mechanical stress on the controlled release of proteins from a biodegradable polymer implant," *J Biomed Mater Res*, vol. 35, no. 4, pp. 433–441, Jun. 1997, doi: 10.1002/(SICI)1097-4636(19970615)35:4<433::AID-JBM3>3.0.CO;2-I.

[205] J. Y. Lichtenberg, Y. Ling, and S. Kim, "Non-Specific Adsorption Reduction Methods in Biosensing," *Sensors*, vol. 19, no. 11, p. 2488, May 2019, doi: 10.3390/s19112488.

[206] D. Diamond, R. A. Relyea, and M. McCaul, "Understanding and mitigating global change with aquatic sensors: current challenges and future prospects," *Frontiers in Sensors*, vol. 4, Dec. 2023, doi: 10.3389/fsens.2023.1284043.

[207] B. Li *et al.*, “Molecular imprinting-based indirect fluorescence detection strategy implemented on paper chip for non-fluorescent microcystin,” *Nat Commun*, vol. 14, no. 1, p. 6553, Oct. 2023, doi: 10.1038/s41467-023-42244-z.

[208] Y. Yang, X. Liu, S. Meng, S. Mao, W. Tao, and Z. Li, “Molecularly imprinted polymers-isolated AuNP-enhanced CdTe QD fluorescence sensor for selective and sensitive oxytetracycline detection in real water samples,” *J Hazard Mater*, vol. 458, p. 131941, Sep. 2023, doi: 10.1016/j.jhazmat.2023.131941.

[209] R. Liu and C.-C. Ko, “Molecularly Imprinted Polymer-Based Luminescent Chemosensors,” *Biosensors (Basel)*, vol. 13, no. 2, p. 295, Feb. 2023, doi: 10.3390/bios13020295.

[210] J. Wu, Y. Qin, X. Mei, L. Cai, W. Hao, and G. Fang, “Self-Enhanced Near-Infrared Copper Nanoscale Electrochemiluminescence Probe for the Sensitive Detection of Ciprofloxacin in Foods,” *Foods*, vol. 14, no. 3, p. 538, Feb. 2025, doi: 10.3390/foods14030538.

[211] T. Curk, J. Dobnikar, and D. Frenkel, “Rational design of molecularly imprinted polymers,” *Soft Matter*, vol. 12, no. 1, pp. 35–44, 2016, doi: 10.1039/C5SM02144H.

[212] M. S. Kang, E. Cho, H. E. Choi, C. Amri, J.-H. Lee, and K. S. Kim, “Molecularly imprinted polymers (MIPs): emerging biomaterials for cancer theragnostic applications,” *Biomater Res*, vol. 27, no. 1, Feb. 2023, doi: 10.1186/s40824-023-00388-5.